SELECTIVE PLASMA ETCHING OF POLYMER MATRIX COMPOSITES FOR IMPROVEMENT OF THEIR SURFACE PROPERTIES

Harinarayanan Puliyalil

Doctoral Dissertation
Jožef Stefan International Postgraduate School
Ljubljana, Slovenia

Supervisor: Prof. Dr. Uroš Cvelbar, Jožef Stefan International Postgraduate School & Jožef Stefan Institute, Ljubljana, Slovenia
Co-Supervisor: Prof. Dr. Miran Mozetič, Jožef Stefan International Postgraduate School & Jožef Stefan Institute, Ljubljana, Slovenia

Evaluation Board:
Asst. Prof. Dr. Miha Čekada, Chair, Jožef Stefan International Postgraduate School & Jožef Stefan Institute, Ljubljana, Slovenia

Prof. Dr. Sabu Thomas, Member, Mahatma Gandhi University, Kottayam, India

Asst. Prof. Dr. Janez Kovač, Member, Jožef Stefan International Postgraduate School & Jožef Stefan Institute

MEDNARODNA PODIPLOMSKA ŠOLA JOŽEFA STEFANA
JOŽEF STEFAN INTERNATIONAL POSTGRADUATE SCHOOL



Harinarayanan Puliyalil

SELECTIVE PLASMA ETCHING OF POLYMER MATRIX COMPOSITES FOR IMPROVEMENT OF THEIR SURFACE PROPERTIES

Doctoral Dissertation

SELEKTIVNO PLAZEMSKO JEDKANJE KOMPOZITOV S POLIMERNO MATRIKO ZA IZBOLJŠANJE NJIHOVIH POVRŠINSKIH LASTNOSTI

Doktorska disertacija

Supervisor: Prof. Dr. Uroš Cvelbar

Co-Supervisor: Prof. Dr. Miran Mozetič

Ljubljana, Slovenia, August 2016

……To my beloved family and friends

Acknowledgments

My deepest gratitude is to my supervisor, Prof. Uroš Cvelbar. I have been amazingly fortunate to have an advisor who also gave me the freedom to explore on my own. Also I would like to thank my co-supervisor Prof. Miran Mozetič, Prof. Janez Kovač and Prof. Sabu Thomas for their valuable suggestions and guidance throughout my PhD studies.

Special thanks to Dr. Gregor Filipič for his inspiration and support. I also thank my fellow researchers, all technicians and staff in the Department of Surface Engineering and Optoelectronics (F-4), Jožef Stefan Institute. I sincerely thank Dr. Ana Drmota, Dr. Peter Kernel (both from company Kolektor Group), Nejc Rozman (Slovenian National Building and Civil Engineering Institute, Slovenia) and Dr. Janez Zavašnik (Center for electron microscopy and microanalysis, Jožef Stefan Institute, Slovenia) for their scientific and technical support.

I wish to express my sincere thanks to the Jožef Stefan Institute and the Jožef Stefan International Postgraduate School (MPŠ) for the financial support provided from the Slovenian Research Agency (ARRS) and European Social Fund (Evropski socialni sklad), respectively. My PhD studies were namely partially co-financed by the European Union from the European Social Fund in the frame of operative program for development of human resources for period 2007-2013. I sincerely thank the people at MPŠ for their willingness to help, the thesis evaluation board members for their valuable suggestions for writing my thesis, all the research collaborators and co-authors of the published articles for the great collaborations.

Most importantly, none of this would have been possible without the continuous support and patience of my family. My profound thanks and gratitude are extended with full respect, honour, and love to my beloved parents and other family members.

It is a pleasure to thank all my friends who are my constant support to make me more inspired and energetic throughout my PhD research. I remember with gratitude the help, caring and constant encouragement provided by my friends Eldho, Nithin, Subin, Akhil, Runcy, Rathish, Ashik, Girish, Kristina and Našata.

Abstract

The emphasis of this PhD thesis is on the selective plasma etching of glass-filled polyphenolic composite for improving their various surface properties. Compared to the complementary or competing etch techniques, plasma etching is fast, controllable and does not adversely affect the bulk properties of the material. By changing the feeding gas composition, better control over the etching process and resulting surface chemistry are achieved.

As a primary investigation, the surface of the composite material was modified inside CF_4 gas discharge. The exposure of reactive F and CF_x plasma species incorporated various carbon−fluorine bonds on the surface, which decreased the wettability of the exposed surface. Along with the plasma treatment, the surface roughness increased as a result of surface polymer removal and consequent filler exposure onto the surface. However, the studies of the aging effects revealed that the hydrophobicity was mostly influenced by the bonding states of carbon rather than the changes in the surface roughness. Further, the dynamic contact angle measurements were employed to enlighten the mechanisms behind existence of water droplet on the hydrophobic surface. In addition, the effects of surface temperature during the treatment and resulting hydrophilic recovery were considered.

Further, the electrical insulation properties of the polyphenolic composite surface were also improved by the successful removal of the surface polymer inside low pressure O_2 or gas mixture O_2/Ar plasma. The etching process was optimized by combining plasma diagnostics measurements. The polymer etching rate was mostly connected with the O atom flux onto the surface, which was increased by increasing the degree of O_2 dissociation by Ar addition. This enlightened the role of various plasma species in the etching process. After the surface polymer removal in O_2/Ar plasma, the electrical insulation properties sufficiently increased, which was adequate for the material to be used in commercial devices, according to the available safety regulations. This increase in insulation properties was achieved in a few minutes of plasma treatment. The new-achieved methodology of surface preparation avoided the need of using expensive fillers in composite technology for the fabrication of insulating devices.

The experimental work of this PhD thesis was rounded with comparison of selective removal of the surface polymer and the etching rates achieved in various commercially important feeding gases. The highest etching rates were measured inside O_2 plasma compared to N_2, H_2 or NH_3 plasmas due to the high affinity of atomic O species towards the interaction with carbonaceous polymer layer. By combining spectroscopic methods with various surface analyses, we identified various plasma-surface chemical interactions, which are promising for the fundamental understanding of the surface processes.

Povzetek

Doktorska disertacija obravnava problem selektivnega plazemskega jedkanja polifenolnih kompozitov s steklenimi polnili za izboljšanje njihovih površinskih lastnosti. V primerjavi s komplementarnimi ali konkurenčnimi tehnikami jedkanja je plazemsko jedkanje hiter in kontroliran postopek, ki ne vpliva na notranje lastnosti materiala. S spreminjanjem sestave plina, ki ga dovajamo v razelektritev, pa lahko uspešno kontroliramo proces jedkanja in končno kemijo površine.

V začetnem delu smo za raziskave izbrali spreminjanje površinskih lastnosti kompozitov s plazemsko razelektritvijo v plinu CF_4. Izpostava kompozita nastalim plazemskim F in CF_x reaktivnim vrstam omogoči nastanek različnih ogljiko-fluorovih vezi na površini, ki znižajo njeno omočljivost in omogočijo nastanek hidrofobnega stanja. Vzporedno s plazemsko obdelavo naraste tudi hrapavost površine, kar je posledica odstranjevanja polimera in posledičnega razkritja polnil na površini. Študije staranja površine so pokazale, da je hidrofobnost površine posledica vezavnih stanj ogljika in ne toliko sprememb v hrapavosti. Ti mehanizmi so bili dokazani tudi z meritvami dinamičnega kontaktnega kota kapljic. V delu smo se dotaknili tudi povezave med površinsko temperaturo vzorcev med obdelavo in zmanjšanjem hidrofobnega stanja površine.

S plazemsko obdelavo površine v kisiku ali njegovi mešanici smo uspešno selektivno odstranili tudi polimers površine polifenolnega kompozita in s tem izboljšali njegove električno izolacijske lastnosti. To smo dosegli z obdelavo v nizko tlačni plazmi O_2 in mešanici O_2/Ar. Pri tem smo optimizirali tudi proces jedkanja s pomočjo plazemske diagnostike. Ugotovili smo, da je hitrost jedkanja večinoma povezana z gostoto toka nevtralnih atomov O na površino. Ta se v plazemskemu sistemu poveča, ko kisiku dodamo argon in s tem povečamo disociacijo O_2. Plazemska diagnostika nam je omogočila tudi razumevanje vloge drugih plazemskih vrst v procesu jedkanja. Rezultat površinske odstranitve polimera je povečanje izolacijskih lastnosti površine do te mere, da zadovoljujejo zahtevanim varnostnim predpisom. Te zahteve dosežemo že po nekaj minutah obdelave s plazmo. Razvita tehnologija odstranjevanja polimera pa izenači uporabo bolj cenovno neugodnih polnil pri izdelavi kompozita za doseganje istih standardov.

Eksperimentalno delo v tej doktorski disertaciji je zaokroženo s primerjavo selektivnega odstranjevanja polimera s površine polifenolnih kompozitov in hitrosti jedkanja v plazmah, ki jih generiramo iz različnih komercialnih plinov. Največje hitrosti jedkanja so izmerjene v plazmi O_2 v primerjavi z N_2, H_2 in NH_3, predvsem zaradi večje verjetnosti za interakcijo atomarnih vrst O s polimerno plastjo, ki vsebuje ogljik. S kombinacijo spektroskopskih metod in površinskih analiz pa smo razkrili tudi različne interakcije med plazmo in površino, ki omogočajo vpogled v temeljno razumevanje površinskih procesov, povezanih s selektivnim jedkanjem.

Contents

List of Figures xv

Abbreviations xvii

1 Introduction 1
1.1 Plasma Science and Technology 1
1.2 Plasma-Surface Interactions 1
1.3 Surface Modification of Polymer Materials 2
1.4 Origin of Selectivity in Plasma Etching of Polymers 3
1.4.1 Properties of plasma 3
1.4.2 Physical properties of the polymer material 3
1.4.3 Structural features of the polymer material 4
1.5 Selective Plasma Etching of Polymer-Matrix Composites 4
1.6 Motivation for the Selective Etching of Polyphenolic Composites 5
1.7 Thesis Objectives and Outline 6
1.8 Scientific Articles Used in This Thesis 9

2 Selective Plasma Etching of Polymeric Substrates for Advanced Applications 11

3 Surface Wetting Behavior of CF_4 Plasma Selectively Etched Polyphenolic Composite 37

4 Selective Plasma Etching for Improving the Electrical Insulation Properties 47

5 Optimization of Plasma Etching Process in Ar/O_2 Plasma for Improved Surface Tracking Properties 55

6 Comparison of Selective Plasma Etching in Various RF Gas Discharges 63

7 Conclusions and Future Outlook 73

References 75

Bibliography 77

Biography 79

List of Figures

Figure 1.1: Plasma-surface interaction graphs of a) physical sputtering process b) Eley-Rideal process and c) Langmuir-Hinshelwood process 2

Figure 1.2: Functionalization of the aromatic ring of the polymer chain by neutral oxygen atom quenching 4

Figure 1.3: Synthesis of graphene nanoribbons from polymethyl methacrylate-carbon nanotube composite film by Ar plasma selective etching 5

Abbreviations

AFM	. . . atomic force microscopy
CCP	. . . capacitively coupled plasma
CNW	. . . carbon nanowall
CNT	. . . carbon nanotube
CTI	. . . comparative tracking index
CVD	. . . chemical vapor deposition
DC	. . . direct current
EDXS	. . . energy dispersive X-ray spectroscopy
G_s	. . . number of chain scissions per 100 eV of energy absorbed
GNR	. . . graphene nanoribbon
HDPE	. . . high-density polyethylene
ICP	. . . inductively coupled plasma
IEC	. . . International Electrotechnical Commission
K_{rel}	. . . relative etching rate of polymer
LDPE	. . . low-density polyethylene
MW	. . . microwave
MWCNT	. . . multiwalled carbon nanotube
m-SWCNT	. . . metal single walled carbon nanotube
N_{ion}	. . . number density of ion
NW	. . . nanowire
OES	. . . optical emission spectroscopy
PDMS	. . . polydimethyl siloxane
P(S-r-MMA-r-GMA)	. . . random copolymers of styrene, methyl methacrylate, and glycidyl methacrylate
PET	. . . polyethylene terephthalate
PECVD	. . . plasma enhanced chemical vapor deposition
PMMA	. . . polymethyl methacrylate
PS	. . . polystyrene
PTFE	. . . polytetrafluoroethylene
PP	. . . polyrpopylene
PVA	. . . polyvinyl alcohol
RIE	. . . reactive ion etching
SBS	. . . styrene-butadiene-styrene
SEM	. . . scanning electron microscopy
SPERISE	. . . simultaneous plasma enhanced reactive ion synthesis and etching
s-SWCNT	. . . semiconducting single walled carbon nanotube
TGA	. . . thermogravimetric analysis
$W_{B.E.}$	. . . binding energy of surface atom
$W_{K.E.}$	. . . kinetic energy of ion
WCA	. . . water contact angle
XPS	. . . X-ray photoelectron spectroscopy

Chapter 1

Introduction

1.1 Plasma Science and Technology

Plasma is often defined as the fourth state of matter composed of positively or negatively charged ions, electrons, neutral atoms, metastables, excited molecules, photons, etc. The development in the field of plasma science enabled the synthesis of complex nanostructures including carbon nanotubes, graphene sheets, quantum dots, organic and inorganic nanowires, etc. Novel plasma processing is involved in two main directions: plasma etching and plasma deposition. Plasma enhanced deposition techniques are efficient in building up complex micro or nanostructures to surface coatings. Particular examples relate to the creation of novel materials including carbon allotropes as well as hard metallic or non-metallic protective coatings [1-3]. On the other hand, gas plasma etching is a revolutionary extension of the technology which allows to achieve the fabrication of integrated circuit boards, surface cleaning, surface patterning, hydrophobic and hydrophilic surfaces, and many more. Plasma etching is a fast and environmentally benign technique, and is largely involved in material fabrication for physics, chemistry, biology and medicine [4,5]. Plasma etching is widely employed as a powerful technique for the surface modification of various organic and inorganic substrates. However, for the purpose of this research topic, I will emphasize in this thesis the plasma surface modification of materials selected from the group of polymer-matrix composites.

The aim of this chapter is to give an introduction to the field of plasma surface modifications. The section 1.2 shortly describes interactions possible at the plasma-surface interface. In Section 1.3, some more fundamental aspects of surface modification of polymers are described. Section 1.4 provides insight into different factors which influence the polymer etching rates and the ground for selectivity in plasma etching. Later in Section 1.5, a short note on plasma selective etching of polymeric composites is presented, followed by the motivation to the research done (1.6) and the thesis objectives and outline (1.7).

1.2 Plasma-Surface Interactions

When various plasma species interact with a surface, a number of physical and chemical events are possible at the plasma-surface interface. When a charged species with high momentum and energy is allowed to interact with a solid surface, the energy and momentum of the incoming species will be transferred to the lattice atoms which are consequently released as separated particles into the gaseous phase (Figure 1.1). This process is termed as physical sputtering, where kinetic interactions prevail over potential interactions. The energy of the particles involved in such processes usually lies between several 100 eV to a few keV. If the energy of the incoming ion is not sufficient enough to break the surface bonds, it will merely transfer a part of its energy onto the surface, resulting in a local thermal spike [6]. Such localized heating can generate phonons that may supply activation energy vital for bond breakings on the surface. Besides this, the incoming high energy ions can be impinged into the material, resulting in ion implantation. On the other hand, neutral atoms are characterized by very low kinetic energy. A sample on floating potential inside the plasma always has negative potential, which accelerates the incoming positive ions onto the surface. In contrast to this, neutral atoms do not experience

any acceleration in the presence of such potential and are driven by diffusion. When neutral atoms are interacting with the surface, the chemical changes are induced mostly by the recombination of atomic species on the surface. Such chemical reactions on the surface are guided through two major processes: Eley-Rideal process and Langmuir-Hinshelwood process.
Eley-Rideal process is analogous to physical sputtering, where chemical reactions are involved in the surface removal of the bulk atoms (chemical sputtering). In this process, the incoming particle directly reacts with the surface atoms without getting accommodated on the surface, followed by desorption of the neutral molecule formed. Contrary to chemical sputtering, Langmuir-Hinshelwood process is associated with the adsorption and accommodation of the incoming particle before the chemical reaction on the surface. The surface recombination can also happen between two neutral atomic species on the surface of material, regenerating the parent plasma feeding gas [7]. Such recombination reactions do not induce any chemical changes on the surface. However, these reactions can dissipate energy in the form of heat, resulting in localized surface heating. The probability of such surface recombination is largely influenced by the nature of interacting solid surface as well as the neutral atoms involved in the process.

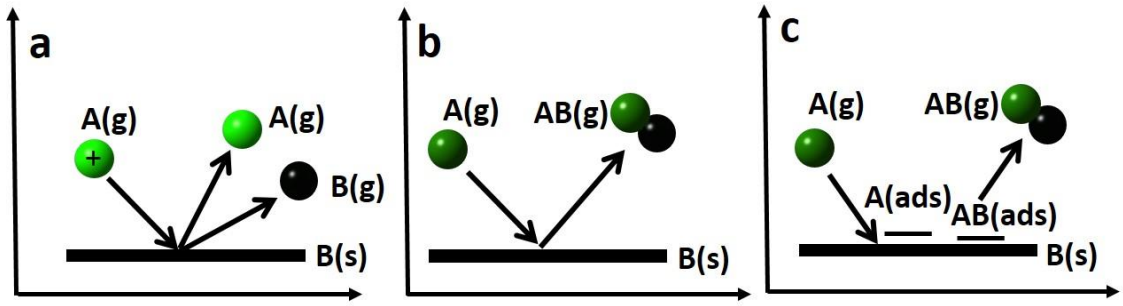


Figure. 1.1: Interaction graphs of a) physical sputtering process $A(g) + B(s) \rightarrow A(g) + B(g)$ b) Eley-Rideal process [A(g) + B(s) → AB(g)] c) Langmuir-Hinshelwood process [A(ads) + B(s) → AB(ads) → AB(g)]. B denotes bulk atom, A an incident energetic particle, while s, g and ads denote a bound (solid), free (gaseous) and adsorbed species, respectively. Based on [7].

1.3 Surface Modification of Polymer Materials

Polymer materials are largely exploited for a wide variety of commercial purposes including plastic bags, medical devices, household items, automotive parts, various thermal and electrical insulation coatings and biomaterials. Their remarkable qualities such as low density, excellent mechanical properties, easy processability, cost effectiveness and high flexibility make them a suitable candidate for such applications. However, many of the polymer materials fail to satisfy our requirements when it comes to some special demands such as adhesion, water repellency or biocompatibility, which are substantially influenced by the surface chemistry and topography. In order to achieve the desired topography and surface chemistry, various surface pre-treatments including plasma functionalization or etching, wet chemical etching and ultraviolet (UV) irradiation are largely employed. However, due to better anisotropy of the etching process and increased environmental concern, plasma etching is preferred to wet chemical treatments for the surface activation or etching of polymer substrates. On the other hand, UV irradiation is an eco-friendly technique for the surface modification of polymer materials. However, the efficiency of this process is relatively low, where no efficient etching and consequent topographic changes are achieved [8].
In contrary to wet chemical etching or UV irradiation, plasma treatment is one of the most versatile techniques that can provide the desired surface wettability, adhesion properties, the degree of surface crystallinity and surface roughness without affecting the bulk properties. Furthermore, different gas plasmas (O_2, N_2, Ar, F_2, etc.) produce unique surface characteristics for wide varieties of applications. For example, O_2 plasma can efficiently

improve the surface energy of the polymeric materials, whereas fluorine containing plasmas reduce the surface energy and increase the chemical inertness [9]. On the other hand, noble gas plasmas can induce surface cross linking, especially for branched polymers. In many previous reports, amine functionalization has shown significant influence on the adhesion properties of various bio-molecules including amino acids or proteins [10].

The etching rate inside the plasma is largely dependent on the type and energy of the particles interacting with the substrate during the processing. However, for the treatment of polymer materials, predominantly ion free and neutral atom rich plasmas are preferred. Such plasmas avoid excessive surface heating due to ion bombardment that can cause unfavorable effects to the bulk properties of the treated polymer. Such plasmas are mostly generated at lower pressures (~100 Pa) within high frequency discharges. The high frequency applied accelerates the electrons, whereas the heavier ions cannot follow the frequency. This yields a highly dissociated and weakly ionized plasma. Microwave (MW) discharges are characterized by insignificant ionic effects due to their low plasma potential whereas the neutral gas temperature is moderately high (~1000 K) [11]. On the other hand, radiofrequency (RF) discharges are capable of producing plasmas with lower neutral gas temperature. It should be noted that the etching rate and the plausible chemical modifications inside various plasmas are correlated with the properties of the plasma and the exposed material.

1.4 Origin of Selectivity in Plasma Etching of Polymers

Gas plasma etching of polymers can be used for tailoring the surface structure of phase separated polymeric systems by the preferential removal of one particular polymer phase over the other. The difference in the etching rates for different polymers or polymer phases originates from multiple factors. Firstly, the etching selectivity originates from the effects of various physical properties and chemical structure of the polymer material [12-13]. In addition to that, the influences caused by various interacting plasma species cannot be excluded. Thus by controlling plasma parameters or choosing suitable candidates for the plasma processing, it is possible to achieve preferential removal of one material over the other. This is the outset of selectivity in plasma etching. The influence of various plasma parameters and the physical and chemical properties of polymer materials which influence the etching selectivity are discussed in this section.

1.4.1 Properties of plasma

The polymer etching rate and etching selectivity throughout the plasma processing is connected with the energy and type of plasma species interacting with the polymer. During the plasma processing, the ionic species do not chemically react with the exposed surface. On the other hand, they mostly contribute their energy towards surface heating, which will accelerate the etching process. Apart from that, various neutral atomic species inside the plasma show difference in their ability in polymer etching and related etching selectivity, which is mostly connected with their potential energy. The comparison of activation energies required for the gas phase reaction between n-butane with various neutral atomic species in the vapor state discloses that O (^{1}D) and F atoms do not need any activation energy for the chemical reaction to start, which reduces the selectivity towards various hydrocarbon bonds [14]. Although the other oxygen atomic species O (^{3}P) is reactive, the spontaneous reaction is prevented by the activation energy barrier. This indicates that this species can distinguish various chemical bonds much better than O (^{1}D) or F species. Due to the same reason, atomic Br species are relatively non-reactive compared to those of atomic Cl species [15].

1.4.2 Physical properties of the polymer material

Among various physical properties of the polymer materials, the influence of crystallinity on the plasma oxidation rate was studied extensively. Irrespective of the feeding gas or type of discharge, the etching rate is maximal for the amorphous polymer. This was explained on the basis of the orderly packed structure of the crystalline polymers that restricts the polymer chain mobility and fast oxidation [16]. Nevertheless, the crystallinity plays a great

influence on the interaction of the material towards various plasma reactive species including neutral atoms or ions. Despite the interacting material, the ionic species neutralize on the surface with a probability of 1. However, the effects due to the neutral atoms depend on the surface recombination probability that is higher for amorphous polymers [13]. The influence of other physical properties of polymeric materials (glass transition temperature, mechanical strength, etc.) on the feasibility of plasma oxidation has not yet been well explored.

1.4.3 Structural features of the polymer material

The difference in the etching rate of polymers in plasma has a strong connection with their structural characteristics including types of monomer units, cross link density and side chain branching. Generally, the polymers derived from monomer units bearing aromatic rings have lower etching rates than those derived from pure aliphatic moieties. This is attributed to the efficient quenching of the incoming neutral atom species by the aromatic ring to incorporate a new functional group, which does not yield any activation of the macromolecular chain (Figure 1.2) [17]. However, when there is some branching on the aliphatic macromolecular chain, the plasma activates the side chain and persuades cross linking on the surface [18]. In such circumstances, surface cross linking prevails over polymer etching and the etching rate for aliphatic polymers is lower compared to aromatic polymers.
The functional groups present on the polymer are one of the factors which can influence the etching rate in various gas plasmas. In many cases, O or F functionalized polymers revealed higher etching rates than their parent hydrocarbon analogues. This is evident due to the reaction between the polymer and highly reactive atomic F or O species which are liberated into the plasma as a result of polymer chain fragmentation. Taylor and Wolf reported a systematic comparison of etching rates for various classes of polymeric substrates relating to the energy required for breaking the polymer backbone [17]. Regardless of the etching mechanism, the etching rate displayed a linear relationship with the total bond energy of the polymer backbone. During plasma-surface interactions, the bond fragmentation is always expected at a position with the lowest bond energy [19-20]. Thus to conclude, the distinct etching rates of various polymer phases are utilized for the removal of unstable amorphous phase from the surface, polymer surface nanostructuring, transformation of the dimensionality of polymer fibers from macro to nanoscale, and many more.

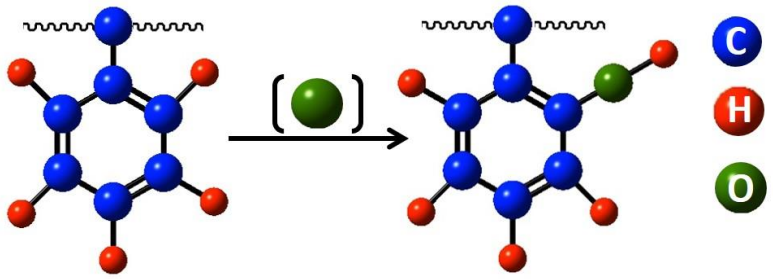


Figure. 1.2: Functionalization of the aromatic ring of the polymer chain by neutral oxygen atom quenching to form phenols.

1.5 Selective Plasma Etching of Polymer-Matrix Composites

As previously stated, different materials are etched at different rates inside plasma, depending upon the chemical stability of the material. Compared to various inorganic materials (glass, minerals, or clay) and carbonaceous materials (allotropes of carbon), polymers exhibit very high etching rates [21-22]. These organic/inorganic materials are largely used as additives for the fabrication of numerous polymer composites. The process of compositing allows to improve the physical and chemical characteristics of polymers by combining the properties of individual constituent materials. In many cases, the surface modification of such composites is necessary to improve the adhesion of other materials on

the surface. Due to the chemical dissimilarities between the polymer and the embedded fillers, the selective removal of the matrix or the embedded filler is achievable.
In the early development stages of the technology, plasma selective etching was implemented for surface cleaning, increasing or decreasing the surface energy of the composite material, studying the filler dispersion in the polymer matrix, etc. However, in some recent reports, plasma selective etching of polymer composites is presented as a novel technique for advanced applications including the fabrication of graphene nanoribbons (GNR), graphene nanomesh and complex nanostructures on polymeric or metallic substrates including nanowires, nanocone arrays, etc. As an example, the fabrication of GNR from multiwalled carbon nanotubes (MWCNT)/polymethyl methacrylate (PMMA) composites by using Ar plasma selective etching is schematically presented in Figure 1.3 [23]. More examples of plasma selective etching of polymers and their related composites and the current state of art is illustrated in Chapter 2.

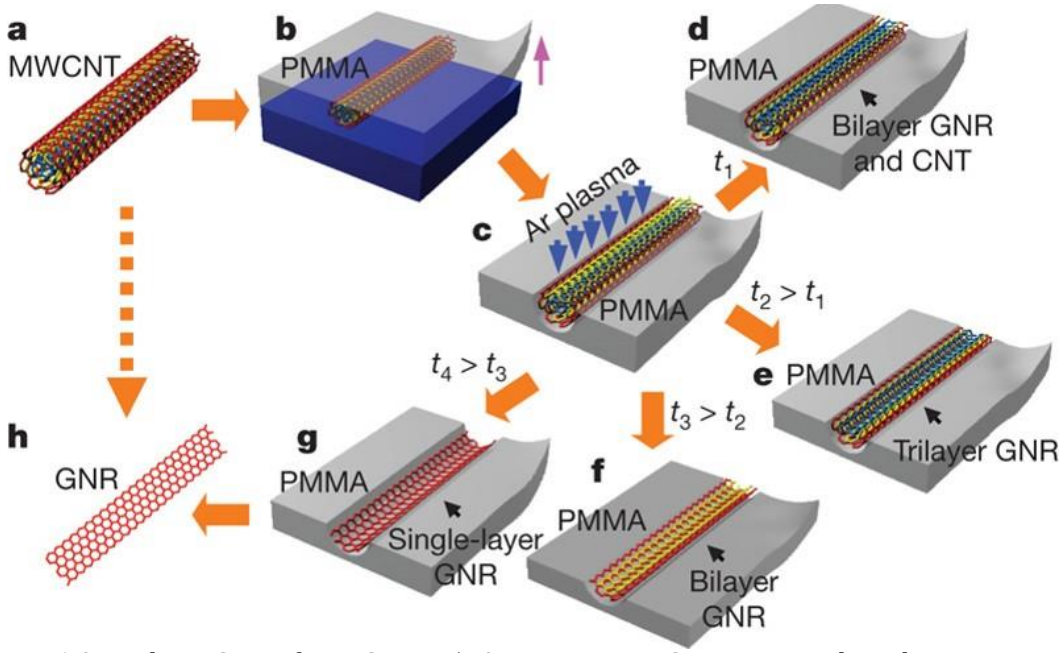


Figure 1.3: Making GNRs from CNTs. a) A pristine MWCNT was used as the starting raw material. b) The MWCNT was deposited on a Si substrate and then coated with a PMMA film. c) The PMMA–MWCNT film was peeled from the Si substrate, turned over and then exposed to an Ar plasma. d–g) Several possible products were generated after etching for different times: GNRs with CNT cores were obtained after etching for a short time t_1 d) tri-, bi- and single-layer GNRs were produced after etching for times t_2, t_3 and t_4 , respectively ($t_4 > t_3 > t_2 > t_1$; e–g) h) The PMMA was removed to release the GNR. Courtesy of Liying Jiao, *et al*. Reproduced with permission from [23].

1.6 Motivation for the Selective Etching of Polyphenolic Composites

The demand for polymers and their composites has increased in the past decades due to their cheap production cost, easy processability and excellent thermal, physical and chemical properties. Among various polymeric materials, polyphenolic resins are widely used in grinding wheels, friction linings, refractory products and other aggressive environments due to multiple advantages [24-26]. They can withstand very high temperatures under mechanical load and exhibit chemical inertness towards harsh chemical environments. Compared to many other polymers, polyphenolic resins produce a low amount of smoke with a lower level of toxic components during combustion. Additionally, phenolic resins cover a large amount of material requirements in electrical insulation devices. To improve the mechanical strength and chemical inertness of polyphenolic resins, compositing with suitable fillers is essential for many applications. However, among numerous available fillers, glass fibers and glass beads are preferred due to their low production cost. Moreover, during the polymerization process, the monomers can efficiently cross link over glass fillers and provide excellent thermal and mechanical

properties. When such composites are used as thermal or electrical insulators, the possible thermal degradation of the polymer gives rise to small molecular fragments including CO, CO_2 and H_2O, whereas glass fillers stay mostly unaffected.

When polymer materials are used in electrical insulation devices, their performance level should meet the requirements according to International Electrotechnical Commission (IEC) standards [27]. The material has to pass the comparative tracking index (CTI) test, which is a measure of the ability of polymer material to restrict the char formation and sequential short circuit at high voltage electric arc. CTI of a polymer material is the maximum voltage at which there is no tracking (surface sparking, burning or formation of electrically conductive path) after wetting the surface with 50 drops of 0.1% NH_4Cl solution, having a conductivity less than 1 mSm^{-1} [28].

The failure during this test happens as an after effect of surface carbonization that results in a conductive path. Despite the higher temperature resistance, lower CTI performance makes glass-filled polyphenolic resins unfit for electrical insulation applications in warm and damp conditions. This is limited due to the carbonization of the thin protruding polymer layer.

The aim of this thesis is to implement novel selective plasma etching of glass-filled polyphenolic composite for the improvement of their surface properties. By utilizing the difference in etching rate between the polymer resin and the glass fillers embedded, the protruding surface polymer can be removed in various low-temperature RF gas discharges. Further, the investigation will extend for testing the electrical insulation properties of the modified surface according to IEC standards. In addition, the study is extended into the systematic comparison of polymer etching processes in various RF discharges. The effects of various gas plasmas on the surface chemistry and surface hydrophilicity are stressed as well.

1.7 Thesis Objectives and Outline

As mentioned in the preceding sections, polyphenolic resin composites are potent candidates to be used in mechanical and electrical insulating devices. However, the main drawback of glass-filled polyphenolic resin is its poor performance level during the standard CTI tests, which decides the quality of the material for electrical insulation applications. The standard performance levels and corresponding tracking index values according to IEC regulations are presented in table 1.1. According to the IEC norms, materials within performance level 0 which are of the upmost quality (CTI >600V). For polymeric materials to be used in commercial devices, the materials should be at least in performance level 2, where the CTI should be in the range from 250–399 V. Unfortunately, the performance level of glass-filled polyphenolic composites lies in performance level 3 (175–249 V). One solution could be to replace the glass fillers in the matrix with different fillers such as melamine salts, which is not cost effective. Nevertheless, the thin surface polymer layer can still restrain the performance level due to its surface charring. Thus the best alternative to this problem is to selectively remove the surface polymer to expose the embedded glass fillers, which do not form condensed char and act as a barrier against tracking.

Table 1.1: Performance level categories for the electrical safety assessment.

Comparative tracking index (V)	Performance level
≥600	0
400−599	1
250−399	2
175−249	3
100−174	4
<100	5

Among various available techniques, selective plasma etching is commonly used for the surface modification and preferential removal of polymer matrix or embedded fillers from a composite surface. Plasma etching allows precise control over etching rate, etching selectivity, and directionality of etching. For this reason, the goal of this thesis emphasize

towards the selective etching of the polymer-matrix from the glass-filled polyphenolic composites to improve the electrical insulation properties. Since the composites used for these experiments are important for engineering applications in automotive and insulating devices, the method of plasma selective etching becomes interesting for both academic and industrial researchers. In addition to that, the goal of this thesis includes the understanding of surface chemistry and wettability in various gas discharges, which are important for the fabrication of superhydrophilic/hydrophobic surfaces. To reduce the thermal damage due to ion bombardment, neutral atom rich and weakly ionized plasmas are used for the experiments, which can be generated by inductively coupled RF discharges at low pressures.

Thesis Objectives are:

1. **Understand the effects of low-temperature plasma treatments on surface chemistry, topography and wettability of various industrially related composite surfaces;**

   Plasma surface modification is known to change the wetting properties of surfaces based on the chemical and morphological changes. Various gas discharges including O_2, N_2, NH_3, etc. are known to increase the surface energy by successful incorporation of polar functional groups and simultaneous creation of micro/nanochannels on the surface which allow the spreading of the water droplet. On the other hand, the fluorine-containing plasmas usually tend to decrease the surface energy and provide hydrophobicity to the modified surface. The mechanisms and the factors behind the existence of water droplet on a hydrophobic surface are studied more in detail for the interest of the scientific community. Even though the physical and chemical effects of plasmas have been studied extensively, the effects of various functional groups and the aging effects have not been well explored yet.
   In Chapter 3, the influence of CF_4 plasma and its selective etching on the hydrophobic behavior of polyphenol resin embedded with glass fillers is presented. As a case study of phenomena, interplay between topography and functional groups is investigated. By comparing the surface topography with dynamic contact angle, the mechanism behind the existence of hydrophobicity on the surface is presented.

2. **To study the effects of selective plasma etching for improving the electrical insulation properties of glass-filled polyphenolic composites;**

   As previously mentioned (Section 1.6), the glass-filled polyphenolic composites are one of the cheapest candidates used as efficient thermal and electrical insulators. However, the superficial polymer layer can cause short circuits and fire while operating in electrical insulation devices. So it is necessary to selectively remove this polymer to expose the glass fillers onto the surface.
   For this purpose, the surface polymer layer is selectively oxidized inside weakly ionized O_2 plasma by utilizing the inertness of the glass fillers towards O atoms and ions (Chapter 4). The results demonstrate that the insulation properties of the composite material significantly increase as a function of polymer removal and the CTI values are merely affected by the degradable carbon layer on the surface. Further, to confirm the effects of glass fillers on the surface, the samples with different filler content are exposed to plasma and test for CTI. The addition of Ar into O_2 plasma can increase the etching efficiency and further improve the CTI performances as presented in Chapter 5.

3. **To determine the influence of various plasma parameters on the etching efficiency and optimization of the process;**

   The studies carried out in Chapter 4 already reveal that the CTI performance can be significantly improved by the selective polymer removal. However, to have a better understanding about the influence of various reactive species, the optimization of the process is essential. Additionally, the results in Chapter 4 reveal that the surface temperature raises to a value slightly above 300 °C during the treatment process. Such elevated temperature on the surface can significantly affect the bulk properties of the

material. Thus it is necessary to control the surface temperature during the treatment, which is an after effect of multiple factors including ion collision, polymer oxidation and neutral atom recombination.

In Chapter 5, O_2/Ar plasma is generated by an RF discharge to selectively remove the surface polymer from polyphenolic composite and the role of different plasma species in the etching process is discussed. By combining Langmuir and Ni catalytic probe measurements, the concentrations of various atomic and ionic species in the system is estimated. The results obtained from the measured etching rate and the plasma parameters clarify the assumption that the ion and radical flux onto the surface are the key parameters which decide the etching rate. The influence of various atomic and ionic species on the etching efficiency will be discussed. On the other hand, the ionic species inside the system contribute to surface temperature and enhance the etching rate. The results point towards the possible direct involvement of metastable species in the etching process. Further, it is confirmed that the molecular oxygen is incapable of inducing polymer etching at the tested conditions.

4. **To systematically compare the etching process in various gas plasmas created within inductively coupled RF discharge;**

Among commonly used RF gas discharges, O_2 plasma displays extremely high etching rate towards various carbonaceous materials. The efficient etching inside O_2 plasma is presented in Chapters 4 and 5. However, due to the simplicity and uniqueness towards achieving certain material properties, the other gases such as N_2, H_2 or NH_3 are widely used for numerous commercial purposes. Due to this, the systematic studies on the polymer etching rate and etching selectivity inside various gas discharges created within RF frequency are necessary.

In Chapter 6, the etching rates inside O_2, N_2, H_2 and NH_3 are compared as a function of discharge power. In all the gas discharges used, the surface polymer is removed exposing the fillers. Irrespective of the discharge power, O_2 plasma shows the highest etching rate. NH_3 discharge yields good etching rate, but it is slightly lower compared to that of O_2 plasma. On the other hand, the measured etching rates are very low inside H_2 or N_2 plasma. To have a more clear understanding of the etching process and etching efficiency, the plasma is qualitatively characterized by emission spectroscopy. Further, the etching mechanism is proposed by comparing the surface chemistry with the stability of various bond types and the chemical structure of the interacting polymer.

1.8 Scientific Articles Used in This Thesis

[1] H. Puliyalil and U. Cvelbar, "Selective Plasma Etching of Polymeric Substrates for Advanced Applications," *Nanomaterials*, vol. 6, pp. 108, 2016.

[2] H. Puliyalil, N. Recek, G. Filipič, M. Čekada, I. Jerman, M. Mozetič, S. Thomas, U. Cvelbar, "Mechanisms of hydrophobization of polymeric composites etched in CF_4 plasma," *Surface and Interface Analysis*, 2016, DOI: 10.1002/sia.6104.

[3] H. Puliyalil, U. Cvelbar, G. Filipič, A. D. Petric, R. Zaplotnik, N. Recek, M. Mozetič, S. Thomas, "Plasma as a tool for enhancing insulation properties of polymer composites," *RSC Advances*, vol. 5, pp. 37853-37858, 2015.

[4] H. Puliyalil, G. Filipič, and U. Cvelbar, "Selective Plasma Etching of Polyphenolic Composite in O_2/Ar Plasma for Improvement of Material Tracking Properties," *Plasma Processes and Polymers*, 2016, vol. 13, pp. 737-743, 2016.

[5] H. Puliyalil, G. Filipič, J. Kovač, M. Mozetič, S. Thomas, U. Cvelbar, " Tackling chemical etching and its mechanisms of polyphenolic composites in various reactive low temperature plasmas," Submitted to: *RSC Advances*, Manuscript number: RA-ART-06-2016-015923

Chapter 2

Selective Plasma Etching of Polymeric Substrates for Advanced Applications

This chapter presents the overview of selective plasma etching of polymer materials and its composites, where various factors which affect the selectivity of plasma etching are discussed in detail. The advantages of selective plasma etching over other complementary techniques are discussed, and relevant examples presented. In addition, we outlined the applications of selective plasma etching of polymer materials that are important in multidisciplinary branches of science including physics, chemistry, biology, medicine, material science and engineering. This chapter gives a clear overview of the topic and current state-of–the-art.

Regarding my contribution: I made an entire literature overview of the topic and jointly prepared the manuscript with co-authors.

nanomaterials

MDPI

Review

Selective Plasma Etching of Polymeric Substrates for Advanced Applications

Harinarayanan Puliyalil [1,2,†] and Uroš Cvelbar [1,2,*,†]

[1] Jožef Stefan International Postgraduate School, Jamova cesta 39, 1000 Ljubljana, Slovenia; hari.puliyalil@ijs.si
[2] Jožef Stefan Institute, Jamova cesta 39, 1000 Ljubljana, Slovenia
* Correspondence: uros.cvelbar@ijs.si; Tel.: +386-14773536
† These authors contributed equally to this work.

Academic Editors: Krasimir Vasilev and Melanie Ramiasa
Received: 2 February 2016; Accepted: 30 May 2016; Published: 7 June 2016

Abstract: In today's nanoworld, there is a strong need to manipulate and process materials on an atom-by-atom scale with new tools such as reactive plasma, which in some states enables high selectivity of interaction between plasma species and materials. These interactions first involve preferential interactions with precise bonds in materials and later cause etching. This typically occurs based on material stability, which leads to preferential etching of one material over other. This process is especially interesting for polymeric substrates with increasing complexity and a "zoo" of bonds, which are used in numerous applications. In this comprehensive summary, we encompass the complete selective etching of polymers and polymer matrix micro-/nanocomposites with plasma and unravel the mechanisms behind the scenes, which ultimately leads to the enhancement of surface properties and device performance.

Keywords: plasma etching; selectivity; surface chemistry; nanomesh; nanostructuring; polymer composite; biomaterials; adhesion; etch mask; radical atoms

1. Introduction

Plasma technology is one of the fastest developing branches of science, which is replacing numerous conventional wet-chemical methods in high-tech laboratories and industries, with a huge impact in renewable energy, environmental protection, biomedical applications, nanotechnology, microelectronics, and other fields. Plasma, the complex mixture of ions, radicals, electrons, and excited molecules has replaced conventional methods to develop various nanostructured materials with complex morphology and advanced properties (e.g., the production of vertically aligned carbon nanotubes (CNTs), which is difficult to achieve with other synthetic methods [1,2]). Owing to fast multi-scale production, it is a preferred method for the synthesis of other nanomaterials such as nanowires (NWs), carbon nanowalls (CNW), graphene sheets, *etc.* [3–5]. Through this, plasma in nanoscience also impacts the field of renewable energy and environmental protection, where we endeavor to replace hydrocarbon energy resources with solar energy or hydrogen fuel cells [6,7]. An additional benefit of plasma technology is the wet free doping of semi-conducting nanomaterials with heteroatoms to alter the band gap energy and conductivity for various applications [8–10]. In the overview of the applications in biology and medicine, plasma is found in various applications, from plasma surgery and the manufacture of artificial implants to the straightforward disinfection of the medical equipment.

The main processing routes in plasma technology are simply concluded into deposition and etching. For achieving the best material performance, these two techniques are either used individually or in a combination. Plasma-enhanced chemical vapor deposition (PECVD) is a technique complementary to thermally excited chemical vapor deposition (CVD) and is used for creating thin

layer coatings, micro- or nanostructures, and even the deposition of complex functional materials [11]. Various applications of plasma deposition techniques are found in numerous articles, and some examples are given in [12–15]. On the other hand, plasma etching originates from the interactions between plasma particles with various substrates. The interactions are either physical or chemical; the particles with high kinetic energy are utilized to knock out the atomic or molecular species from the surface, whereas in the latter case the interaction of particles is purely potential. The physical interactions are mostly linked to ionized plasma species, while potential is linked to neutral or excited species.

Plasma etching, referred many times as plasma chemical etching or dry etching, of both organic and inorganic materials was reported for material fabrication in multidisciplinary applications. Compared to the wet chemical etching, plasma etching is capable of controlled and precise etching at very small scales (~10 nm). Additionally, plasma etching limits the disadvantages, for example, via contamination or solvent absorption during the treatment process. Some of the major advantages and disadvantageous of wet chemical etching *versus* plasma etching are listed in Table 1. In this review, we will mostly focus on the plasma etching of organic materials, which typically undergo etching relatively faster than inorganic materials. The difference in the etching arises from the stability of materials towards various chemical species. As an example, when we compare with liquid chemistry, alkali metals react explosively with water or acids, whereas transition or inner transition metals react very slowly or even stay inert. In the same way, different organic or inorganic materials react at different rates with various plasma species. This advantage of the disparate reactivity of substrates towards plasma is then utilized for fabricating important micro-/nanostructured materials.

Table 1. Comparison of wet chemical etching *versus* plasma etching.

	Wet Chemical Etching	**Plasma Etching**
Etchant:	Chemical (acids, alkali, *etc.*).	Reactive gas (radicals, ions, *etc.*).
Etch rate and selectivity:	High.	Good, controllable.
Advantageous:	Low equipment cost, fast processing and easy to implement.	Capable of small scale etching (~10 nm), no contamination issues, no hazardous chemicals, ecologically benign technology.
Disadvantageous:	Inadequate to define small feature size less than 1 μm, handling of hazardous chemicals, contamination issues, ecologically unfriendly technology with need of waste processing.	High equipment cost, implementation dependent on application, potential radiation damage.
Directionality:	Only isotropic etching.	Can be isotropic or anisotropic.

In the field of material fabrication, the organic materials, especially polymer materials, are replacing many inorganic substrates. Simple fabrication and low production costs are the two great advantages for employing polymer materials. However, to minimize certain disadvantages of pure polymers, their properties are improved by making composites from multiple organic materials using multiplication of material properties or even reducing their dimensions to the nanoscale. To achieve this, the preferential removal of materials is desired, which is simply achieved by plasma etching. This approach was found to be the best method for many applications to achieve desired surface structures, morphology, or chemistry [16,17]. One should stress the effects on the surface chemistry, especially when it comes to organic materials, as it is typically more important than the morphology for certain applications such as adhesion. Plasma etching always alters the surface energy by the successful incorporation or formation of chemical groups during the interaction of plasma particles with materials [18].

Up to now, no reviews have reported specifically on the topic of plasma selective etching, which has innumerable applications in the field of materials science. This review concentrates on the applications of selective etching. However, prior to that, a short discussion is made on the important

types of plasmas based on particle species, their energy, and the result of interaction with the surface, namely sputtering, reactive ion etching, or neutral radical chemical etching. All these interactions then drive the representative applications of plasma etching schematically presented in Figure 1. Sputtering, which involves the removal of various substrates merely by high-energy particle collision is not very important for the selective etching of materials. On the contrary, the reactive ion etching and the neutral plasma chemical etching are found to be efficient for the preferential removal of one material over the other. Following this, the applications of the plasma modified polymeric substrates are described. The main objective of this article is to focus on the characteristics of polymer materials, which are decisive for the etching rate and stability towards high-energy particles. Plasma processing of various polymer composites and their advanced applications are outlined as well.

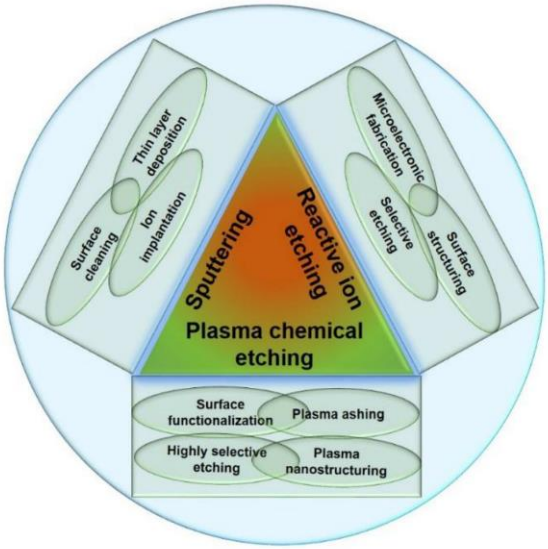


Figure 1. Schematic representation of various uses of different plasma processes.

2. Plasma Processing

2.1. Sputtering

Sputtering deposition is widely employed as a robust method in a thin film preparation for countless applications. The basic principle of the sputtering technique is the generation of high-energy ions, which are then accelerated and guided towards the substrate where they knock out surface atoms as ions into the vapor phase. The so-generated ions are also guided and deposited on the coated substrate where they form a thin layer. However, this deposition process is beyond the scope of this paper. More interesting are energetic surface collisions, where material is removed from the surface.

While considering the process, one should create an ion-rich environment that enables the acceleration of generated particles by applying an external electric or magnetic field. The number density and kinetic energy of the ions (N_{ion} and $W_{K.E.}$, respectively) should be sufficiently large to overcome the energy barrier created by the binding energy of the surface atoms ($W_{B.E.}$). The sputtering process is efficient when the kinetic interactions significantly prevail over chemical and thermal interactions, which typically occurs at ion energies ranging higher than several 100 eV or even higher than 1 keV [19]. However, the sputtering process efficiency in atom removal is significantly dependent upon the material sputtered. One simple schematic representation of the plasma-sputtering chamber is presented in Figure 2a.

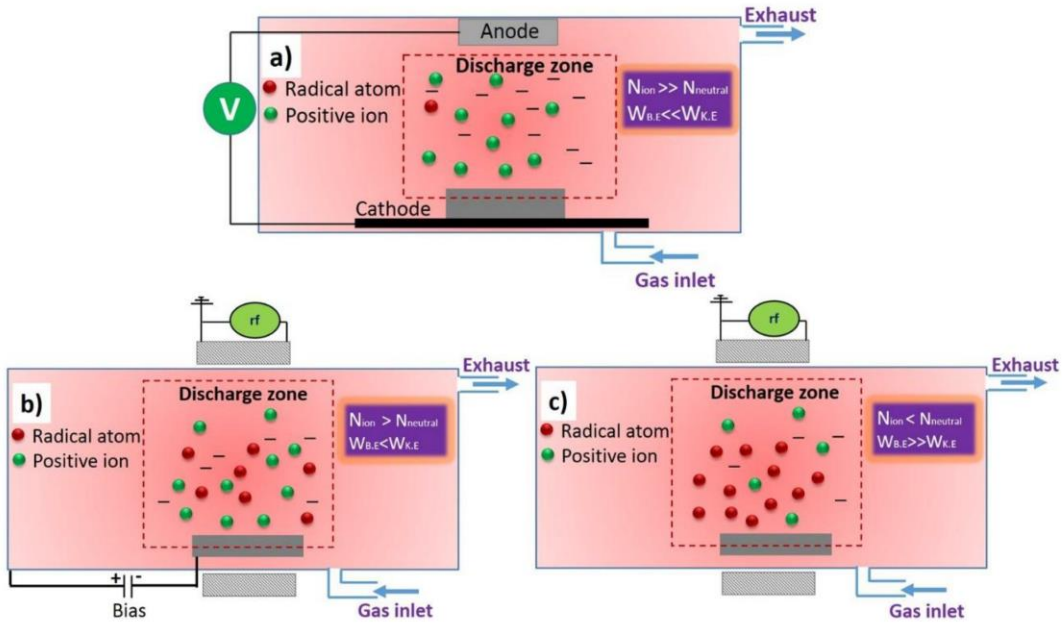


Figure 2. Schematic representation of various plasma processing systems for (**a**) sputtering; (**b**) reactive ion etching; and (**c**) highly dissociated weakly ionized plasma for chemical etching.

The major drawback of the sputtering process is its inefficiency for the surface modification of delicate materials including polymers. The problem is that the high-energy particle–surface interactions are uncontrollable and completely damage the surface mostly through cascade collisions inside the material, which provide almost no selectivity. Moving away from high-energy ions, which cause only the pure kinetic-physical interactions of ions with surfaces (via two body collisions), there is a gray zone of so-called chemical sputtering, where some chemical reactions between the incident beam and substrate occur. This process involves mostly lower energy ions (typically with energies around 100 eV) and is commonly applied to remove the surface contaminates such as hydrocarbons [20].

2.2. Reactive Ion Etching

Reactive ion etching (RIE) was mostly developed and improved by the microelectronic industry in the last few decades for trenching and patterning the surfaces. The RIE process is very diverse and uses various plasma combinations, with species ranging from merely low-energy ions (10 eV to several 100 eV) to combinations of ions with radicals, excited atoms, and electrons. These combinations are mostly generated with glow discharges, where the ratio of ($W_{K.E.}$) to ($W_{B.E.}$) is much lower than in the case of sputtering (Figure 2b). In these processes, the etching material is typically DC-biased in order to increase the effect of ion collection and acceleration towards the surface. The process is most commonly done inside a chamber with low pressure of a selected gas, where plasma is generated in a high-frequency discharge [21]. In such systems, where the surface potential is controlled, the interacting ions are directed, their energy distribution controlled by bias voltage. Nevertheless, other reactive species including neutrals inside the plasma play a significant role in determining the etching rate and etching anisotropy. Like in the case of any plasma process, the etching rate inside a reactive ion chamber is partially dependent on the discharge parameters that influence plasma properties. Therefore, the increase in the discharge power improves the etching rate, since the dissociation efficiency increases with the applied power. On the other hand, the generation of self-bias potential at reduced pressure improves the etching efficiency by energizing the particles [22].

The most reported discharge systems used for RIE are capacitively coupled RF plasma (CCP) and inductively coupled RF plasma (ICP). In CCP plasma, the ion energy varies as a function of applied

power, whereas an increase in gas pressure reduces the acceleration of ions by collisions with the background gas. The ion energy flux to the surface is increased by bias voltage, which imparts a high kinetic energy to the particles. This makes complications by reducing the control or selectivity over the etching process. However, lowering the pressure also results in an increase in the collision mean free path, which restricts the existence of plasma at the point in which the mean free path approaches a value that is of the same order than the distance between the electrodes [22,23]. On the other hand, ICP is capable of generating high particle densities without any additional biasing, even at higher gas pressures [24].

The etching rate in RIE processing varies from a few nm to a few hundred nm per minute depending on the conditions used for the processing [25]. Optimization of the process is extremely important because of the problems encountered during RIE such as bowling, undercutting, or mask scattering, all of which adversely affect the aspect ratio of the processing, especially during the fabrication of circuit boards [26]. To improve the etching rate and aspect ratio, RIE is sometimes combined with other processing techniques including magnetic-field-induced beam control, lithography, ultraviolet (UV) irradiation, *etc.* [27,28].

2.3. Neutral Radical Plasma Chemical Etching

Very frequently, processes like ion sputtering and even RIE lead to thermal damages of the surface or even of bulk properties, which make them improper for the etching of temperature-sensitive materials such as polymers. In order to avoid overheating by ion bombardment or even by increased neutral gas temperature, it is wise to use mostly neutral plasma species like neutral atoms. This is achieved with so-called cold plasmas mostly generated at lower pressures (around 100 Pa) with high-frequency discharges. The high frequency applied accelerates the electrons, whereas the heavier ions cannot follow frequency, which results in a high dissociation and low ionization of the feeding gas (Figure 2c). When treatments are performed in the post-glow or after-glow regions, the discharge features practically no ions. Microwave discharges are popular for the plasma treatment of materials because they are characterized by low plasma potential, which has the advantage of insignificant ionic effects, but the neutral gas temperature is normally high. On the other hand, RF discharges have the electron temperature of about 5 eV for plasma gases such as O_2, where the observed neutral gas temperature is lower compared to microwave discharge. In such high frequency discharges, the dissociation is almost linearly enlarged with the increase in discharge power, independent of the gas flow [29].

Highly dissociated plasma is not only applicable for polymer etching, but also for other applications such as chemical reduction, nanostructuring, and plasma cleaning [30–32]. The reactions of polymers and other materials will be more elucidated in the following chapters, where different neutral atoms contribute a major part to etching through adsorption and recombination processes [33–35]. The recombination of atoms at preferential spots on the surface originates from the roughness of the surface and plays a crucial role, even in deciding the nanostructure growth [24,36]. The surface interactions and bond-breaking mechanisms during the interactions of non-equilibrium plasmas with various carbonaceous materials are also reported [37,38].

3. Applications of Plasma Functionalization and Etching of Polymers

Polymer materials cover a large segment of our material requirements for packaging, microelectronics, photonic devices, medical implants, sealing applications, water repellent coatings, thermal and electrical insulators, sensing materials, *etc.* [39–42]. Plasma-assisted surface functionalization and etching were proven to provide the desired surface energy and morphological changes to the polymeric surface [43,44]. Although various chemical treatments such as soaking in acidic medium are efficient and inexpensive methods for improving the surface energy of polymeric materials, they are associated with persisting residuals after treatment and, to a large extent, connected to environmental pollution [45,46]. Plasma modification consists of surface functionalization, which

is considered to be a primary step in which surface chemistry is altered by bond breaking and the incorporation of functional groups. Thereafter, the removal of material takes place through the bonding of surface atoms with impinging radicals, which recombine and leave the surface. Through this mechanism, the organic surface contaminants or weakly bonded surface layer are removed. An alternative to plasma pre-treatment is UV irradiation, which mostly results in surface functionalization, but it is not sufficient for material etching. Moreover, wet chemical treatments as the second alternative are limited by the type of incorporated functional groups [47]. By taking these factors into consideration, plasma treatments are preferably used in polymer treatments for a wide variety of applications.

Among various applications of plasma surface treatments, improving the adhesion of various metals on polymer substrates is an important task. The major challenge in metallizing polymeric surfaces is their lower surface energy, which confronts the adhesion of metallic particles. By incorporating suitable polar functional groups by plasma exposure, this deficiency is easily solved. For instance, Pascu *et al.* presented both microwave and RF plasma treatments of polyvinylidene fluoride with N_2 and NH_3 as working gases for the incorporation of polar nitrogen containing groups including amines, nitriles, or imines. These incorporated polar functionalities then aided to increase the amount and adhesive strength of the deposited copper [48]. Metallized polymers including polyethylene terephthalate (PET) are important in the fabrication of microelectronic and photonic devices, where the intermixing of the metal and polymer showed the significant improvement of their properties when material was exposed to post-deposition annealing in Ar or Ar/O_2 plasma [49]. The treatment of the samples was done with Ar/O_2 plasma generated at low pressures (50–100 Pa) within RF discharge at power 35 W. The process increased the surface roughness and porosity, allowing the diffusion of coated Au/Ag metal from the surface into the bulk. To obtain the best adhesion, the plasma treatment conditions were optimized to minimize fracture at the interface between the metal film and polymer substrate [50,51]. The adhesion of Cu layer on polyamide also increased with O_2 plasma treatment at 200 W and 8 Pa for 3 min prior to Cu metallization. The peel strength of the deposited Cu on polyamide increased to a value of 250 g/mm, which was almost 280 times higher than that of the non-treated sample [50]. Irrespective of the gas or discharge condition used for the treatment, the metal coatings of polymers should be done immediately after the plasma surface modification in order to eradicate the drawbacks arising from the aging effects [52,53].

In addition to the improved adhesion of inorganic particles, plasma treatments have a significant role in fabricating surfaces, which are customized for the adhesion of various organic or biomolecules. Surface treatment with oxidizing plasma source gases such as O_2, NH_3, N_2, Air, or even noble gas mixtures is found efficient to enhance the surface energy and thereby adhesion of various bio materials onto the surface [54,55]. The surface roughness and polarity provided by plasma exposure are utilized to increase the adsorption of anti-blood clotting agents such as heparin onto various polymeric substrates. This operation is extended in application for manufacturing artificial organs [56]. In addition to this, the cell growth on various polymeric surfaces efficiently increases after suitable plasma pre-treatments as a simultaneous effect of improved surface contact area and the electron rich behavior. The incorporated functional groups allow for the nucleation and adsorption of desired biomaterials on the surface of the implant used by which the spatial alignment of the bio-molecules on the surface is regulated [57,58]. Another supportive application of plasma etching in the bio-medical field is plasma sterilization of surgical devices, drug packaging, or processing of other medical objects [59,60]. For example, on exposure to reactive O_2 plasma neutral radical in the afterglow, the blood proteins and microorganisms showed exponential etching rate, whereas the PET substrate exhibited only a linear etching rate [61]. These distinct etching rates help to remove toxins or other organic contaminants from the surface without affecting the surgical equipment or medical material. Further applications of plasma degradation of materials extend into novel applications such as decontamination of toxic warfare agents, the cleaning of dental devices, and even the precise removal of cancerous cells [62–64].

Besides the improved surface energy of polymeric substrates, plasma treatment is also able to incorporate low-energy functionalities on the polymeric surface. This is largely applied in the fabrication of water-repellent surfaces, which are significantly important in terms of generating better anti-aging or anti-corrosive properties of membranes for oil-water separation, and of fluid transportation control [65,66]. The self-cleaning ability of materials is expressed in terms of the water contact angle, where the surface with a contact angle above 150° is termed as the superhydrophobic surface [67]. Plasma etching efficiently creates superhydrophobic surfaces by two major mechanisms: firstly by providing sufficient roughness to the surface by the etching process and secondly by providing a sufficient number of low-energy functional groups [68]. Typically used fluorine containing plasmas have an ability to simultaneously incorporate sufficient amounts of low-energy functional groups as well as create the desired surface roughness through etching. In the cases of fluorinated polymers including Teflon (polytetrafluoroethylene—PTFE), even fluorine-free gases are sufficient enough to generate hydrophobicity merely by increasing the surface roughness by polymer etching [66,69]. An example of this are nanocone structures on Teflon surface achieved after etching the surface with O_2 plasma (25 Pa and 50 W) for 10 min. In this case, the water contact angle achieved was 134°. Such nano-featured surface is achieved also by etching anisotropy, which is created with deposits like polymer beads. The surface decorated with polystyrene (PS) beads with a 10-μm diameter prior to the plasma process can create nanocones during etching as well (Figure 3) [69]. The sufficient roughness is boosted by the additional deposition of Au nanoparticles on top of the nanocones, which leads to a superhydrophobic surface response. In certain cases, the roughness on the etched surface is influenced by the sputtered deposits from the plasma chamber wall, which act as a mask to protect the polymer but provide similar anisotropy for etching [70].

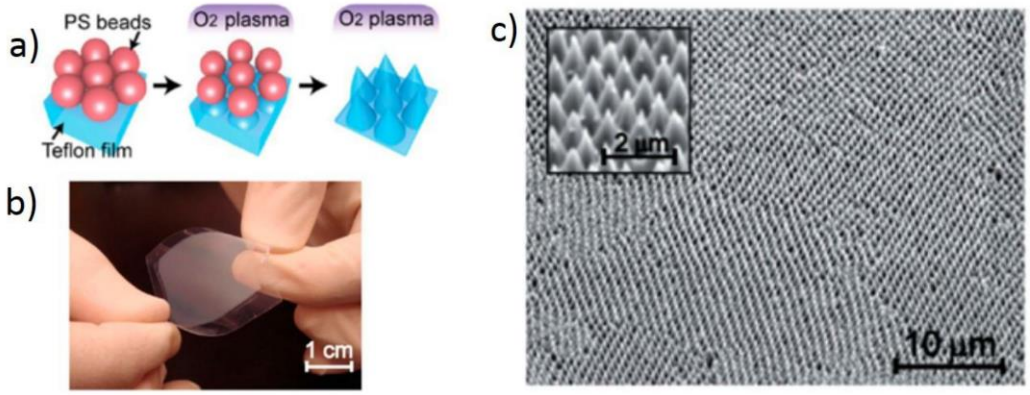


Figure 3. (**a**) Scheme of the fabrication process of Teflon nanocone arrays; (**b**) Photograph showing a macroscopic view of flexible Teflon nanocone array; (**c**) Scanning electron microscopy (SEM) images of the tilted nanocone array. Inset: detailed view of Teflon nanocones (Reproduced with permission from [69]. Copyright American Chemical Society, 2014).

4. The Origin of Plasma Etching Selectivity

The importance of the dry etching of polymeric materials for numerous applications such as masking or nanostructuring has increased the demand for systematic studies on the stability of various polymeric materials towards reactive plasma particles. The stability of the polymer definitely depends on the type of polymer/monomer units present (homo or copolymer, aliphatic or aromatic, crystalline or amorphous, *etc.*) as well as the energy and type of plasma particle interacting with it. Herein, the important factors are directly related to the stability of polymers towards plasma particles, which result in selective etching that will be presented and discussed.

One of the primary structural features that are considered is the aliphatic and aromatic moiety on the polymer backbone. The etching rates for aromatic polymers are relatively lower compared to

aliphatic ones due to the extra energy stabilization (~36 kcal/mole), provided by the aromaticity of the rings in the polymeric chain. One more explanation to support the distinct etching rate is that the aliphatic rings degrade easily to form volatile molecules, whereas the aromatics generally form more non-volatile fragments and are not easily removed from the surface [71]. However, plasma-initiated degradation can occur on the bond–ring junctions, which are connected through relatively unstable secondary or tertiary carbon atoms. This argument can question the extra stability of the aromatic polymer chains exposed to the plasma. An appropriate argument was given by Taylor and Wolf, who stated that the extra stability of the aromatic polymers, irrespective of the position of the aromatic ring, originated from the ability of aromatic rings to quench the reactive plasma particles [72]. The quenching is typically directed through the abstraction of the hydrogen from the aromatic ring by the incoming reactive atom and the formation of a functionalized ring (Figure 4). This reaction prevents the formation of any active sites or dangling bonds on the polymer chain and prevents the chain cleavage. Additionally, the energy released during this process will be readily reduced by contributing to the vibrational energy of the polymer backbone [73]. Some early reports on the gas phase reactions of aromatic rings with oxygen plasma radicals significantly support this argument [74,75]. During such reactions, the hydroxylation was mostly directed towards the ortho position regardless of the size of the substituents on the ring due to the higher degree of neucleophilicity of oxygen radicals. This observation points out that the reactions are mostly guided through a kinetic route to give rise to reaction products that are thermodynamically less stable [74].

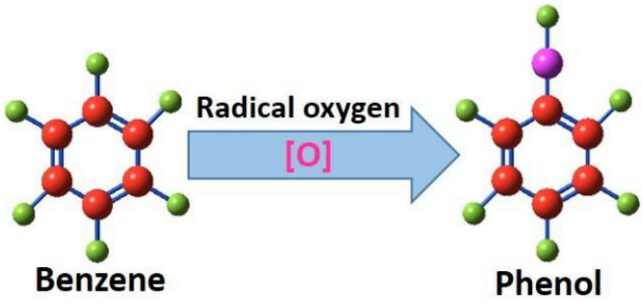


Figure 4. The schematic of reaction involved in the radical quenching by the aromatic ring to form functional group instead of ring cleavage.

Liming *et al.* provided an excellent example to present the etching efficiency and selectivity of plasma towards various chemical bonds [76]. The stability of various bonds was accurately distinguished by high-energy hydrogen radicals and ions, used to selectively etch away the edge atoms of graphene sheets and to convert them into graphene nanoribbons (GNR). As observed from atomic force microscopy (AFM) imaging, the observed etching rate for single layer graphene was 0.27 nm/min, whereas multi-layer graphene disclosed an etching rate of 0.1 nm/min (Figure 5). By keeping the surface temperature to an optimum value of 300 °C, the defect-free hydrogen terminated graphene nanoribbons were synthesized. The selectivity originated from the lower chemical stability of the edge carbon towards plasma particles compared to the atoms embedded in the mid-region of the graphene sheet [77]. In the same manner, while considering the polymeric substrates, regardless of the etching mechanism, the etching rate was mostly connected with the energy required for breaking the polymer backbone, as demonstrated by Taylor and Wolf. They compared the etching rate of different polymers (k_{rel}) with the number of chain scissions per 100 eV of energy absorbed (G_s) (Table 2). The etching rate displayed a linear relationship with the bond-breaking energy of the polymer backbone [72].

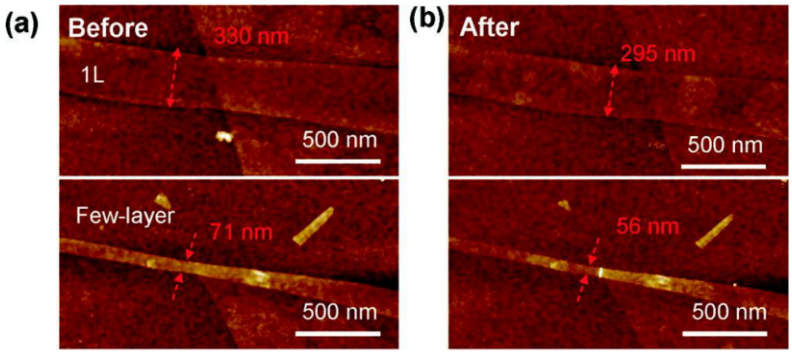


Figure 5. Atomic force microscopy (AFM) images of two small pieces of graphene (top: a monolayer (1 L) graphene strip; bottom: a few-layer graphene strip). (**a**) Before and (**b**) after selective hydrogen plasma edge etching for 60 min at 300 °C (Reproduced with permission from [76]. Copyright American Chemical Society, 2010).

Table 2. Relative rates of O_2 plasma removal (k_{rel}) and G_s-values for selected polymers (Reproduced with permission from [72]. Copyright John Wiley and Sons, 2004).

No.	Polymer	k_{rel}	G_s
1	Poly(α-methylstyrene)	1.11	0.3
2	Polyphenyl methacrylate	1.33	——
3	Polyviny1 methyl ketone	1.48	——
4	Polymethy1 methacrylate (PMMA)	2.37	1.2
5	Polymethyl methacrylate-co-methacrylonitrile (94:6 mol %)	2.70	2.03
6	Polyisobutylene	3.56	4
7	Polybutene-1 sulfone	7.11	8

Another important parameter which determines the etching selectivity is the energy required for the initiation of chemical reaction (activation energy). For example, the chemical oxidation of Mg in air is highly exothermic. However, the reaction will not commence unless sufficient heat is provided such that the reactants can reach the intermediate transition state (activated complex). Once the reaction starts, the exothermic energy released will be used for the reaction to proceed. The comparison of activation energies required for the reaction between n-butane with various neutral species in the vapor state discloses that O (^{1}D) and F atoms do not need any activation energy for the chemical reaction to start, which reduces the selectivity towards various hydrocarbon bonds. Although O (^{3}P) species are reactive, the energy of activation is found to be 1 eV to react with the hydrocarbon, which indicates that this species can distinguish various chemical bonds much better than O (^{1}D) or F species [73,78]. Likewise, the Cl atomic species are highly reactive without any bond selectivity towards the reacting polymer due to no activation energy barrier. On the other hand, Br atoms are relatively non-reactive due to an energy barrier of around 1.8 eV. Moreover, the etching rate can also be controlled through the combination of various reactive species, which can be regulated by controlling the feeding gas composition and discharge parameters. In one recent report, it was demonstrated that adding O_2 into CF_4 plasma increased the etching rate [79]. This phenomenon was due to the involvement of excited oxygen radicals in the electron impact dissociation of CF_4, which leads to a higher dissociation and more F atomic species [80].

Hegemann *et al.* compared the etching rates for various polymers with different chemical structures inside the noble gas-generated plasmas and concluded that the polymer backbones that contained oxygen functionalities etched away relatively faster. For example, polymethyl methacrylate (PMMA), PET, *etc.* showed relatively higher etch rates compared to the hydrocarbon polymers inside Ar plasma generated at 300 W and a pressure of 20 Pa (Figure 6) [81]. The explanation for the higher

etch rates for functionalized polymers was due to the secondary reactive oxygen atomic species released into the system as a result of polymer bond cleavage. More surprisingly, polypropylene (PP) exhibited a lower etching rate compared to PS, which was in contradiction to the hypothesis of radical quenching mechanism proposed for the extra stability of aromatic polymers. However, this was explained by the efficient cross-linking on the PP surface upon exposure to plasma due to the side chain activation [81].

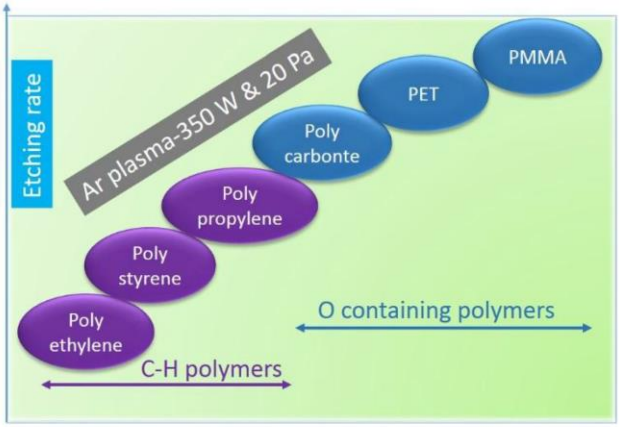


Figure 6. Etching rates for various polymer substrates in Ar plasma based on [81].

Plasma surface interactions have a strong correlation with the crystallinity of the polymer used, where the etching rate is typically reduced with the increase in crystallinity [82]. The reason for this can be different neutral atom recombination probabilities on surfaces. For example, the neutral O atom recombination probability is 8.3×10^{-4}–2.1×10^{-4} for amorphous PET or 4×10^{-4}–2.5×10^{-5} for semi-crystalline PET [83]. Thus, the extension of interactions between the polymer and the neutral atomic species that induce etching differ with respect to crystallinity, which cannot hold for charged species. The ion flux to the surface is independent of the crystallinity. The increased value of the neutral atom recombination coefficient provided higher contribution to the surface temperature which induced more deformation to the amorphous material, as reflected by the roughness measurements before and after plasma exposure [83–85]. The treatment of LDPE (low density polyethylene) and HDPE (high density polyethylene) inside CF_4 plasma revealed similar results. The etching rate for LDPE was 1.5 nm/min more than that of the HDPE inside CF_4 plasma generated by capacitively coupled RF discharge, where the morphological changes also displayed significant differences with respect to crystallinity [86]. Nair *et al.* recently reported the removal of an amorphous carbon layer from the multiwalled carbon nanotube (MWCNT) with low-energy ions, radicals and metastable species, where the crystalline phase remained relatively intact. The extra stability provided by the crystallization energy additionally supported the etch-resistant behavior of crystalline polymers [87]. From all of the above-mentioned results, the relative etching rates for various polymeric substrates inside the widely used oxygen plasma are summarized in Figure 7.

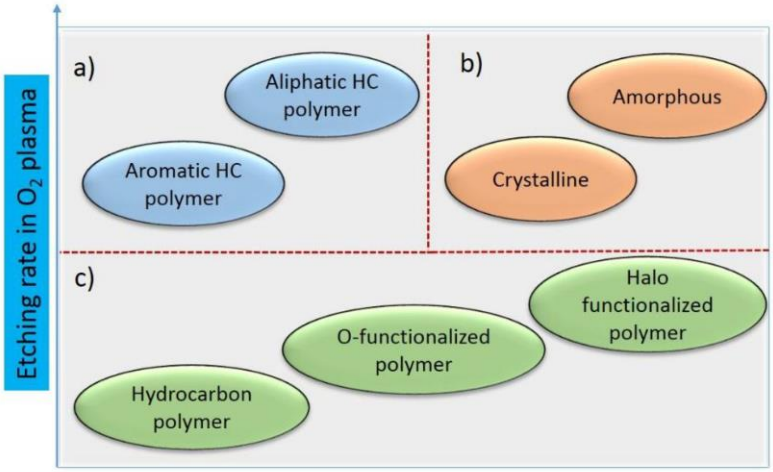


Figure 7. General schematic of the etching rate for various types of polymeric materials in O_2 plasma. (**a**) Dependence of etching rate on the aliphatic/aromatic behavior of the monomer units; (**b**) Etching rate dependence on the crystallinity; (**c**) Functionality dependence of the polymer with etching rate.

An important class of polymers that needs to be separately addressed is that of block copolymers, since they are largely used in block copolymer lithography for the semiconductor industry. The chemical dissimilarities between the two polymer domains permit the selective etching of one component over the other, when a suitable treatment method is used. After the selective etching of the less stable polymer, the unaffected component will form the template pattern. One of the most widely used copolymers is the PS/PMMA system, where both of the components have distinct chemical stabilities. For achieving spherical and cylindrical structures, PMMA is easily removed with a suitable wet chemical treatment [88]. However, the wet chemical etching is limited due to capillary forces when the polymers possess lamellar arrangement. In order to avoid these problems, plasma selective etching is implemented and used for a number of copolymer systems: for example, polystyrene–poly ferrocenylisopropylmethylsilane diblock copolymer, styrene–butadiene–styrene (SBS) triblock copolymer, polystyrene–polydimethylsiloxane block copolymer, polyhydroxybutyrate-co-hydroxyvalerate, *etc.* [89–91]. The most fundamental object while choosing the copolymer for plasma etch patterning is the selection of proper blocks that have distinct etching rates towards various plasma particles [92].

The oxidation probability of the polymer is independent of the density of plasma particle species in the proximity of the samples, but the etching still depends on plasma particle properties and their fluxes to surface [93]. In many cases, the etch-resistant properties of polymer materials are dependent on the type of discharge used, where the difference in the etching rate originates from the energies and flux of various reactive species including neutral atoms and ions generated [37,94,95]. The etching rate is also well correlated to the surface temperature originated from the ion bombardment, neutral atom recombination, and exothermic carbon oxidation [96–98]. In order to achieve the highest etching rates, a higher surface temperature is always preferred. However, the surface temperatures above the glass transition temperature of the polymer can critically affect the bulk properties. Due to this, the radical and ion flux should be optimized, whereas in many cases the pulse mode plasma treatment over continuous mode will be more appropriate to control the temperature related effects [99–101].

5. Applications of Plasma Selective Etching of Composite Materials

Plasma selective etching is utilized in many applications for material fabrication especially in micro- and nano-structuring. One of the important examples is the transplantation of nanostructures like nanotubes. Li *et al.* demonstrated a method for growing CNTs inside Si trench with Ni catalysts.

The challenge faced was the transfer of the designed nanotubes onto suitable receptors. This difficulty was solved by extracting the nanotubes with an epoxy matrix in the form of pellets, followed by oxygen plasma selective etching of the epoxy matrix in order to release well aligned and densely packed CNT arrays [102]. By taking advantage of the difference in etching selectivity of various chemical bonds towards plasma, the metal single-walled carbon nanotube (m-SWCNT) were also obtained. One of the challenges for creating m-SWCNTs is the higher chemical etching rate of m-SWCNTs compared to semi-conducting single-walled carbon nanotubes (s-SWCNT) [103]. However, by taking advantage of the weaker stability of smaller diameter s-SWCNT due to the C–C bond bending, a mild hydrogen plasma treatment yielded m-SWCNT from a mixture of m- and s-SWCNT [104]. This etching selectivity is only diameter-dependent, unlike the m- or s- character of SWCNT, and could yield a 100% recovery and easy scaling up of one type of SWCNT from the mixture [105].

Graphene-based electrodes are used in wide variety of semiconducting devices such as field effect transistors, sensors, supercapacitors, *etc.* [106]. In the transistor applications, one of the most important parameters is the gap dimension between the electrodes. Graphene sheets, which are separated by micro- or nanoscale distance, played a significant role in the fabrication of numerous electronic devices. The fabrication of such devices is extremely hard by wet chemical treatment due to the lack of precision in etching over nanoscale dimensions. As demonstrated by Liao *et al.*, plasma-assisted mask etching can provide precise control over the gap between graphene sheets ranging from a few micrometers to hundreds of nanometers [107]. Furthermore, the electrical properties of graphene sheets are highly dependent on their specific surface area. For this, graphene sheets can be converted into different porous forms including graphene nanomesh, crumpled graphene, folded graphene, and graphene foam in order to exploit the exceptionally large surface area [108–110]. Such high surface area graphene sheets are also easy to obtain by means of polymeric or metallic mask-assisted plasma selective etching. In a presented example, the spin coating of PMMA on graphene-supported silica, when covered with porous anodized aluminum oxide resulted in a suitably masked surface for plasma etching. Treatment of this composite with O_2 plasma for 30 s resulted in pores with diameters of 67 nm on the graphene surface, which produces the graphene mesh with a very high surface area of 100 μm^2 [111]. The origin of etching selectivity during the processing was based on the tolerance of the Al mesh towards plasma compared to the PMMA layer. The observed difference in the etching rates of PS and P(S-r-MMA-r-GMA) (a random copolymers of styrene, methyl methacrylate, and glycidyl methacrylate) was 1.17 and 1.42 nm/s, respectively, inside O_2 plasma (50 W, 10 sccm, 1.3 Pa), compared to 0.76 and 0.96 nm/s, respectively, inside the CHF_3/O_2 gas mixture (300 W, 45 sccm CHF_3 and O_2 5 sccm, 8 Pa). Exploiting this, the patterned copolymer template was fabricated, which provided an easy route for creating nanoperforations on graphene sheets. Such prepared graphene with a large surface area has been used in electronic and sensing devices [112]. Additionally, the combination of holography and photoresist-assisted O_2 plasma selective etching was demonstrated for providing a low-cost production route to synthesize graphene nanomesh [113]. Additional examples are also seen where self-assembled masks are used for the perforation of graphene sheets during selective etching [114]. Such masks provide controlled exposure of the graphene layer to the plasma reactive species and yield precise mesh sizes and ribbon widths between successive meshes. This allows control over the electronic characteristics of graphene [115]. During the etching of such graphene composite surfaces, the selective edge oxidation and O_2 physisorption on the inner walls of the mesh add secondary benefits to chemo-sensing applications [116].

Another particular application of selective plasma modification and etching was to improve gas permeation properties of composite membranes [117]. After plasma treatment with corona discharge, the polyamide 6/polyethersulfone (PA6/PES) composite membrane exhibited significant improvement in separation of CO_2, N_2, and O_2 by incorporating functional groups and increasing the surface roughness [118]. Unfortunately, the changes induced to the distinct composite components were not studied individually. When a polybutadiene/polycarbonate (PB/PC) membrane was exposed to the Cl-containing plasma, it was observed that the modified surface chemistry had very little influence,

whereas the separation towards N_2 and O_2 were dominantly affected by the variation in surface morphology [119]. Other than for permeation applications, selective plasma-assisted mask O_2/Ar etching of Nafion membrane has been used in the preparation of patterned metal-polymer composite membranes for robotics and other applications [120].

Unzipping CNTs under plasma exposure is known to ease the preparation of novel materials including hollow CNTs or GNR. To make such preparative methods easier, the simplest method is to expose CNTs embedded in a polymer matrix to reactive plasmas. Exposure of the vertically aligned CNT in the polymer matrix to plasma opened the tips of the embedded CNTs. This route also included the removal of the polymer matrix at higher rates and then exposing the tube tips and further opening of the CNT tips [121]. In another relevant example, plasma selective etching enabled the successful synthesis of single-layer GNR from CNTs embedded in PMMA composite. The method provided excellent control over edge smoothness and uniformity in width for the fabricated ribbon structures [122].

Due to its simplicity, and the higher rate of dimension tolerance compared to wet chemical etching procedures, plasma etching is well exploited in the semiconducting industry for printing integrated circuit boards. One of the disadvantages often given for plasma processing is the high production cost due to expensive low-pressure plasma systems, which can be bridged only with long-term operation. Silicon wafers, as one of the most used materials in the semiconductor industry, is efficiently etched mostly by halogen-containing plasmas or by their mixture with other gases in the presence of a suitable etch mask. The etch mask on the surface generates an unbalanced etching rate of the surface and creates desired patterns on the wafer [123]. For achieving the etching selectivity between the semiconducting layer and the photoresist, the control of the plasma species inside is needed. By adding certain gases, it is possible to scavenge the radicals and ions, which presents an alternative route to controlling the species inside the plasma and the corresponding etching selectivity, without changing the discharge parameters [124]. One of the major drawbacks of RIE technology is the non-uniform etching on the sidewalls. It operates in such a way that the radicals get accumulated nearer to the edge of the wafer instead of the center, which increases the etch rate towards the edges. Additionally, the ion current is favorably drawn over the wafer edge, and the etch rates for the silicon wafer show an increase from the center to the edge and the consequent edge breakings [125]. Performance level and many of the disadvantages of RIE processing such as anti-notch performances, quality of the profile, surface finishing, *etc.* are tuned by adjusting the applied frequency or pulsing [125]. Even in the presence of these disadvantages, plasma etching is far better than other conventional methodologies.

An important application of the diverse material etching rates in plasma is used to deal with the nanostructuring of the polymeric substrates. Polymer-based 1D and 2D nanostructures have potential applications in sensing and energy devices [126,127]. Although template-assisted synthetic methods are well-known, controlling the dimensions during template removal still represents an obstacle. Plasma-assisted mask etching has proven to be an alternative to overcome these problems. An example is the exposure of metallic nanoparticles deposited on polymer surfaces to reactive gas plasma, which yields the dense polymeric NWs. The metallic coating or, say, metallic material islands (nanodots) merely acted as an etch mask to provide a rough surface to mobilize the NW growth [128]. For this purpose, a mixture of Ar, O_2, and CF_4 gases was leaked into the inductively coupled plasma chamber at constant flow ratios of 15, 10, and 30 sccm. The plasma discharge was generated at 400 W where an additional 100 W was used for biasing to accelerate and direct the ions to the surface. In this way, the polymeric NWs with an aspect ratio of up to 700 were produced on the surface of a large number of polymers including PET, Kapton, Dura film, PS, and polydimethyl siloxane (PDMS). The length of the NWs exhibits a linear trend with the exposure time, whereas the diameter remains constant at a value around 100 nm for a given thickness of the mask on the surface. On the other hand, the density of the NWs is strongly influenced by the thickness of the coated metal. The scanning electron microscopy (SEM) images of NW with respect to various thicknesses of the mask and the relationship of the etching rate with the plasma exposure time are presented in Figure 8.

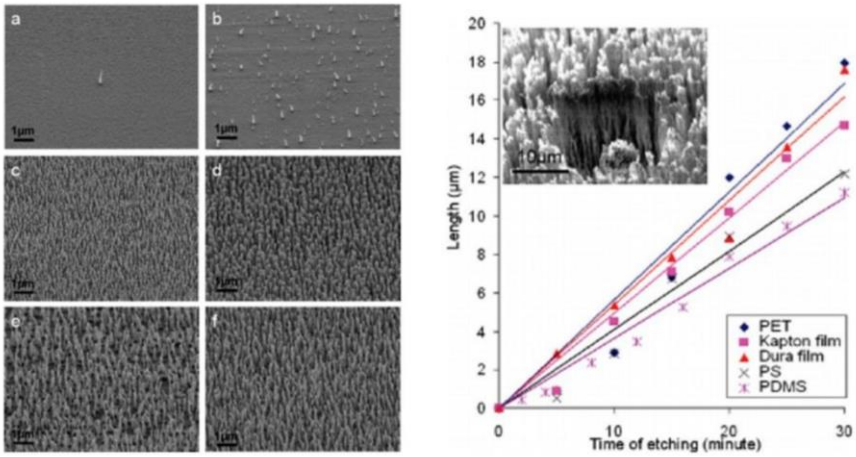


Figure 8. SEM images of the density-controlled fabrication of polymer nanowire (NW) arrays of Kapton by covering the initial surface with (**a**) 0.75; (**b**) 1.5; (**c**) 3; (**d**) 4.5; (**e**) 10; and (**f**) 15 nm of Au before inductively coupled plasma (ICP) etching. The graph represents the length-controlled growth of NWs of polyethylene terephthalate (PET), Kapton film, Durafilm, polystyrene (PS), and polydimethyl siloxane (PDMS). The inset is a SEM image of a NW array on Durafilm after 30 min of etching (Reproduced with permission from [128]. Copyright American Chemical Society, 2009).

In many of the presented examples, the surface nanostructuring is achieved by using an appropriate mask/template. Nevertheless, it was not necessary to introduce a mask prior to processing. A typical example is found where simultaneous plasma-enhanced reactive ion synthesis and etching (SPERISE) is employed. This technique was first used during the treatment of a Si wafer inside HBr-O_2 gas plasma (Figure 9a). In the primary step, the halogen species interact with the surface, and Si atoms are released into the vapor phase. This excited Si is then combined with the O and Br reactive species to form an etch-resistant silicon oxy bromide complex, which is deposited back on the surface. These deposits then act as masks and support the non-uniform etching on the surface. As a result of this processing, the mushroom-like Si NWs are formed, where an etch mask is left on the top (Figure 9b). The removal of the etch mask is done later with relatively simple mild chemical treatment [129].

Another application of plasma selective etching includes the study of filler dispersion inside the composite matrix. The filler dispersion inside the polymer matrix is the deciding factor for its bulk properties including ductility, hardness, impact resistance, *etc*. Conventional methods such as cryogenic breaking are generally used to monitor the dispersion of the fillers [130,131]. However, this method lacks precision for the determination of dispersion due to the possible displacement of the fillers during the distortion of the matrix. To overcome this, dissociated plasma etching is applied where the surface polymer layer is selectively removed to expose the embedded fillers. A fast and selective removal of the surface polymer from the composite materials including powder coatings and paint films with the dissociated oxygen plasma followed by SEM imaging enables the monitoring of the filler dispersion [132–135]. The same strategy allowed for the optimization of the bonding process efficiency of powder coatings with other materials, where bonding is enabled through disclosed but still embedded fillers. Due to the inhomogeneity in the plasma etching of various components inside the composite material, the resulting surface acquires relatively high surface roughness due to the exposed fillers. Along with suitable plasma functionalities, increased surface roughness is gained, which additionally improves the metallization of the surface [136,137]. Similarly, the fabrication of counter electrodes for solar cell application was done from a PP/CNT nanocomposite, where O_2 plasma reactive ion etching was used to remove the thick protruding layer of PP on the surface to expose the embedded CNTs. As a result, the charge transfer resistance of the composite surface is diminished to much lower values [138].

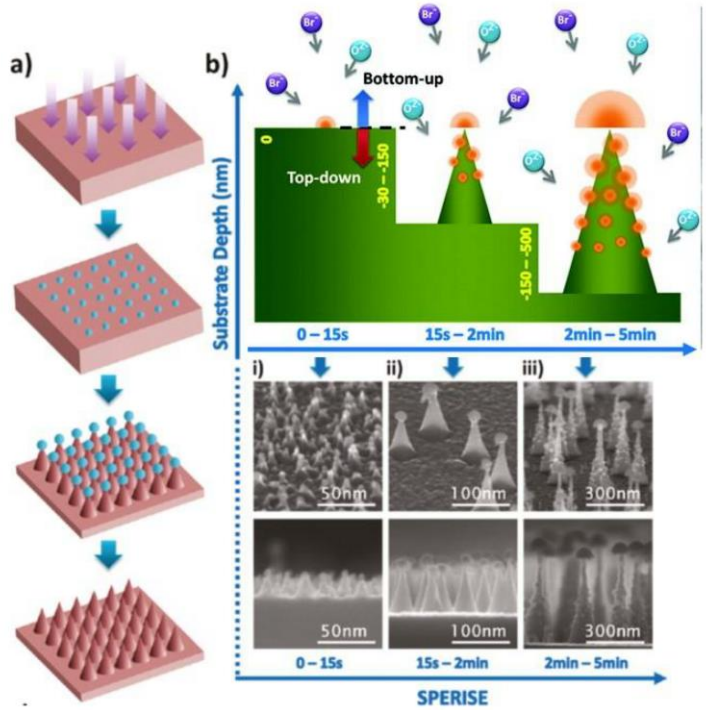


Figure 9. Simultaneous plasma enhanced reactive ion synthesis and etching (SPERISE) process and Si nanocone formation mechanism. (**a**) Process flow of the nanomanufacturing process: Pseudo randomly distributed silicon oxybromide nanodots are synthesized on the planar silicon substrate surface in the first few seconds of the SPERISE process. The oxide nanodots grow to hemispheres by a phase-transition nucleation process and act as a protective nanomask for the simultaneous reactive ion etching of the silicon underneath. Depending on the growth rate of the oxide hemispheres and the crystalline structures of the silicon substrates, nanocones with different aspect ratios are formed. The silicon oxybromide nanohemispheres on top of the nanocones are removed by wet etching; (**b**) Detailed schematic drawing of the three typical stages in the SPERISE process: Bromine and oxygen reactive ions interact with silicon to form synthesized oxide hemisphere and dots (orange) and etched silicon cone structure (green). Both the illustrations and corresponding SEM images at (i) 0–15 s; (ii) 15 s–2 min; and (iii) 2–5 min in the SPERISE process manifest this unique nanomanufacturing method (Reproduced with permission from [129]. Copyright American Chemical Society, 2011).

The applications of plasma selective etching are further extended for achieving improved bio- and chemo-sensing properties of semiconducting materials. As shown in one recent report, the gas-sensing properties of a composite membrane prepared by electrospinning process from the aq. solution of polyvilnyl alcohol (PVA) and SnO_2 was improved by O_2 plasma treatment. The resulting SnO_2 material showed a notable sensing response towards very low concentrations of ethanol vapor (~1 ppb). The enhanced sensitivity was featured because of the high specific surface area of the ripple-like structures obtained after plasma treatment followed by annealing at 500 °C [139]. However, the metal oxide nanodevices are less preferred due to their inability to operate at room temperature for sensing applications that could be replaced by conducting polymers, carbon allotropes or their suitable composites [140–142]. The sensing ability of such materials, especially in the context polymeric composites are further improved by plasma modification of the surface. As demonstrated by Raghu and co-workers, plasma modifications of the MWCNT composite with conducting polymers indicated greater effects on sensitivity and selectivity towards various volatile organic compounds [143]. However, a better understanding of how plasma improves the sensitivity and selectivity is still to be studied extensively for improving the sensor properties. While in the case of bio-sensors, the

sensitivity is found to be controlled by the covalent attachment of the bio-molecule to the sensing material. For this application, the removal of the polymer matrix and the functionalization of the exposed MWCNTs on the surface of a pristine PS/MWCNT composite yielded an opportunity to covalently attach antibodies and to fabricate advanced immunosensors [144].

One of the most recent applications of plasma chemical etching was the improvement of the insulation properties of polymeric composites. The insulating properties of various polymeric materials are standardized in terms of comparative tracking index (CTI) as per international electrotechnical commission (IEC) grading. The origin of poor insulating properties of composite materials is an aftereffect of the polymer charring on the surface at a high voltage electric arc. This issue is commonly tackled by adding suitable fillers, which forms little or no char on the surface [145]. However, this is inadequate due to the thin polymer layer on top of the embedded fillers. The simplest solution to overcome this situation is the selective removal of the surface polymer layer by an optimized plasma discharge. The cold O_2 plasma removal of the surface polymer from the glass embedded phenolic resin composite was demonstrated to improve CTI performances up to 56% (Figure 10) [101]. The performance level increased with the decrease in the surface polymer content along the prolonged plasma treatment times.

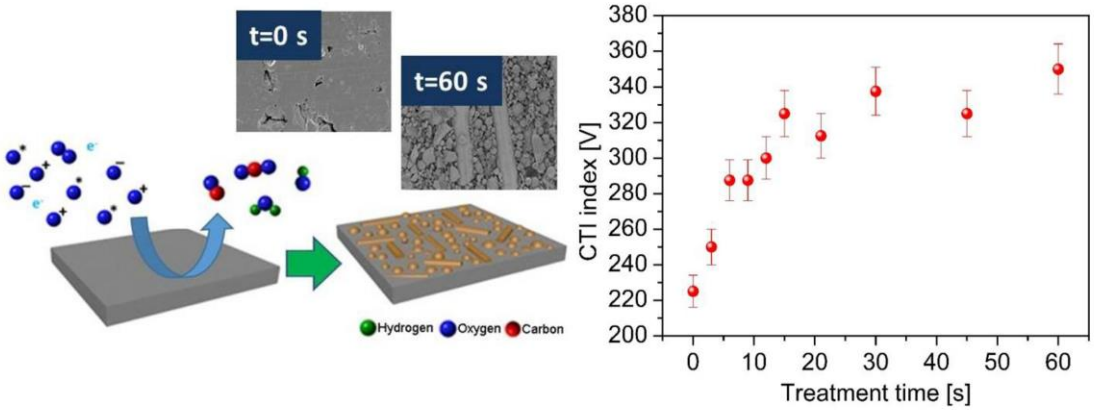


Figure 10. Plasma surface interaction of the glass-filled composite with corresponding SEM images for non-treated and plasma-treated samples for 60 s. The graph represents the variation of comparative tracking index (CTI) performance with plasma exposure time (Reproduced with permission from [101]. Copyright Royal Society of Chemistry, 2015, Year.").

6. Conclusions and Research Challenges to Tackle

This review attempted to outline the interdisciplinary applications of plasma etching and the selective etching of polymer-based materials from different branches of science. Moreover, it looks at the origin of selectivity and attempts to find answers bringing together an understanding of plasma properties with very diverse results of plasma–surface interactions through the note to nanomaterials. Among various plasma modifications, neutral dense and ion free cold plasmas are have been found to be efficient, especially for treating delicate polymeric and biomaterials to avoid unwanted surface damages and thermal effects. The plasma-induced functionalization and etching of polymer substrates is preferred to wet chemical etching and UV irradiation for designing the surface chemistry, surface morphology, and surface energy. These plasma induced modifications enable the attachment of various materials and biomolecules onto the surface. Additionally, plasma-induced hydrophobization of the surface can effectively increase the water-resistant behavior of the surface to improve anti-aging, anti-fouling, and corrosion-resistant properties. Such improvements in the surface properties are directly connected to structural and morphological changes.

The high-energy particles inside the plasma are able to distinguish various bond types under controlled process parameters. Utilizing the difference in the chemical stability of various bond types on the same molecule, delicate materials such as GNRs have been fabricated. The comparison of etching rate for different classes of polymeric materials has revealed that the difference in the etch rate is connected with both physical and chemical properties of the material. The presence of aromatic moieties has reduced the etching rate by radical quenching, whereas the surface cross-linking has reduced the etching rate for branched polymers. Generally, the etch rates are lower for hydrocarbon polymers compared to functionalized macromolecules. Additionally, a higher extension of crystallinity has reduced the plasma etch rates for various polymers, presented through reports on a few examples, namely, PET, LDPE, and HDPE. Thus, existing differences in the etching rates for various polymeric substrates have been employed in the surface structuring of block copolymers in applications, especially for the semiconductor industry. The pronounced applications of plasma selective etching of composite materials have been found to be efficient for reducing the dimensionalities of materials such as CNT or graphene sheets for advanced applications in electronics, electrical, and sensing devises. Furthermore, the preferential etching of composite surfaces has been effectively used for a simple and low-cost synthesis of polymer NWs with a controlled aspect ratio.

The plasma etching rate and etching selectivity of micro/macro molecules are well connected with the strength of the available bonds in the material. However, the side reactions such as radical quenching and surface cross-linking significantly affect the etching rate. Thus, the optimization of the process parameters is essential for achieving etching selectivity in different systems. Plasma is used as a single operating tool in only one/a few step(s) throughout multistep processes for demanding applications. More frequently used plasma has been found as one of the steps in multi-processing. This is clearly visible in many of the discussed examples, including the synthesis of GNR, graphene nanomesh, patterning the surface of block copolymers, *etc*. In some of the presented examples, the involved wet chemistry had slight adverse effects on the properties of the final product. An additional challenge in front of the plasma community is the pinpoint control of various plasma species and their reactions on the atomic or molecular level. Such developments are important, especially for such remarkable applications as plasma nanoscience and plasma medicine.

Acknowledgments: This work was partially funded by the Slovenian Research Agency (ARRS) projects L2-6769 and program P2-0082. Harinarayanan Puliyalil would like to thank G. Filipič for valuable discussions, and the Jožef Stefan International Postgraduate School (MPŠ) for the grant from the Innovative Scheme for Research.

Conflicts of Interest: The authors declare no conflict of interest. The founding sponsors had no role in the design of the study; in the collection, analyses, or interpretation of data; in the writing of the manuscript, and in the decision to publish the results.

References

1. Ostrikov, K.; Cvelbar, U.; Murphy, A.B. Plasma nanoscience: Setting directions, tackling grand challenges. *J. Phys. D* **2011**, *44*. [CrossRef]
2. Zhang, Z.; Han, S.; Wang, C.; Li, J.; Xu, G. Single-walled carbon nanohorns for energy applications. *Nanomaterials* **2015**, *5*, 1732–1755. [CrossRef]
3. Bo, Z.; Yang, Y.; Chen, J.; Yu, K.; Yan, J.; Cen, K. Plasma-enhanced chemical vapor deposition synthesis of vertically oriented graphene nanosheets. *Nanoscale* **2013**, *5*, 5180–5204. [CrossRef] [PubMed]
4. Filipič, G.; Cvelbar, U. Copper oxide nanowires: A review of growth. *Nanotechnology* **2012**, *23*. [CrossRef] [PubMed]
5. Guo, S.; Dong, S. Graphene nanosheet: Synthesis, molecular engineering, thin film, hybrids, and energy and analytical applications. *Chem. Soc. Rev.* **2011**, *40*, 2644–2672. [CrossRef] [PubMed]
6. Ashik, U.P.M.; Wan Daud, W.M.A.; Abbas, H.F. Production of greenhouse gas free hydrogen by thermocatalytic decomposition of methane—A review. *Renew. Sustain. Energy Rev.* **2015**, *44*, 221–256. [CrossRef]

7. Mariotti, D.; Mitra, S.; Svrcek, V. Surface-engineered silicon nanocrystals. *Nanoscale* **2013**, *5*, 1385–1398. [CrossRef] [PubMed]
8. Park, S.H.; Chae, J.; Cho, M.-H.; Kim, J.H.; Yoo, K.-H.; Cho, S.W.; Kim, T.G.; Kim, J.W. High concentration of nitrogen doped into graphene using N_2 plasma with an aluminum oxide buffer layer. *J. Mater. Chem. C* **2014**, *2*, 933–939. [CrossRef]
9. Meena, J.S.; Chu, M.-C.; Chang, Y.-C.; You, H.-C.; Singh, R.; Liu, P.-T.; Shieh, H.-P.D.; Chang, F.-C.; Ko, F.-H. Effect of oxygen plasma on the surface states of ZnO films used to produce thin-film transistors on soft plastic sheets. *J. Mater. Chem. C* **2013**, *1*, 6613–6622. [CrossRef]
10. Pumera, M. Heteroatom modified graphenes: Electronic and electrochemical applications. *J. Mater. Chem. C* **2014**, *2*, 6454–6461. [CrossRef]
11. Kumar, A.; Ann Lin, P.; Xue, A.; Hao, B.; Khin Yap, Y.; Sankaran, R.M. Formation of nanodiamonds at near-ambient conditions via microplasma dissociation of ethanol vapour. *Nat. Commun.* **2013**, *4*. [CrossRef] [PubMed]
12. Attri, P.; Arora, B.; Choi, E.H. Utility of plasma: A new road from physics to chemistry. *RSC Adv.* **2013**, *3*, 12540–12567. [CrossRef]
13. Meyyappan, M. A review of plasma enhanced chemical vapour deposition of carbon nanotubes. *J. Phys. D* **2009**, *42*. [CrossRef]
14. Meyyappan, M. Plasma nanotechnology: Past, present and future. *J. Phys. D* **2011**, *44*. [CrossRef]
15. Vasilev, K.; Griesser, S.S.; Griesser, H.J. Antibacterial surfaces and coatings produced by plasma techniques. *Plasma Process. Polym.* **2011**, *8*, 1010–1023. [CrossRef]
16. Aria, A.I.; Lyon, B.J.; Gharib, M. Morphology engineering of hollow carbon nanotube pillars by oxygen plasma treatment. *Carbon* **2015**, *81*, 376–387. [CrossRef]
17. Coburn, J.W.; Winters, H.F. Ion- and electron-assisted gas-surface chemistry—An important effect in plasma etching. *J. Appl. Phys.* **1979**, *50*, 3189–3196. [CrossRef]
18. Denes, F.S.; Manolache, S. Macromolecular plasma-chemistry: An emerging field of polymer science. *Prog. Polym. Sci.* **2004**, *29*, 815–885. [CrossRef]
19. Bohlmark, J.; Lattemann, M.; Gudmundsson, J.T.; Ehiasarian, A.P.; Aranda Gonzalvo, Y.; Brenning, N.; Helmersson, U. The ion energy distributions and ion flux composition from a high power impulse magnetron sputtering discharge. *Thin Solid Films* **2006**, *515*, 1522–1526. [CrossRef]
20. Smith, T. Sputter cleaning and etching of crystal surfaces (Ti, W, Si) monitored by auger spectroscopy, ellipsometry and work function change. *Surf. Sci.* **1971**, *27*, 45–59. [CrossRef]
21. Oehrlein, G.S. Reactive-ion etching. *Phys. Today* **1986**, *39*, 26–33. [CrossRef]
22. Lee, H.; Oberman, D.B.; Harris, J.S. Reactive ion etching of GaN using CHF_3/Ar and C_2ClF_5/Ar plasmas. *Appl. Phys. Lett.* **1995**, *67*, 1754–1756. [CrossRef]
23. Levchenko, I.; Keidar, M.; Xu, S.; Kersten, H.; Ostrikov, K. Low-temperature plasmas in carbon nanostructure synthesis. *J. Vac. Sci. Technol. B* **2013**, *31*. [CrossRef]
24. Ostrikov, K.; Levchenko, I.; Cvelbar, U.; Sunkara, M.; Mozetic, M. From nucleation to nanowires: A single-step process in reactive plasmas. *Nanoscale* **2010**, *2*, 2012–2027. [CrossRef] [PubMed]
25. Tachi, S.; Tsujimoto, K.; Okudaira, S. Low-temperature reactive ion etching and microwave plasma etching of silicon. *Appl. Phys. Lett.* **1988**, *52*, 616–618. [CrossRef]
26. Coburn, J.W.; Winters, H.F. Conductance considerations in the reactive ion etching of high aspect ratio features. *Appl. Phys. Lett.* **1989**, *55*, 2730–2732. [CrossRef]
27. Cybart, S.A.; Roediger, P.; Ulin-Avila, E.; Wu, S.M.; Wong, T.J.; Dynes, R.C. Nanometer scale high-aspect-ratio trench etching at controllable angles using ballistic reactive ion etching. *J. Vac. Sci. Technol. B* **2013**, *31*. [CrossRef]
28. Zeze, D.A.; Cox, D.C.; Weiss, B.L.; Silva, S.R.P. Lithography-free high aspect ratio submicron quartz columns by reactive ion etching. *Appl. Phys. Lett.* **2004**, *84*, 1362–1364. [CrossRef]
29. Mozetič, M.; Vesel, A.; Monna, V.; Ricard, A. H density in a hydrogen plasma post-glow reactor. *Vacuum* **2003**, *71*, 201–205. [CrossRef]
30. Filipič, G.; Baranov, O.; Mozetič, M.; Ostrikov, K.; Cvelbar, U. Uniform surface growth of copper oxide nanowires in radiofrequency plasma discharge and limiting factors. *Phys. Plasmas (1994-Present)* **2014**, *21*. [CrossRef]

31. Wang, A.; Qin, M.; Guan, J.; Wang, L.; Guo, H.; Li, X.; Wang, Y.; Prins, R.; Hu, Y. The synthesis of metal phosphides: Reduction of oxide precursors in a hydrogen plasma. *Angew. Chem.* **2008**, *120*, 6141–6143. [CrossRef]
32. Vratnica, Z.; Vujosevic, D.; Cvelbar, U.; Mozetic, M. Degradation of bacteria by weakly ionized highly dissociated radio-frequency oxygen plasma. *IEEE Trans. Plasma Sci.* **2008**, *36*, 1300–1301. [CrossRef]
33. Vesel, A.; Mozetic, M. Surface functionalization of organic materials by weakly ionized highly dissociated oxygen plasma. *J. Phys. Conf. Ser.* **2009**, *162*. [CrossRef]
34. Hartney, M.A.; Greene, W.M.; Soane, D.S.; Hess, D.W. Mechanistic studies of oxygen plasma etching. *J. Vac. Sci. Technol. B* **1988**, *6*, 1892–1895. [CrossRef]
35. Pearton, S.J.; Norton, D.P. Dry etching of electronic oxides, polymers, and semiconductors. *Plasma Process. Polym.* **2005**, *2*, 16–37. [CrossRef]
36. Filipič, G.; Baranov, O.; Mozetič, M.; Cvelbar, U. Growth dynamics of copper oxide nanowires in plasma at low pressures. *J. Appl. Phys.* **2015**, *117*. [CrossRef]
37. Cvelbar, U. Interaction of non-equilibrium oxygen plasma with sintered graphite. *Appl. Surf. Sci.* **2013**, *269*, 33–36. [CrossRef]
38. Cvelbar, U.; Mozetič, M.; Junkar, I.; Vesel, A.; Kovač, J.; Drenik, A.; Vrlinič, T.; Hauptman, N.; Klanjšek-Gunde, M.; Markoli, B.; *et al.* Oxygen plasma functionalization of poly(*p*-phenilene sulphide). *Appl. Surf. Sci.* **2007**, *253*, 8669–8673. [CrossRef]
39. Wang, K.; Zhang, X.; Zhang, X.; Yang, B.; Li, Z.; Zhang, Q.; Huang, Z.; Wei, Y. Fabrication of cross-linked fluorescent polymer nanoparticles and their cell imaging applications. *J. Mater. Chem. C* **2015**, *3*, 1854–1860. [CrossRef]
40. Tsougeni, K.; Papageorgiou, D.; Tserepi, A.; Gogolides, E. "Smart" polymeric microfluidics fabricated by plasma processing: Controlled wetting, capillary filling and hydrophobic valving. *Lab Chip* **2010**, *10*, 462–469. [CrossRef] [PubMed]
41. Yang, X.; Zhou, G.; Wong, W.-Y. Recent design tactics for high performance white polymer light-emitting diodes. *J. Mater. Chem. C* **2014**, *2*, 1760–1778. [CrossRef]
42. Uysal Unalan, I.; Cerri, G.; Marcuzzo, E.; Cozzolino, C.A.; Farris, S. Nanocomposite films and coatings using inorganic nanobuilding blocks (NBB): Current applications and future opportunities in the food packaging sector. *RSC Adv.* **2014**, *4*, 29393–29428. [CrossRef]
43. Vlachopoulou, M.-E.; Kokkoris, G.; Cardinaud, C.; Gogolides, E.; Tserepi, A. Plasma etching of poly(dimethylsiloxane): Roughness formation, mechanism, control, and application in the fabrication of microfluidic structures. *Plasma Process. Polym.* **2013**, *10*, 29–40. [CrossRef]
44. Jacobs, T.; De Geyter, N.; Morent, R.; Desmet, T.; Dubruel, P.; Leys, C. Plasma treatment of polycaprolactone at medium pressure. *Surf. Coat. Technol.* **2011**, *205*, S543–S547. [CrossRef]
45. Charbonnier, M.; Romand, M. Polymer pretreatments for enhanced adhesion of metals deposited by the electroless process. *Int. J. Adhes. Adhes.* **2003**, *23*, 277–285. [CrossRef]
46. Yu, H.-D.; Regulacio, M.D.; Ye, E.; Han, M.-Y. Chemical routes to top-down nanofabrication. *Chem. Soc. Rev.* **2013**, *42*, 6006–6018. [CrossRef] [PubMed]
47. Pochner, K.; Beil, S.; Horn, H.; Blömer, M. Treatment of polymers for subsequent metallization using intense UV radiation or plasma at atmospheric pressure. *Surf. Coat. Technol.* **1997**, *97*, 372–377. [CrossRef]
48. Pascu, M.; Debarnot, D.; Durand, S.; Poncin-Epaillard, F. Surface modification of pvdf by microwave plasma treatment for electroless metallization. In *Plasma Processes and Polymers*; Wiley-VCH Verlag GmbH & Co. KGaA: Weinheim, Germany, 2005; pp. 157–176.
49. Macková, A.; Švorčík, V.; Strýhal, Z.; Pavlík, J. RBS and AFM study of Ag and Au diffusion into pet foils influenced by plasma treatment. *Surf. Interface Anal.* **2006**, *38*, 335–338. [CrossRef]
50. Lin, Y.S.; Liu, H.M. Enhanced adhesion of plasma-sputtered copper films on polyimide substrates by oxygen glow discharge for microelectronics. *Thin Solid Films* **2008**, *516*, 1773–1780. [CrossRef]
51. Li, W.T.; Charters, R.B.; Luther-Davies, B.; Mar, L. Significant improvement of adhesion between gold thin films and a polymer. *Appl. Surf. Sci.* **2004**, *233*, 227–233. [CrossRef]
52. Zille, A.; Fernandes, M.M.; Francesko, A.; Tzanov, T.; Fernandes, M.; Oliveira, F.R.; Almeida, L.; Amorim, T.; Carneiro, N.; Esteves, M.F.; *et al.* Size and aging effects on antimicrobial efficiency of silver nanoparticles coated on polyamide fabrics activated by atmospheric DBD plasma. *ACS Appl. Mater. Interfaces* **2015**, *7*, 13731–13744. [CrossRef] [PubMed]

53. Boyd, R.D.; Kenwright, A.M.; Badyal, J.P.S.; Briggs, D. Atmospheric nonequilibrium plasma treatment of biaxially oriented polypropylene. *Macromolecules* **1997**, *30*, 5429–5436. [CrossRef]
54. Bazaka, K.; Jacob, M.V.; Crawford, R.J.; Ivanova, E.P. Plasma-assisted surface modification of organic biopolymers to prevent bacterial attachment. *Acta Biomater.* **2011**, *7*, 2015–2028. [CrossRef] [PubMed]
55. Poncin-Epaillard, F.; Brosse, J.C.; Falher, T. Cold plasma treatment: Surface or bulk modification of polymer films? *Macromolecules* **1997**, *30*, 4415–4420. [CrossRef]
56. Yasuda, H.; Gazicki, M. Biomedical applications of plasma polymerization and plasma treatment of polymer surfaces. *Biomaterials* **1982**, *3*, 68–77. [CrossRef]
57. Inglis, W.; Sanders, G.H.W.; Williams, P.M.; Davies, M.C.; Roberts, C.J.; Tendler, S.J.B. A simple method for biocompatible polymer based spatially controlled adsorption of blood plasma proteins to a surface. *Langmuir* **2001**, *17*, 7402–7405. [CrossRef]
58. Wang, H.; Kwok, D.T.K.; Wang, W.; Wu, Z.; Tong, L.; Zhang, Y.; Chu, P.K. Osteoblast behavior on polytetrafluoroethylene modified by long pulse, high frequency oxygen plasma immersion ion implantation. *Biomaterials* **2010**, *31*, 413–419. [CrossRef] [PubMed]
59. Oehr, C. Plasma surface modification of polymers for biomedical use. *Nucl. Instrum. Methods Phys. Res. Sect. B* **2003**, *208*, 40–47. [CrossRef]
60. Halfmann, H.; Bibinov, N.; Wunderlich, J.; Awakowicz, P. A double inductively coupled plasma for sterilization of medical devices. *J. Phys. D* **2007**, *40*. [CrossRef]
61. Vesel, A.; Kolar, M.; Stana-Kleinschek, K.; Mozetic, M. Etching rates of blood proteins, blood plasma and polymer in oxygen afterglow of microwave plasma. *Surf. Interface Anal.* **2014**, *46*, 1115–1118. [CrossRef]
62. Stoffels, E.; Flikweert, A.J.; Stoffels, W.W.; Kroesen, G.M.W. Plasma needle: A non-destructive atmospheric plasma source for fine surface treatment of (bio)materials. *Plasma Sources Sci. Technol.* **2002**, *11*. [CrossRef]
63. Herrmann, H.W.; Henins, I.; Park, J.; Selwyn, G.S. Decontamination of chemical and biological warfare (CBW) agents using an atmospheric pressure plasma jet (APPJ). *Phys. Plasmas* **1999**, *6*, 2284–2289. [CrossRef]
64. Lazović, S.; Puač, N.; Miletić, M.; Pavlica, D.; Jovanović, M.; Bugarski, D.; Mojsilović, S.; Maletić, D.; Malović, G.; Milenković, P.; *et al.* The effect of a plasma needle on bacteria in planktonic samples and on peripheral blood mesenchymal stem cells. *New J. Phys.* **2010**, *12*. [CrossRef]
65. Feng, L.; Li, S.; Li, Y.; Li, H.; Zhang, L.; Zhai, J.; Song, Y.; Liu, B.; Jiang, L.; Zhu, D. Super-hydrophobic surfaces: From natural to artificial. *Adv. Mater.* **2002**, *14*, 1857–1860. [CrossRef]
66. Zhang, X.; Shi, F.; Niu, J.; Jiang, Y.; Wang, Z. Superhydrophobic surfaces: From structural control to functional application. *J. Mater. Chem.* **2008**, *18*, 621–633. [CrossRef]
67. Erbil, H.Y.; Demirel, A.L.; Avcı, Y.; Mert, O. Transformation of a simple plastic into a superhydrophobic surface. *Science* **2003**, *299*, 1377–1380. [CrossRef] [PubMed]
68. Puliyalil, H.; Filipič, G.; Cvelbar, U. Recent advances in the methods for designing superhydrophobic surfaces. In *Surface Energy*; Aliofkhazraei, M., Ed.; InTech: Rijeka, Croatia, 2015; pp. 311–335.
69. Toma, M.; Loget, G.; Corn, R.M. Flexible teflon nanocone array surfaces with tunable superhydrophobicity for self-cleaning and aqueous droplet patterning. *ACS Appl. Mater. Interfaces* **2014**, *6*, 11110–11117. [CrossRef] [PubMed]
70. Tsougeni, K.; Vourdas, N.; Tserepi, A.; Gogolides, E.; Cardinaud, C. Mechanisms of oxygen plasma nanotexturing of organic polymer surfaces: From stable super hydrophilic to super hydrophobic surfaces. *Langmuir* **2009**, *25*, 11748–11759. [CrossRef] [PubMed]
71. Korshak, V.V.; Svetlana, V.V. Dependence of thermal stability of polymers on their chemical structure. *Russ. Chem. Rev.* **1968**, *37*, 885. [CrossRef]
72. Taylor, G.N.; Wolf, T.M. Oxygen plasma removal of thin polymer films. *Polym. Eng. Sci.* **1980**, *20*, 1087–1092. [CrossRef]
73. Moss, S.J.; Jolly, A.M.; Tighe, B.J. Plasma oxidation of polymers. *Plasma Chem. Plasma Process.* **1986**, *6*, 401–416. [CrossRef]
74. Zadok, E.; Sialom, B.; Mazur, Y. Oxygen atoms produced by microwave discharge: Reaction with arenes. *Angew. Chem. Int. Ed. Engl.* **1980**, *19*, 1004–1005. [CrossRef]
75. Zadok, E.; Rubinraut, S.; Frolow, F.; Mazur, Y. Reactions of di-, tri-, and hexamethylbenzenes with oxygen(3P) atoms in liquid and on adsorbed phases. *J. Am. Chem. Soc.* **1985**, *107*, 2489–2494. [CrossRef]
76. Xie, L.; Jiao, L.; Dai, H. Selective etching of graphene edges by hydrogen plasma. *J. Am. Chem. Soc.* **2010**, *132*, 14751–14753. [CrossRef] [PubMed]

77. Xiang, H.; Kan, E.; Wei, S.-H.; Whangbo, M.-H.; Yang, J. "Narrow" graphene nanoribbons made easier by partial hydrogenation. *Nano Lett.* **2009**, *9*, 4025–4030. [CrossRef] [PubMed]
78. Kerr, J.A. *Handbook of Bimolecular and Termolecular Gas Reactions*; Taylor & Francis: Boca Raton, FL, USA, 1987.
79. Mogab, C.J.; Adams, A.C.; Flamm, D.L. Plasma etching of Si and SiO_2—The effect of oxygen additions to CF_4 plasmas. *J. Appl. Phys.* **1978**, *49*, 3796–3803. [CrossRef]
80. Chun, I.; Efremov, A.; Yeom, G.Y.; Kwon, K.-H. A comparative study of $CF_4/O_2/Ar$ and $C_4F_8/O_2/Ar$ plasmas for dry etching applications. *Thin Solid Films* **2015**, *579*, 136–143. [CrossRef]
81. Hegemann, D.; Brunner, H.; Oehr, C. Plasma treatment of polymers for surface and adhesion improvement. *Nucl. Instrum. Methods Phys. Res. Sect. B* **2003**, *208*, 281–286. [CrossRef]
82. Wohlfart, E.; Fernández-Blázquez, J.P.; Knoche, E.; Bello, A.; Pérez, E.; Arzt, E.; del Campo, A. Nanofibrillar patterns by plasma etching: The influence of polymer crystallinity and orientation in surface morphology. *Macromolecules* **2010**, *43*, 9908–9917. [CrossRef]
83. Junkar, I.; Cvelbar, U.; Vesel, A.; Hauptman, N.; Mozetič, M. The role of crystallinity on polymer interaction with oxygen plasma. *Plasma Process. Polym.* **2009**, *6*, 667–675. [CrossRef]
84. Chernomordik, B.D.; Russel, H.B.; Cvelbar, U.; Jasinski, J.B.; Kumar, V.; Deutsch, T.; Sunkara, M.K. Photoelectrochemical activity of as-grown, α-Fe_2O_3 nanowire array electrodes for water splitting. *Nanotechnology* **2012**, *23*. [CrossRef] [PubMed]
85. Lazović, S.; Puač, N.; Spasić, K.; Malović, G.; Cvelbar, U.; Mozetič, M.; Radetić, M.; Petrović, Z.L. Plasma properties in a large-volume, cylindrical and asymmetric radio-frequency capacitively coupled industrial-prototype reactor. *J. Phys. D Appl. Phys.* **2013**, *46*. [CrossRef]
86. Olde Riekerink, M.B.; Terlingen, J.G.A.; Engbers, G.H.M.; Feijen, J. Selective etching of semicrystalline polymers: CF_4 gas plasma treatment of poly(ethylene). *Langmuir* **1999**, *15*, 4847–4856. [CrossRef]
87. Nair, L.G.; Mahapatra, A.S.; Gomathi, N.; Joseph, K.; Neogi, S.; Nair, C.P.R. Radio frequency plasma mediated dry functionalization of multiwall carbon nanotube. *Appl. Surf. Sci.* **2015**, *340*, 64–71. [CrossRef]
88. Black, C.T.; Guarini, K.W.; Milkove, K.R.; Baker, S.M.; Russell, T.P.; Tuominen, M.T. Integration of self-assembled diblock copolymers for semiconductor capacitor fabrication. *Appl. Phys. Lett.* **2001**, *79*, 409–411. [CrossRef]
89. Chuang, V.P.; Ross, C.A.; Gwyther, J.; Manners, I. Self-assembled nanoscale ring arrays from a polystyrene-*b*-polyferrocenylsilane-*b*-poly(2-vinylpyridine)triblock terpolymer thin film. *Adv. Mater.* **2009**, *21*, 3789–3793. [CrossRef]
90. Lammertink, R.G.H.; Hempenius, M.A.; van den Enk, J.E.; Chan, V.Z.H.; Thomas, E.L.; Vancso, G.J. Nanostructured thin films of organic–organometallic block copolymers: One-step lithography with poly(ferrocenylsilanes) by reactive ion etching. *Adv. Mater.* **2000**, *12*, 98–103.
91. Jung, Y.S.; Ross, C.A. Orientation-controlled self-assembled nanolithography using a polystyrene—Polydimethylsiloxane block copolymer. *Nano Lett.* **2007**, *7*, 2046–2050. [CrossRef] [PubMed]
92. Kim, S.Y.; Nunns, A.; Gwyther, J.; Davis, R.L.; Manners, I.; Chaikin, P.M.; Register, R.A. Large-area nanosquare arrays from shear-aligned block copolymer thin films. *Nano Lett.* **2014**, *14*, 5698–5705. [CrossRef] [PubMed]
93. Mozetič, M. Controlled oxidation of organic compounds in oxygen plasma. *Vacuum* **2003**, *71*, 237–240. [CrossRef]
94. Panda, S.; Economou, D.J.; Meyyappan, M. Effect of metastable oxygen molecules in high density power-modulated oxygen discharges. *J. Appl. Phys.* **2000**, *87*, 8323–8333. [CrossRef]
95. Dai, L.; Griesser, H.J.; Mau, A.W.H. Surface modification by plasma etching and plasma patterning. *J. Phys. Chem. B* **1997**, *101*, 9548–9554. [CrossRef]
96. Chen, F.F.; Smith, M.D. Plasma. In *Van Nostrand's Scientific Encyclopedia*; John Wiley & Sons, Inc.: Hoboken, NJ, USA, 2005. [CrossRef]
97. Donnelly, V.M.; Kornblit, A. Plasma etching: Yesterday, today, and tomorrow. *J. Vac. Sci. Technol. A* **2013**, *31*. [CrossRef]
98. Mozetič, M.; Ostrikov, K.; Ruzic, D.N.; Curreli, D.; Cvelbar, U.; Vesel, A.; Primc, G.; Leisch, M.; Jousten, K.; Malyshev, O.B.; *et al.* Recent advances in vacuum sciences and applications. *J. Phys. D* **2014**, *47*. [CrossRef]
99. Kontziampasis, D.; Constantoudis, V.; Gogolides, E. Plasma directed organization of nanodots on polymers: Effects of polymer type and etching time on morphology and order. *Plasma Process. Polym.* **2012**, *9*, 866–872. [CrossRef]

100. Vourdas, N.; Kontziampasis, D.; Kokkoris, G.; Constantoudis, V.; Goodyear, A.; Tserepi, A.; Cooke, M.; Gogolides, E. Plasma directed assembly and organization: Bottom-up nanopatterning using top-down technology. *Nanotechnology* **2010**, *21*. [CrossRef] [PubMed]
101. Puliyalil, H.; Cvelbar, U.; Filipic, G.; Petric, A.D.; Zaplotnik, R.; Recek, N.; Mozetic, M.; Thomas, S. Plasma as a tool for enhancing insulation properties of polymer composites. *RSC Adv.* **2015**, *5*, 37853–37858. [CrossRef]
102. El-Aguizy, T.A.; Jeong, J.-H.; Jeon, Y.-B.; Li, W.Z.; Ren, Z.F.; Kim, S.-G. Transplanting carbon nanotubes. *Appl. Phys. Lett.* **2004**, *85*, 5995–5997. [CrossRef]
103. Che, Y.; Wang, C.; Liu, J.; Liu, B.; Lin, X.; Parker, J.; Beasley, C.; Wong, H.S.P.; Zhou, C. Selective synthesis and device applications of semiconducting single-walled carbon nanotubes using isopropyl alcohol as feedstock. *ACS Nano* **2012**, *6*, 7454–7462. [CrossRef] [PubMed]
104. Hou, P.-X.; Li, W.-S.; Zhao, S.-Y.; Li, G.-X.; Shi, C.; Liu, C.; Cheng, H.-M. Preparation of metallic single-wall carbon nanotubes by selective etching. *ACS Nano* **2014**, *8*, 7156–7162. [CrossRef] [PubMed]
105. Zhang, G.; Qi, P.; Wang, X.; Lu, Y.; Li, X.; Tu, R.; Bangsaruntip, S.; Mann, D.; Zhang, L.; Dai, H. Selective etching of metallic carbon nanotubes by gas-phase reaction. *Science* **2006**, *314*, 974–977. [CrossRef] [PubMed]
106. Di, C.-A.; Wei, D.; Yu, G.; Liu, Y.; Guo, Y.; Zhu, D. Patterned graphene as source/drain electrodes for bottom-contact organic field-effect transistors. *Adv. Mater.* **2008**, *20*, 3289–3293. [CrossRef]
107. Liao, Z.; Wan, Q.; Liu, H.; Tang, Q. Realization of size controllable graphene micro/nanogap with a micro/nanowire mask method for organic field-effect transistors. *Appl. Phys. Lett.* **2011**, *99*. [CrossRef]
108. Jiang, L.; Fan, Z. Design of advanced porous graphene materials: From graphene nanomesh to 3d architectures. *Nanoscale* **2014**, *6*, 1922–1945. [CrossRef] [PubMed]
109. Song, X.; Hu, J.; Zeng, H. Two-dimensional semiconductors: Recent progress and future perspectives. *J. Mater. Chem. C* **2013**, *1*, 2952–2969. [CrossRef]
110. Zang, J.; Ryu, S.; Pugno, N.; Wang, Q.; Tu, Q.; Buehler, M.J.; Zhao, X. Multifunctionality and control of the crumpling and unfolding of large-area graphene. *Nat. Mater.* **2013**, *12*, 321–325. [CrossRef] [PubMed]
111. Zeng, Z.; Huang, X.; Yin, Z.; Li, H.; Chen, Y.; Li, H.; Zhang, Q.; Ma, J.; Boey, F.; Zhang, H. Fabrication of graphene nanomesh by using an anodic aluminum oxide membrane as a template. *Adv. Mater.* **2012**, *24*, 4138–4142. [CrossRef] [PubMed]
112. Kim, M.; Safron, N.S.; Han, E.; Arnold, M.S.; Gopalan, P. Fabrication and characterization of large-area, semiconducting nanoperforated graphene materials. *Nano Lett.* **2010**, *10*, 1125–1131. [CrossRef] [PubMed]
113. Ding, J.; Du, K.; Wathuthanthri, I.; Choi, C.-H.; Fisher, F.T.; Yang, E.-H. Transfer patterning of large-area graphene nanomesh via holographic lithography and plasma etching. *J. Vac. Sci. Technol. Technol. B* **2014**, *32*. [CrossRef]
114. Sinitskii, A.; Tour, J.M. Patterning graphene through the self-assembled templates: Toward periodic two-dimensional graphene nanostructures with semiconductor properties. *J. Am. Chem. Soc.* **2010**, *132*, 14730–14732. [CrossRef] [PubMed]
115. Liang, X.; Jung, Y.-S.; Wu, S.; Ismach, A.; Olynick, D.L.; Cabrini, S.; Bokor, J. Formation of bandgap and subbands in graphene nanomeshes with sub-10 nm ribbon width fabricated via nanoimprint lithography. *Nano Lett.* **2010**, *10*, 2454–2460. [CrossRef] [PubMed]
116. Paul, R.K.; Badhulika, S.; Saucedo, N.M.; Mulchandani, A. Graphene nanomesh as highly sensitive chemiresistor gas sensor. *Anal. Chem.* **2012**, *84*, 8171–8178. [CrossRef] [PubMed]
117. Fatyeyeva, K.; Dahi, A.; Chappey, C.; Langevin, D.; Valleton, J.-M.; Poncin-Epaillard, F.; Marais, S. Effect of cold plasma treatment on surface properties and gas permeability of polyimide films. *RSC Adv.* **2014**, *4*, 31036–31046. [CrossRef]
118. Zarshenas, K.; Raisi, A.; Aroujalian, A. Surface modification of polyamide composite membranes by corona air plasma for gas separation applications. *RSC Adv.* **2015**, *5*, 19760–19772. [CrossRef]
119. Chen, S.-H.; Chuang, W.-H.; Wang, A.A.; Ruaan, R.-C.; Lai, J.-Y. Oxygen/nitrogen separation by plasma chlorinated polybutadiene/polycarbonate composite membrane. *J. Membr. Sci.* **1997**, *124*, 273–281. [CrossRef]
120. Chen, Z.; Tan, X. Monolithic fabrication of ionic polymer–metal composite actuators capable of complex deformation. *Sens. Actuators A* **2010**, *157*, 246–257. [CrossRef]
121. Nikhil Dilip, P.; Mark, S.M. An investigation of the fracturing process in nitrogen-doped multiwalled carbon nanotubes (N-MWCNTs). Evidence for directional unzipping. *Mater. Res. Express* **2014**, *1*. [CrossRef]

122. Jiao, L.; Zhang, L.; Wang, X.; Diankov, G.; Dai, H. Narrow graphene nanoribbons from carbon nanotubes. *Nature* **2009**, *458*, 877–880. [CrossRef] [PubMed]
123. Poulsen, R.G. Plasma etching in integrated circuit manufacture—A review. *J. Vac. Sci. Technol.* **1977**, *14*, 266–274. [CrossRef]
124. Vitale, S.A.; Berry, S. Etching selectivity of indium tin oxide to photoresist in high density chlorine- and ethylene-containing plasmas. *J. Vac. Sci. Technol. B* **2013**, *31*. [CrossRef]
125. Laermer, F.; Urban, A. Challenges, developments and applications of silicon deep reactive ion etching. *Microelectron. Eng.* **2003**, *67–68*, 349–355. [CrossRef]
126. Liao, Q.; Xu, Z.; Zhong, X.; Dang, W.; Shi, Q.; Zhang, C.; Weng, Y.; Li, Z.; Fu, H. An organic nanowire waveguide exciton-polariton sub-microlaser and its photonic application. *J. Mater. Chem. C* **2014**, *2*, 2773–2778. [CrossRef]
127. Garcia-Frutos, E.M. Small organic single-crystalline one-dimensional micro- and nanostructures for miniaturized devices. *J. Mater. Chem. C* **2013**, *1*, 3633–3645. [CrossRef]
128. Fang, H.; Wu, W.; Song, J.; Wang, Z.L. Controlled growth of aligned polymer nanowires. *J. Phys. Chem. C* **2009**, *113*, 16571–16574. [CrossRef]
129. Chen, Y.; Xu, Z.; Gartia, M.R.; Whitlock, D.; Lian, Y.; Liu, G.L. Ultrahigh throughput silicon nanomanufacturing by simultaneous reactive ion synthesis and etching. *ACS Nano* **2011**, *5*, 8002–8012. [CrossRef] [PubMed]
130. Chandran, N.; Chandran, S.; Maria, H.J.; Thomas, S. Compatibilizing action and localization of clay in a polypropylene/natural rubber (PP/NR) blend. *RSC Adv.* **2015**, *5*, 86265–86273. [CrossRef]
131. Jyotishkumar, P.; Koetz, J.; Tiersch, B.; Strehmel, V.; Özdilek, C.; Moldenaers, P.; Hässler, R.; Thomas, S. Complex phase separation in poly(acrylonitrile−butadiene−styrene)-modified epoxy/4,4′-diaminodiphenyl sulfone blends: Generation of new micro- and nanosubstructures. *J. Phys. Chem. B* **2009**, *113*, 5418–5430. [CrossRef] [PubMed]
132. Kunaver, M.; Mozetič, M.; Klanjšek-Gunde, M. Selective plasma etching of powder coatings. *Thin Solid Films* **2004**, *459*, 115–117. [CrossRef]
133. Kunaver, M.; Klanjsek-Gunde, M.; Mozetic, M.; Kunaver, M.; Hrovat, A. The degree of dispersion of pigments in powder coatings and the origin of some surface defects. *Surf. Coat. Int. Part B* **2003**, *86*, 175–179. [CrossRef]
134. Mozetič, M.; Zalar, A.; Panjan, P.; Bele, M.; Pejovnik, S.; Grmek, R. A method of studying carbon particle distribution in paint films. *Thin Solid Films* **2000**, *376*, 5–8. [CrossRef]
135. Salalha, W.; Dror, Y.; Khalfin, R.L.; Cohen, Y.; Yarin, A.L.; Zussman, E. Single-walled carbon nanotubes embedded in oriented polymeric nanofibers by electrospinning. *Langmuir* **2004**, *20*, 9852–9855. [CrossRef] [PubMed]
136. Ponnamma, D.; Sadasivuni, K.K.; Grohens, Y.; Guo, Q.; Thomas, S. Carbon nanotube based elastomer composites—An approach towards multifunctional materials. *J. Mater. Chem. C* **2014**, *2*, 8446–8485. [CrossRef]
137. Cvelbar, U.; Pejovnik, S.; Mozetiè, M.; Zalar, A. Increased surface roughness by oxygen plasma treatment of graphite/polymer composite. *Appl. Surf. Sci.* **2003**, *210*, 255–261. [CrossRef]
138. Malara, F.; Manca, M.; De Marco, L.; Pareo, P.; Gigli, G. Flexible carbon nanotube-based composite plates as efficient monolithic counter electrodes for dye solar cells. *ACS Appl. Mater. Interfaces* **2011**, *3*, 3625–3632. [CrossRef] [PubMed]
139. Zhang, Y.; Li, J.; An, G.; He, X. Highly porous SnO_2 fibers by electrospinning and oxygen plasma etching and its ethanol-sensing properties. *Sens. Actuators B* **2010**, *144*, 43–48. [CrossRef]
140. Ramgir, N.; Datta, N.; Kaur, M.; Kailasaganapathi, S.; Debnath, A.K.; Aswal, D.K.; Gupta, S.K. Metal oxide nanowires for chemiresistive gas sensors: Issues, challenges and prospects. *Colloids Surf. A* **2013**, *439*, 101–116. [CrossRef]
141. Bandgar, D.K.; Navale, S.T.; Nalage, S.R.; Mane, R.S.; Stadler, F.J.; Aswal, D.K.; Gupta, S.K.; Patil, V.B. Simple and low-temperature polyaniline-based flexible ammonia sensor: A step towards laboratory synthesis to economical device design. *J. Mater. Chem. C* **2015**, *3*, 9461–9468. [CrossRef]
142. Han, J.-W.; Kim, B.; Li, J.; Meyyappan, M. Carbon nanotube based humidity sensor on cellulose paper. *J. Phys. Chem. C* **2012**, *116*, 22094–22097. [CrossRef]
143. Raghu, M.; Suresh, R.; Vijay, P.S. MWCNT–polymer composites as highly sensitive and selective room temperature gas sensors. *Nanotechnology* **2011**, *22*. [CrossRef]

144. Ernest, M.; Jahir, O.; Cecilia, J.-J.; Ana, B.G.-G.; Ana, C.; Laura, M.L.; César, F.-S. Scalable fabrication of immunosensors based on carbon nanotube polymer composites. *Nanotechnology* **2008**, *19*. [CrossRef]
145. Sullalti, S.; Colonna, M.; Berti, C.; Fiorini, M.; Karanam, S. Effect of phosphorus based flame retardants on UL94 and comparative tracking index properties of poly(butylene terephthalate). *Polym. Degrad. Stab.* **2012**, *97*, 566–572. [CrossRef]



© 2016 by the authors; licensee MDPI, Basel, Switzerland. This article is an open access article distributed under the terms and conditions of the Creative Commons Attribution (CC-BY) license (http://creativecommons.org/licenses/by/4.0/).

Chapter 3

Surface Wetting Behavior of CF_4 Plasma Selectively Etched Polyphenolic Composite

Surface chemistry and topography are the two of the most important factors that permit to achieve suitable surface energy and wetting behavior of the plasma modified surfaces. These factors are largely dependent on the interacting plasma species and the exposed material. Herein, we examined various factors such as topography, surface chemistry, plasma species generated and temperature variations on the sample surface during exposure of glass-filled polyphenolic composites to CF_4 plasma.
The results in this paper demonstrate that the surface hydrophobicity mostly depends on the surface chemistry rather than surface roughness, where the number of fluorine atoms bonded to the surface carbon have crucial role in deciding the surface wettability of the treated composites. Additionally, it was revealed that various plasma generated functional groups migrate at different rates from the surface to the bulk of the material, where surface temperature during the treatment is an influential factor.

This chapter addresses thesis Objective 1.

Regarding my contribution: I performed the experiment, surface analysis and jointly wrote the paper with co-authors.

Short communication

SURFACE and INTERFACE ANALYSIS

Received: 16 December 2015 Revised: 19 May 2016 Accepted: 4 July 2016 Published online in Wiley Online Library

(wileyonlinelibrary.com) DOI 10.1002/sia.6104

Mechanisms of hydrophobization of polymeric composites etched in CF_4 plasma

Harinarayanan Puliyalil,[a,b] Nina Recek,[a,b] Gregor Filipič,[a,b] Miha Čekada,[a] Ivan Jerman,[c] Miran Mozetič,[a] Sabu Thomas[d] and Uroš Cvelbar[a,b]*

Achieving optimal hydrophobicity of polymer materials especially polymer–matrix composites is important for many material applications. Herein the interplay of factors determining hydrophobic surface is presented during CF_4 plasma treatments which lead to functionalization as well as selective polymer–matrix etching. The continuous exposure to plasma reactive species induces functionalization and etching on the surface, which decides the surface morphology and surface chemistry. Consequently, exothermic processes during the plasma–surface interactions are another important factor which influences the surface chemistry and etching rate of the material. The results demonstrate that despite etching and increasing surface roughness, the major contribution to hydrophobic character is dependent on the number of carbon atoms populated with fluorine, whereas the temperature is a deciding factor for type of created bonds. **Copyright © 2016 John Wiley & Sons, Ltd.**

Additional supporting information may be found in the online version of this article at the publisher's web site.

Keywords: CF_4 plasma; plasma etching; hydrophobicity; composites

Introduction

The research on super-hydrophobicity attracted a lot of attention because of the self-cleaning abilities of surfaces like observed on plant leaves.[1] In order to achieve super-hydrophobic phenomena and mimic the nature, a number of methods for modification of surfaces were developed including lithography, templating, electrospinning, sol–gel methods, layer by layer deposition, chemical etching, chemical vapour deposition, thin layer functionalization, galvanic deposition, etc.[2,3] Among these methods, plasma supported chemical etching or material deposition was found to be the most efficient for hydrophobization of polymeric surfaces. From perspective use of plasmas, the simplest way to achieve this is by plasma etching of material or with thin-layer surface functionalization. This holds particularly for fluorine containing plasmas including CF_4, CHF_3, SF_6 or similar, which can increase the surface roughness via etching by ions or functionalize thin layer of polymer surface with hydrophobic fluorine functional groups.[4,5]

In this respect, plasma etching/functionalization is a more efficient and faster process than chemical vapour deposition or other lithographic approaches.[6,7] Up to date, there are many reports on various gas plasma treatments on polymeric substrates to induce extremely good water repelling surfaces. Altering the surface topography to various nano/micro hierarchical structures is also important in addition to the functionalization. Providing sufficient roughness to the surface will allow the water drop to occupy more volume and stabilize in its globular shape.[8,9] To achieve such extremely water repelling systems, various plasma systems which operate at low and atmospheric pressure have been developed.[10–12]

When dealing with polymer–matrix composites and their hydrophobicity, the surface roughness is mostly determined by amount of polymer that is removed by plasma and the shape and distribution of fillers which get exposed. In contrast to surface roughness, the surface functionalization in the case of composites is not straightforward. The chemical composition of the surface changes after the fillers are exposed, and the plasma–surface interactions become more complex, and thus the wanted functionalization is more challenging.[13] In the last decade, the effect of various factors affecting the water repellence behaviour of polymeric surfaces, including fluorination and surface roughening in CF_4, was studied extensively. In many cases, the surface hydrophobicity was found to be influenced mostly by the surface functionalities, whereas the effects of surface roughness could not be excluded completely. Apart from pure polymeric materials, these studies have to be extended into more complex polymeric composite systems which have prominent applications in large scale industrial applications. Moreover, the effects of various C—F bond types incorporated on the surface have to be investigated properly.

In this short communication, we try to unravel the interplaying effect of CF_4 plasma etching predominantly of polymer on polymer–matrix composite and its surface functionalization, with

* *Correspondence to: Jožef Stefan International Postgraduate School, Jamova cesta 39, 1000 Ljubljana, Slovenia. E-mail: uros.cvelbar@ijs.si*

a *Jožef Stefan Institute, Jamova cesta 39, 1000, Ljubljana, Slovenia*

b *Jožef Stefan International Postgraduate School, Jamova cesta 39, 1000, Ljubljana, Slovenia*

c *Department for Materials Chemistry, National Institute of Chemistry, Hajdrihova 19, SI-1000, Ljubljana, Slovenia*

d *International and Inter University Centre for Nanoscience and Nanotechnology, Mahatma Gandhi University, Priyadarshini Hills P.O., Kottayam, Kerala, India*

 Copyright © 2016 John Wiley & Sons, Ltd.

the aim of achieving the best hydrophobic conditioning of the surface. For this reason, we explored various factors such as topography, plasma species generated and temperature variations during the treatment, which determined the hydrophobic behaviour of composite surface. As a case study, we compared the effects of plasma treatment on various types of glass filled polyphenolic composites used in automotive and aerospace industry, which are economical and hold excellent thermal resistance as well as mechanical properties.[14,15]

Materials and methods

The polymer–matrix composite materials used were all polyphenolic moulding compound filled with glass fibres, glass balls or both, which are commercially available under name Vyncolit (Sumitomo Bakelite Group). The Composite-1 used was 42% phenolic moulding with 3% of melamine-formaldehyde resin up to 55% glass fibres and glass beads. Composite-2 then contained 50% glass fibres, but not glass beads. Then Composite-3 was made from the same composition as Composite-1, but without melamine-formaldehyde resin. Inductively coupled RF 27.12-MHz plasma was generated in CF_4 gas at pressure 70 Pa and 80 W inside borosilicate tube. During the treatment, the properties of plasma were monitored with various plasma analysis techniques including presented optical emission spectroscopy (OES) with AvaSpec-3648 spectrometer, whereas the sample surface temperature changes are simultaneously measured with IR pyrometer Raytek Raynger MX4+. The etching rate was calculated from the mass lost after exposing the samples to reactive plasma by using an analytical balance from RADWAG advanced weighing technologies. After the treatment, various surface analyses were performed including X-ray photoelectron spectroscopy (XPS) analyses with the PHI-TFA XPS spectrometer, scanning electron microscopy (SEM) with FE-SEM Jeol JSM-7600F, and profilometry with Talysurf Series 2 (Taylor–Hobson). The static water contact angles (WCAs) were measured with SeeSystem (Advex Instruments). Later surface ageing effects were monitored on samples kept in an inert atmosphere at room temperature (25 °C) to avoid the influence of atmospheric moisture and thermal degradation of the surface bonding states. Dynamic contact angles were measured by using a Tensiometer Theta T200 from Biolinscientific by the tilt method.

Results and discussion

Feeding CF_4 gas into the inductively coupled discharges leads to its decomposition into various excited atoms and molecules as well as to plasma–surface interactions of those species [seen from OES presented in Supporting Information Figure S1]. In this created plasma the CF_4 dissociated excited molecules including CF, CF_2 and CF_3 were observed in the OES spectrum (250–400 nm). Mentioned observation is in consensus with the previous reports.[16] Additionally, the strong atomic F emission lines at 691 nm, 703 nm and 712 nm indicate rather large amounts of atomic fluorine.[17,18] These species then readily react with composite surfaces containing mostly

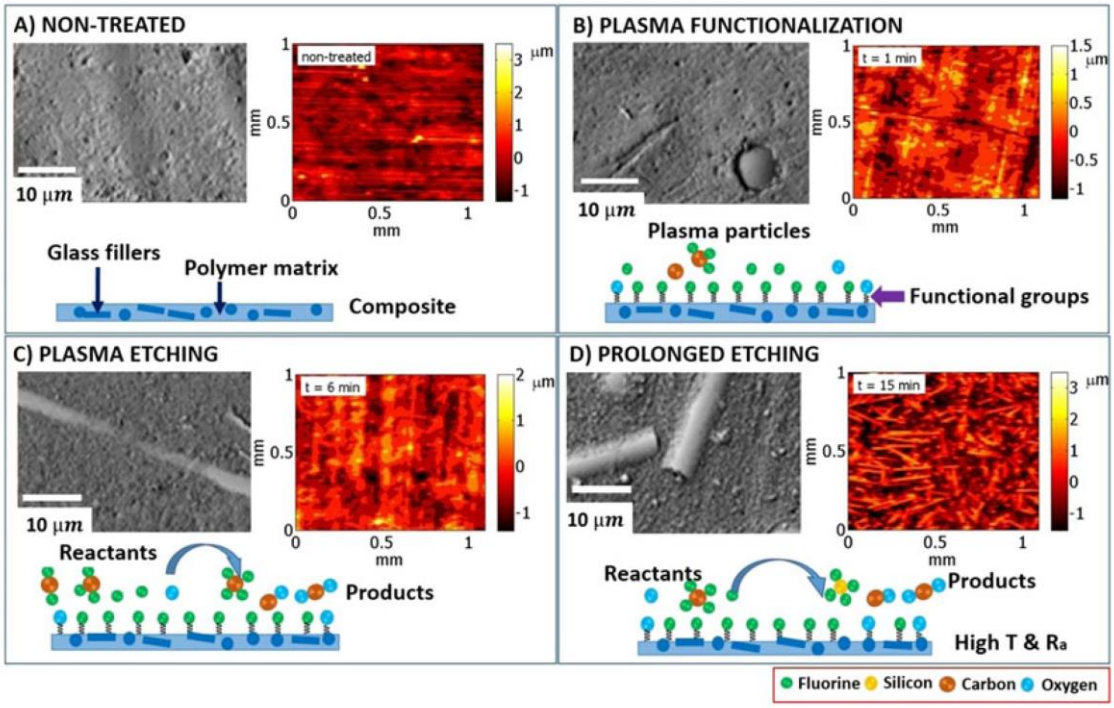


Figure 1. Schematic of the plasma surface interactions along with the corresponding SEM and topographic images of composite 1: A) Non-treated sample where the surface polymer covers the embedded glass fillers. B) After 30 s, the dissociated plasma particles chemically react with the surface polymer to give surface saturated with functional groups. C) After 3 min, continuous exposure to the plasma reactive species resulted the removal of the surface polymer exposing the fillers. D) After 15 min, prolonged interaction of the plasma particles resulted deep etching providing high surface roughness and temperature.

Copyright © 2016 John Wiley & Sons, Ltd.

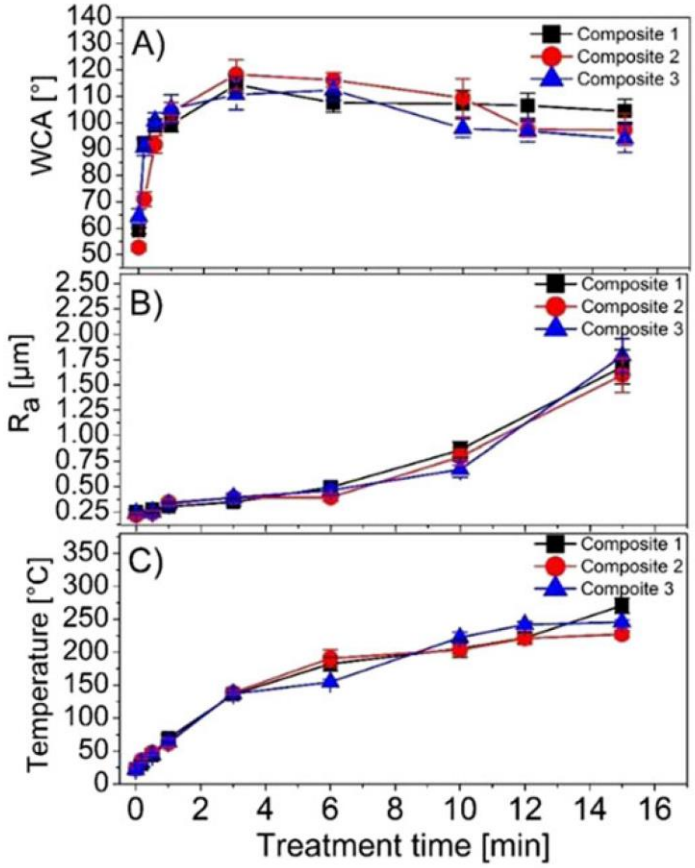


Figure 2. A) Measured water contact angle on each composite surface as a function of treatment time. B) Variation of surface roughness as a function of treatment time. C) Surface temperature measured during the treatment process.

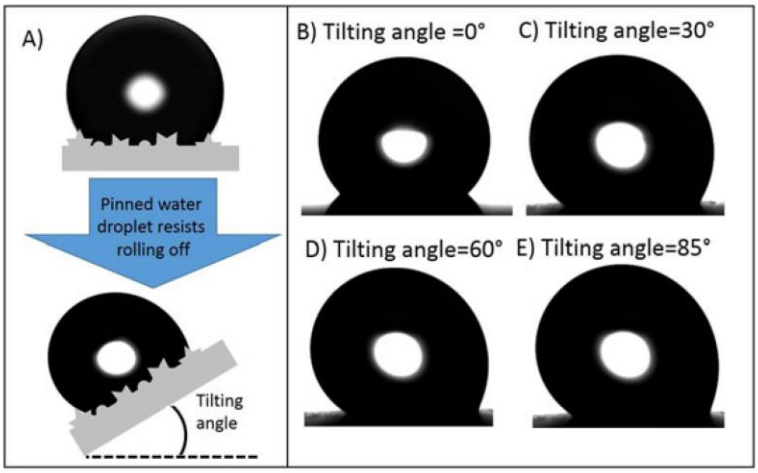


Figure 3. A) Schematic of the pinned water droplet resistance to rolling off from the composite surface. B)–D) The images of the water droplet of volume 10 µl at various sample tilting angles.

 Copyright © 2016 John Wiley & Sons, Ltd.

polyphenol, leading first to functionalization of the surface through incorporation of fluorine groups, and in the following stages to breaking C—C/C—H bonds and desorption of reaction products from the surface. As a result of polymer scissions by plasma O atomic radicals, molecules such as CO were released from surface and observed in their excited states.[13,16] The presence of O reactive species is generally observed during the treatment of polymer materials, which originate from the degradation of desorbed water molecules from the reaction chamber or as a by-product of polymer degradation. Here it is worth noticing that plasma species are highly reactive towards the carbon-containing layer (polymer), but much less towards the glass fillers.[16,19]

The plasma–surface reactions are schematically presented along with corresponding SEM images in Fig. 1. The result of these plasma–surface interactions is reflected in the measured WCA, surface roughness and surface temperature in respect to treatment time (Fig. 2A–2C). The WCA results show fast increase in hydrophobicity which reached the maximum already after 3 min of treatment (Fig. 2A). Independent of the sample components, the WCA showed much similar trends. This revealed that the slight changes in the composition were not affecting the surface functionalization or etching rate. Prolonged exposure later led to WCA saturation and slight decrease. In order to explain this WCA behaviour, the surface modifications in terms of related roughness or created functional groups were explored. Furthermore, the analyses of sample roughness indicated very small changes in morphology in the beginning, but start increasing with higher rates after only 6 min of treatment (Fig. 2B). The water drop on the hydrophobic surface typically exists either in Cassie or Wenzel state. Measurement of dynamic contact angle by the tilt method is one of the suitable experimental techniques to predict the existing state of the water drop on the surface. During the experiments, the water drop was firmly sticking to the composite surface, which restricted the easy rolling of the drop from the surface. Such sticky nature arises because of the pinning of water drop inside the micro textures on the surface, which can be described by Wenzel state mechanism.[20,21] The fact that water droplet stuck to the surface even after changing the tilting angle to 90° even further supported this argument. The images of water droplet as a function of tilting angle are shown in Fig. 3. In the case of surfaces, which exhibit Cassie state mechanism, the droplet with very low volume (~1 μl) can easily roll off even at very low tilting angles.[22] In our experiments, the water droplet did not roll off from the surface even for a droplet volume of 10 μl. Abe *et al.* reported that the hydrophobicity of various polymer particles is mostly influenced by the functionalization over the roughness factor.[23] In our experiments, the results were in agreement with this, and surface roughness showed little influence in the absence of fluorine groups. However, the observed surface temperature of the sample increases to above 200 °C in the course of the treatment, as a result of ion bombardment and chemical reactions between amorphous carbon and inorganic fillers with F reactive species from plasma (Fig. 2C). Such increased temperatures on the surface accelerate the migration of the newly formed functional groups into the bulk or their degradation and might explain the decrease in WCA after 3–6 min of treatment time.[24] In addition to this, surface temperature can significantly influence the etching rate of the material. The etching rates were measured in terms of mass lost from the composite after exposing to the CF_4 plasma reactive species. For lower treatment times (up to 3 min), no etching was measured. However, prolonged treatments showed significant mass loss from the composite material as presented in Fig. 4. As it is seen from the etching rate evolution as a function of exposure time, all three composites used showed very similar etching rates irrespective of the composition of the additives in the matrix.

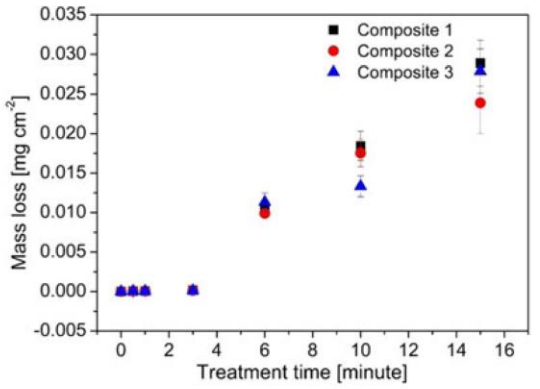


Figure 4. Measured time evolution of etching rates for the composite materials in CF_4 plasma.

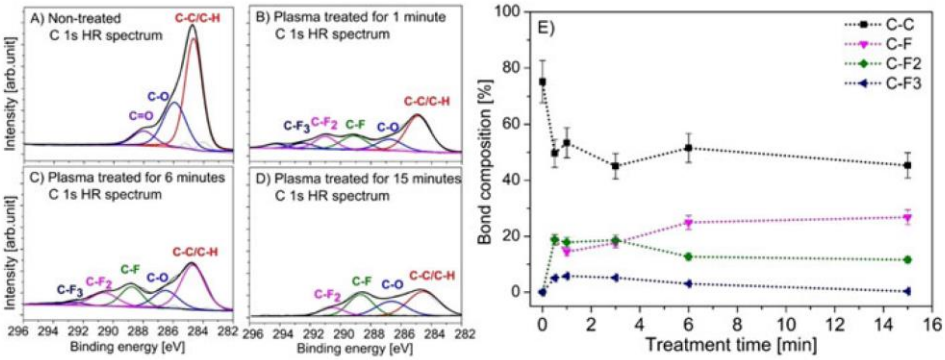


Figure 5. XPS deconvolution C 1s peak of composite 1: A) Non-treated sample, B) treated for 1 min, C) for 6 min and D) for 15 min. E) The composition of different bond types on the surface deduced by deconvolution of C 1s peak.

Copyright © 2016 John Wiley & Sons, Ltd.

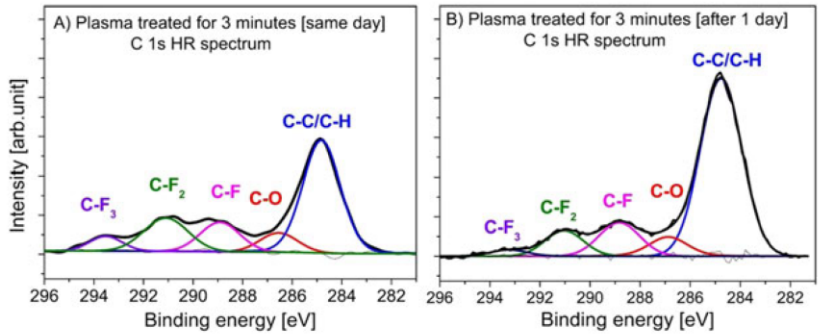


Figure 6. XPS deconvolution C 1s peak of composite 1: A) Sample treated for 3 min and the analysis was done immediately after the treatment. B) The analysis of the same sample after 1 day.

What is happening on the surface is revealed by XPS analysis and deconvolution of C 1s peaks, which for the non-treated sample revealed the C—C/C—H, C—O and C=O bonds at 284.7, 286.5 and 288 eV, respectively (Fig. 5).[25,26] The oxygen functionalities mostly disappeared or they could not be clearly resolved after exposing to CF_4 plasma, because of the replacement of native polymer bonds with C—F_x bonds by functionalization and etching. Instead, the new carbon fluorine bonds formed, which were observed in the deconvoluted spectra at 288.8, 291.2 and 293.5 eV originated from C—F, C—F_2 and C—F_3 entities, respectively.[25] Interestingly, C—F_2 and C—F_3 species increased rapidly in the beginning of the treatment and thereafter decreased, whereas C—F bond type gradually increased throughout the process (Fig. 5E). This is attributed to the elevated temperature which induces faster migration or degradation of the di- and tri-fluoro functionalities from the surface than the mono-fluoro species into the bulk. Additionally, the number of bonding spots in the polymer is reduced because of the etching process. This leads to a hypothesis that the hydrophobicity is dependent on the valency of carbon satisfied by fluorine atoms. However, with the ageing of the polymers the WCA is decreased and settled only at a slightly higher value than the one of non-treated polymer (Figure S4). Thus, the main contribution to the hydrophobic behaviour must be the functionalization of the surface. The surface chemistry revealed also the drastic decrease of C—H bond species, replaced by C—F bonds. In spite of the higher polarization, the fluorocarbon surfaces have a larger molecular cross section (28.3 Å^2) than the corresponding hydrocarbon (18.9 Å^2), so that a water droplet occupies sufficiently more volume. This gives more free-energy benefits to stabilize the surface at a higher contact angle.[27] As presented by Jackel *et al.* the hydrophobicity of a molecular species increases as the value of *x* increases in a C—F_x terminated molecule, which was in accordance with the observed decrease of WCA with the decrease in C—F_3 bond concentration on the surface.[28]

The elemental composition of the samples varied with ageing time. For instance, immediately after treating the sample for 3 min, the C/F ratio was 0.8, where the percentage of surface oxygen was 8.5. After 1 day, the C/F ratio increased to a value of 1.6 along with an increase in the oxygen content to 11%. While comparing the C 1s deconvolution peaks for the samples immediately after the treatment and the same sample after a day, it was revealed that the intensities of the plasma incorporated C—F_x bonds decreased (Fig. 6). Along with this, the intensities of C—C/C—H and C—O bonding states on the surface showed higher concentration. Such migration of plasma incorporated surface bonds and hydrophilic recovery is well known, the rate of which has been known to increase with the temperature.[29] However, comparison of the different C—F_x bond intensity after ageing for 1 day revealed that the migration rate is much higher for the bond types with more number of fluorine atoms bonded to the carbon atom. After 1 day, the C—F_3 bonding states mostly disappeared from the surface. The decrease in the intensity of C—F_2 states was higher than that of C—F bonds, which further supports the previous claims.

Thus, to conclude, the overall processes are presented in Fig. 7. The first step of the processing starts with the activation of the surface which turns in to etching after the saturation of the surface with fluorine functionalities. As the treatment time was increased, an equilibrium will be established between the functionalization and etching. However, the elevated temperature promotes the migration of the functionalities into the bulk and the selective removal increases the surface roughness. Increased surface roughness and decreased functionalities decrease the WCA.

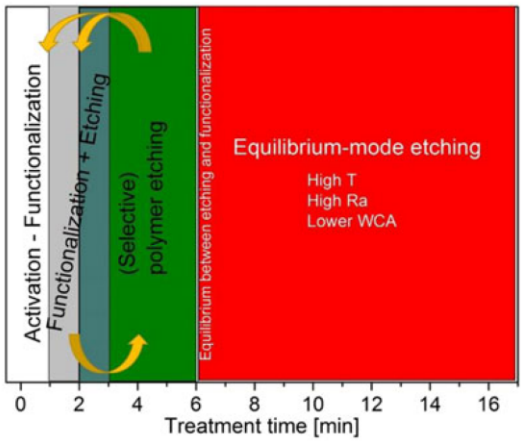


Figure 7. Representation of the effects of various factors on the surface hydrophobic behaviour.

 Copyright © 2016 John Wiley & Sons, Ltd.

Conclusions

The influence of CF_4 plasma and its selective etching on the hydrophobic behaviour of polyphenol–matrix composites with micro sized glass is presented as a case study of phenomena interplay between topography and functional groups. The effect of both surface roughness and created functional groups as well as ratio of polymer/glass and surface temperatures has to be taken into consideration. Fluorination is an immediate process and the amount of fluorine-contained bonds stays constant with the treatment time. However, the amount of C—F_3 and C—F_2 bonds decreases, whereas the amount of C—F bond increases. Fluorocarbon bonds provide larger extent of surface to volume ratio on molecular level. Among plasma generated bonds, C—F_3 bond types contribute more towards the hydrophobicity of the surface. Additionally, the migration rate of C—F_x bonds shows an increase with the increase in number of F atoms attached to the carbon. Respectively, the gradual increase of the WCA is not correspondingly affected by the increasing surface roughness. The longer treatment time increases the temperature of the surface which inherently accelerates the C—F bond diffusion into the bulk or their degradation – it increases the ageing process, and thus the WCA slightly decreases. However, this can be overcome by applying cycling plasma processing achieved via pulse plasma treatments instead of continuous plasma treatment which has higher control over surface temperature.

Acknowledgements

Authors gratefully acknowledge Slovenian Research Agency (ARRS grants L2-6767 and L2-6769) for financial support. H. P. thanks Jozef Stefan International Postgraduate School for the PhD grant and Janez Zavašnik (CEMM) for technical support.

References

[1] C. Neinhuis, W. Barthlott, *Ann. Bot.*, **1997**, *79*, 667.
[2] E. Celia, T. Darmanin, E. Taffin de Givenchy, S. Amigoni, F. Guittard, *J. Colloid Interface Sci.*, **2013**, *402*, 1.
[3] L. Feng, Z. Yan, X. Qiang, Y. Wang, Y. Liu, *Surf. Interface Anal.*, **2015**, *47*, 506.
[4] J. Fresnais, J. P. Chapel, L. Benyahia, F. Poncin-Epaillard, *J. of Adhesion Science and Technology*, **2009**, *23*, 447.
[5] J. P. Fernández-Blázquez, D. Fell, E. Bonaccurso, A. D. Campo, *J. Colloid Interface Sci.*, **2011**, *357*, 234.
[6] C. Canal, F. Gaboriau, S. Villeger, U. Cvelbar, A. Ricard, *Int. J. Pharm.*, **2009**, *367*, 155.
[7] M.-E. Vlachopoulou, G. Kokkoris, C. Cardinaud, E. Gogolides, A. Tserepi, *Plasma Processes Polym.*, **2013**, *10*, 29.
[8] K. Ellinas, A. Tserepi, E. Gogolides, *Langmuir*, **2011**, *27*, 3960.
[9] B. K. Lee, I.-B. Baek, B.-J. Lee, Y. Kim, W. I. Jang, Y. S. Yoon, H. Y. Yu, *Adv. Mater. Interfaces*, **2015**, *2*, 1500141.
[10] K. Matsubara, M. Danno, M. Inoue, H. Nishizawa, Y. Honda, T. Abe, *Surf. Coat. Technol.*, **2013**, *236*, 269.
[11] Z. Zhou, X. Liu, B. Hu, J. Wang, D. Xin, Z. Wang, Y. Qiu, *Surf. Coat. Technol.*, **2011**, *205*, 4205.
[12] A. K. Gnanappa, D. P. Papageorgiou, E. Gogolides, A. Tserepi, A. G. Papathanasiou, A. G. Boudouvis, *Plasma Processes Polym.*, **2012**, *9*, 304.
[13] U. Cvelbar, S. Pejovnik, M. Mozetic, A. Zalar, *Appl. Surf. Sci.*, **2003**, *210*, 255.
[14] C. P. R. Nair, *Prog. Polym. Sci.*, **2004**, *29*, 401.
[15] R. Balaji, M. Sasikumar, A. Elayaperumal, *Polym. Degrad. Stab.*, **2015**, *114*, 125.
[16] M. Gorjanc, K. Jazbec, M. Šala, R. Zaplotnik, A. Vesel, M. Mozetič, *Cellulose*, **2014**, *21*, 3007.
[17] R. d'Agostino, F. Cramarossa, S. De Benedictis, G. Ferraro, *J. Appl. Phys.*, **1981**, *52*, 1259.
[18] R. Barni, S. Zanini, C. Riccardi, *Vacuum*, **2007**, *82*, 217.
[19] R. Zaplotnik, M. Bišćan, Z. Kregar, U. Cvelbar, M. Mozetič, S. Milošević, *Spectrochimica Acta Part B: Atomic Spectroscopy*, **2015**, *103–104*, 124.
[20] C. Ran, G. Ding, W. Liu, Y. Deng, W. Hou, *Langmuir*, **2008**, *24*, 9952.
[21] C.-Y. Gao, G.-X. Meng, X. Li, M. Wu, Y. Liu, X.-Y. Li, X. Zhao, I. Lee, X. Feng, *Surf. Interface Anal.*, **2013**, *45*, 650.
[22] X. Dai, B. B. Stogin, S. Yang, T.-S. Wong, *ACS Nano*, **2015**, *9*, 9260.
[23] K. Matsubara, M. Danno, M. Inoue, H. Nishizawa, Y. Honda, T. Abe, *Appl. Surf. Sci.*, **2013**, *284*, 340.
[24] H. Puliyalil, U. Cvelbar, G. Filipic, A. D. Petric, R. Zaplotnik, N. Recek, M. Mozetic, S. Thomas, *RSC Advances*, **2015**, *5*, 37853.
[25] H. Watanabe, H. Kondo, M. Hiramatsu, M. Sekine, S. Kumar, K. Ostrikov, M. Hori, *Plasma Processes Polym.*, **2013**, *10*, 582.
[26] D. Kontziampasis, T. Trantidou, A. Regoutz, E. J. Humphrey, D. Carta, C. M. Terracciano, T. Prodromakis, *Plasma Processes Polym.*, **2016**, *13*, 324.
[27] V. H. Dalvi, P. J. Rossky, *Proc. Natl. Acad. Sci.*, **2010**, *107*, 13603.
[28] C. Jäckel, M. Salwiczek, B. Koksch, *Angew. Chem. Int. Ed.*, **2006**, *45*, 4198.
[29] D. Jucius, V. Grigaliūnas, V. Kopustinskas, A. Lazauskas, A. Guobienė, *Appl. Surf. Sci.*, **2012**, *263*, 722.

Supporting information

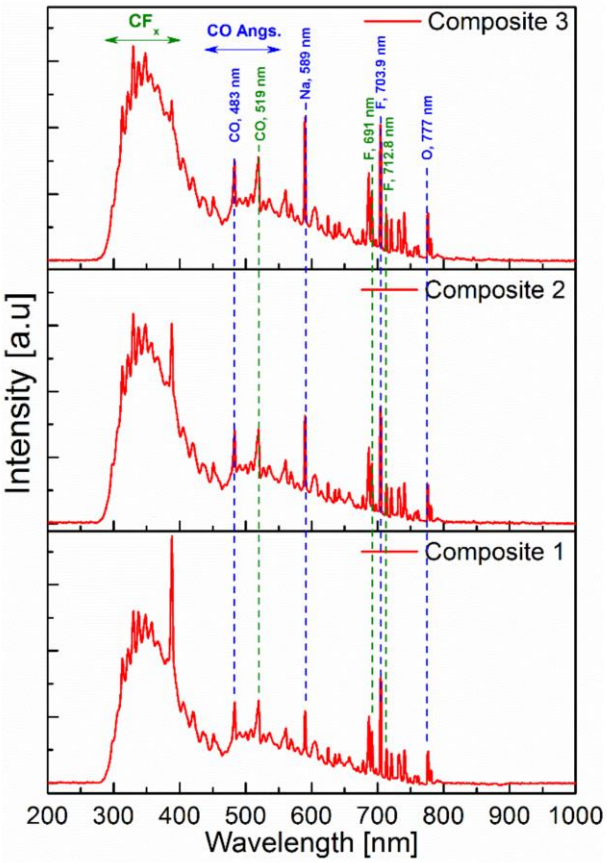
Additional supporting information may be found in the online version of this article at the publisher's web site.

Figure. S1. OES spectrum during the treatment recorded after 5 min of plasma ignition
Figure S2. Contact angle measurements of surface wettability with 1,5 pentanediol for different treatment times.
Figure S3. XPS survey spectrum of composite 3 surface treated for various treatment times.
Figure S4. WCA measurements of surface conditions along the composite sample ageing, when treated for 3, 6 or 15 min.

Copyright © 2016 John Wiley & Sons, Ltd.

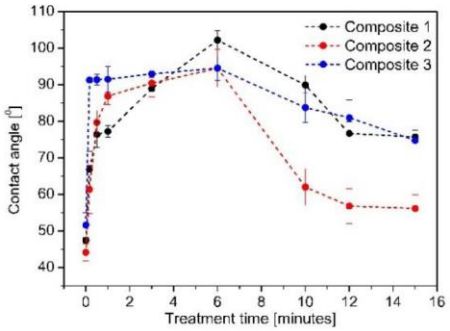
Supporting Information

Figure. S1. Optical emission spectra (OES) during the treatment recorded after 5 minutes of plasma ignition.



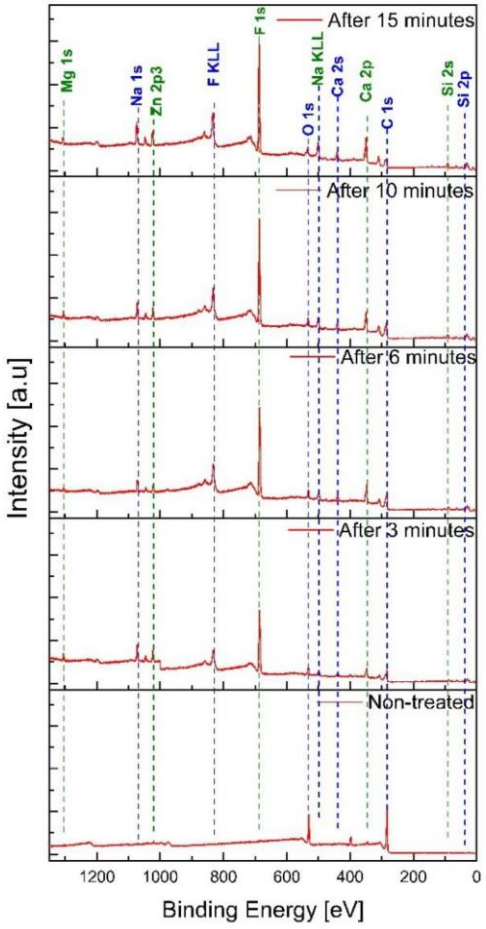
The spectra are relatively similar, except some variations in CF_x molecular bands and emissions from the etch by-products. The OES signals from atomic fluorine confirms that plasma is dissociated. The anomaly in spectra is Na peak (at 589 nm), which comes from etching of polymer matrix and its additives. The sodium salt of organic acids is normally as adhesive or lubricant for compositing to improve the processability of composites spectra we observe also atomic oxygen peaks, which either originate from the etching of by fluorine atoms (SiO_2), polymer or comes from the dissociation of residual water molecules inside the vacuum chamber.

Figure S2. Contact angle measurements of surface with 1,5 pentanediol for different treatment times.



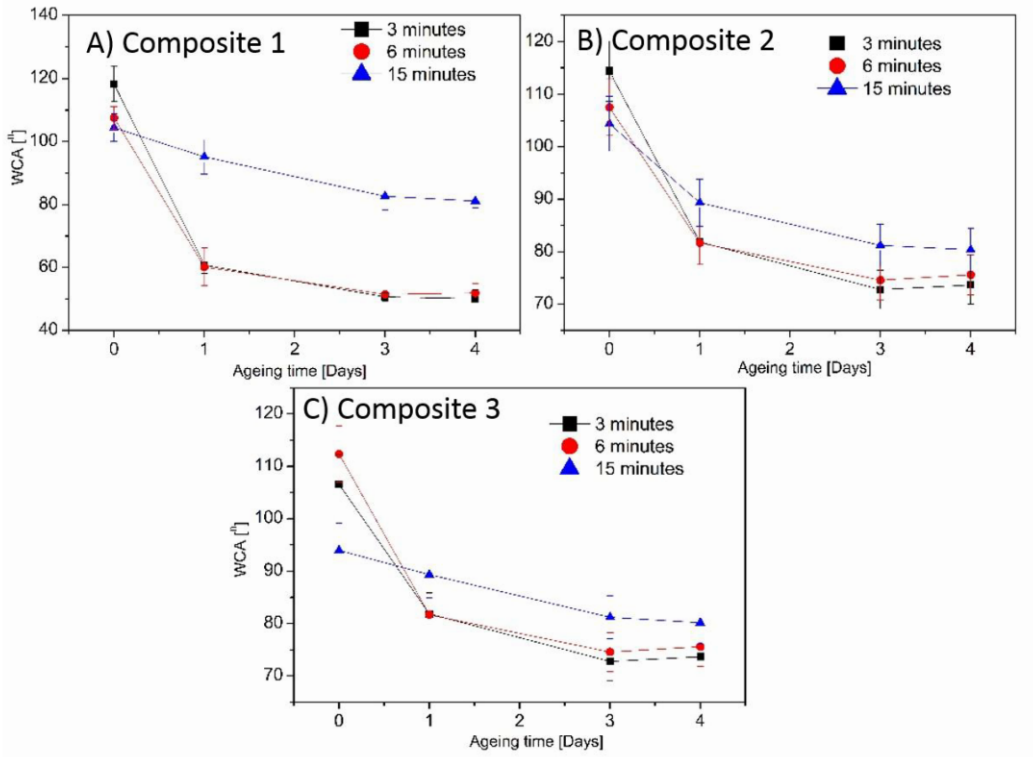
This is a complementary information to WCA measurements with deionized water droplets presented in the paper (Figure 2A). The contact angle measured on the surface with 1,5 pentanediol, which is less polar solvent compared to water is presented in the Figure S2. As observed in the case of WCA, diol shows similar behaviour. The CA is firstly increased and then slightly decreased for prolonged plasma processing of composite surface.

Figure S3. XPS survey spectra of composite 3 surface for various plasma treatment times.



The XPS survey spectra present composition of the surfaces. As seen from results, the amount of carbon on the surface is decreased drastically with treatment time. Moreover, the intensities of F, Si, Na, Ca, etc. are increased at the same time, bringing out the fillers during removal of polymer matrix. On the other hand the F comes from plasma-surface interactions which first result in the functionalized polymers and later inter-binding.

Figure S4. WCA measurements of surface along with the aging effects treated.



The S4 graphs present surface aging measured through WCA measurements. The surface is affected by environment or migration/deterioration of created functional groups. The surface functional groups generated after plasma treatment can either migrate in to the bulk with time or are deteriorated based on environment conditions. To evaluate this, we measured WCA with aging time in controlled inert reduced atmosphere. The results of WCA showed a gradual decrease with aging time, and attained a constant value after 4 days. This is the case of all three types of samples used. After 4 days, the WCA values closely approached the non-treated sample wettability. These measurements also revealed that in our case the surface roughness of composites has very little influence on the water repellence of the surface.

Chapter 4

Selective Plasma Etching for Improving the Electrical Insulation Properties

The electrical insulation properties of glass-filled polyphenolic composites are always limited due to the protruding surface polymer layer that undergoes carbonization when exposed to high voltage electric arc. Herein, a novel method of selective O_2 plasma etching is presented for improving the electrical insulation properties of the polyphenolic composites. The results demonstrate that the removal of surface polymer into volatile molecular forms including CO, CO_2 or H_2O reduced the possible surface carbonization and increased surface tracking properties up to 56%. The electrical insulation properties were directly connected with the concentration of the filler embedded in the matrix as well as the possible surface carbonization during the CTI tests. This approach of selective plasma etching provides an alternative to conventional methods used in composite technology to prevent short circuits and fire under warm and damp conditions.

This chapter addresses thesis Objectives 1 and 2.

Regarding my contribution: I performed the plasma treatments and jointly wrote the paper with co-authors.

RSC Advances

PAPER

View Article Online
View Journal | View Issue



Cite this: *RSC Adv.*, 2015, **5**, 37853

Plasma as a tool for enhancing insulation properties of polymer composites†

H. Puliyalil,[ab] U. Cvelbar,*[ab] G. Filipič,[a] A. D. Petrič,[c] R. Zaplotnik,[a] N. Recek,[ab] M. Mozetič[a] and S. Thomas[d]

Received 7th January 2015
Accepted 20th April 2015

DOI: 10.1039/c5ra00304k

www.rsc.org/advances

The performance of electrical insulating polymers measured by comparative tracking index can be improved by flame retardant fillers in the polymer–matrix, but is not necessary effective due to persisting surface layers. We demonstrated a method for selective etching of polyphenol–matrix composites which leads to improvement of the tracking properties. Selective etching was performed by low pressure inductively coupled oxygen plasma generated at 35 Pa. Species created in discharge were monitored *in situ* during the treatment by optical emission spectroscopy (OES). Their surface reactions were established indirectly from X-ray photoelectron spectroscopy (XPS) and energy dispersive X-ray spectroscopy (EDXS) after plasma treatment. The effective etching was done by oxygen species which removed off surface polymer layer within 10 to 15 s during plasma pulse operation to prevent surface overheating. The selective polymer removal improved tracking properties of the 70% glass filler reinforced composites up to 56%, whereas the performance level decreased with the decrease in filler content. This technology provides an important enhancement of polymer–matrix composites' tracking properties and resistance of composites to electrical short-circuit fire.

1 Introduction

Degradation and stability of polymer materials under various physical and chemical environments has been an interesting subject of studies in the last few decades. The most frequent is thermal degradation which refers to the unfavorable changes in physical, mechanical or electrical properties of materials in contact with heat. Generally, above the degradation temperature, polymers breakdown into chemical fragments. The lighter fragments such as CO, CO_2, *etc.*, desorb from the surface, whereas the heavier fragments remain in a condensed phase.[1]

Carbonization by high voltage arcing is a major disadvantage of polymer materials, when they are used as electrical insulators since it forms a conductive path.[2] Comparative tracking index (CTI) is a common test for materials used in electrical insulation applications. CTI represents a maximum voltage at which no tracking occurs, when 50 drops of ammonium chloride solution are added to the surface of the material as per IEC 60112 standards. This is an important test that determines the performance level of materials, which are used in electrical insulation applications.[3,4] There were attempts to correlate the tracking of various materials at high voltage arcing with the chemical structure as well as the binding energy of the insulating material, but this approach was applicable only for pure polymer materials. The problem is that in composites the additives vary the stability of polymeric materials.[5] On the other hand, CTI performance of various polymers could be enhanced by mixing suitable fillers with polymers. Glass reinforced fillers along with phosphorous or brominated fire retardants were found to be effective in improving the CTI performance of various polyesters and polyamides.[6] For example, addition of 1–2.5 wt% nanoclay into the epoxy matrix made them more resistant to tracking, since the exfoliated clay acted as a barrier and limited tracking, while the pure polymer burnt vigorously during the tests.[7] Similar effects on the tracking properties were reported for various flame retardants in poly(butylene terephthalate).[4] The flammability and CTI tests also confirmed that diethylphosphinic acid aluminum salt which forms condensed form of char enhances the flame retardant properties. On the other hand, melamine polyphosphate which burns completely, improved the CTI performances. Among various polymeric materials, polyphenol composites are important in various electrical insulation applications. Glass filled polyphenols have higher temperature resistance than the alternative polyamide materials filled with melamine salts. However, lower CTI performance makes them unfit for applications in warm and damp conditions.[8]

Use of plasma for the improvement of bulk or surface properties of polymer–matrix composites was reported before.[9]

[a]*Jozef Stefan Institute, Jamova cesta 39, 1000 Ljubljana, Slovenia. E-mail: uros.cvelbar@ijs.si*

[b]*Jozef Stefan International Postgraduate School, Jamova cesta 39, 1000 Ljubljana, Slovenia*

[c]*Research Department, Kolektor Group, Kosovelova 10, SI-5280 Idrija, Slovenia, EU*

[d]*School of Chemical Sciences, Mahatma Gandhi University, Kottayam, Kerala, India*

† Electronic supplementary information (ESI) available. See DOI: 10.1039/c5ra00304k

Surface modification of various polymers by means of plasma treatment was reported to improve the adhesion between fillers and matrix in the bulk. Kafi *et.al.*,[10] found that the atmospheric pressure plasma treatment on jute fibers significantly improved surface characteristics, which improved the flexural and shear strength of the composite when incorporated into the polyester matrix because the mechanical properties of composites are affected by extend of interfacial adhesion between the matrix and the fillers. Oxygen plasma treatment was reported to improve the interfacial compatibility and thereby makes an easy route for the stress transfer at the interfaces between the matrix and the fiber.[11] Moreover both low pressure and atmospheric pressure plasma pretreatments were reported to improve the adhesion between various nanoparticles and polymer substrates, and thus enhance thermal, mechanical and flame retardant properties.[12–15]

Physical surface modifications of polymeric material and possible chemical changes during plasma treatment significantly depend on various plasma discharge parameters including the used gas as well as connected plasma parameters.[16–19] Weakly ionized and highly dissociated plasma generated at low pressure, especially oxygen plasma is known for the selective removal of polymer materials from the composite surfaces. In this process, the reactive oxygen radicals from plasma react with surface atoms including the polymer chains already at room temperature.[20,21] At first, plasma species (neutral atoms, ions) physically adsorb to the surface, and then chemically react with the surface layer of atoms. Result of these reactions is formation of small volatile molecules (*e.g.* OH, CO, *etc.*), which finally desorb away. Etching rate of various components in plasma depends on their binding energy and chemical stability. Many of the commonly used fillers such as glasses, ceramics, metals or graphite are not etched easily in oxygen plasma compared to carbon polymers.[20–22] This makes it possible to remove the polymer from the surface without affecting the bulk or fillers.

Fillers are added to polymer–matrix composites that are used in electrical appliances to further improve the tracking properties. However, even the very thin surface polymer layer still makes an adverse effect on the CTI performance. To the best of our knowledge, there are no reports on the surface modification of composite materials by plasma selective etching for improving the track resistant properties of materials. Herein, we report a novel method for the improvement of CTI performances of glass filled polyphenol composite by the time-resolved selective removal of surface polymer layer by reactive oxygen plasma treatment.

2 Experimental section

2.1 Plasma treatment

Polyphenol composite with glass fibers and glass beads were prepared by injection molding process. The temperature in tool cavity was 160–170 °C. After molding, the plates were cured, 2 h at 160 °C, 4 h at 180 °C and 4 h at 210 °C. The samples with dimensions 2.2 cm × 2.2 cm × 5 mm (*lbh*) were used for the experiments. The plasma was generated using AE-Dressler CESAR plasma generator using an inductively coupled RF discharge at pressure 35 Pa with power of 700 W and oxygen flow rate of 40 sccm. The frequency used for discharge, 13.56 MHz, enabled generation of neutral oxygen atom density of $\sim 10^{22}$ m^{-3} and oxygen ion density of $\sim 10^{17}$ m^{-3}.

A schematic of the experimental setup is presented in Fig. 1. The coil was water cooled, whereas the reactor chamber was cooled with forced air to prevent reactor tube overheating. To prevent overheating of samples, they were treated in pulses of 3 s and sufficient time intervals were kept in between successive pulses for the sample to cool down. Qualitative optical emission spectroscopy (OES) measurements were performed with Avantes AvaSpec-3648, while the sample surface temperature was measured with infrared pyrometer Raytek Raynger MX4+ (IR(T)) during all treatments. Mass spectroscopy analysis of various species during the treatment process was carried out with Pfeifer PrismaPlus QMG 220 Residual Gas Analyser (RGA), 0–100 AMU.

2.2 CTI measurements

Comparative tracking index (CTI) as one of the fundamental standard pass/fail tests used to assess the suitability of the material for electrical insulation purpose was measured according to IEC 60112:2003 standard using PTL Tracking Test Apparatus M31.10.

2.3 Surface analysis

The X-ray photoelectron spectroscopy (XPS) analyses were carried out with the PHI-TFA XPS spectrometer. The analyzed area was 0.4 mm in diameter, at a depth about 3–5 nm. The accuracy of binding energies was ±0.3 eV. The surface of the samples was imaged with a scanning electron microscope (SEM) FE-SEM Jeol JSM-7600F with electron beam energy 2 keV. The surface elemental composition was investigated with Oxford's EDXS unit mounted onto the SEM. Contact angles were measured by imaging the water droplet (2 μl) on the surface by using wettability contact angle (WCA) measuring Advex Instruments system.

Results and discussion

When polymer composites were exposed to reactive oxygen plasma, which was created by RF discharge, the interaction of

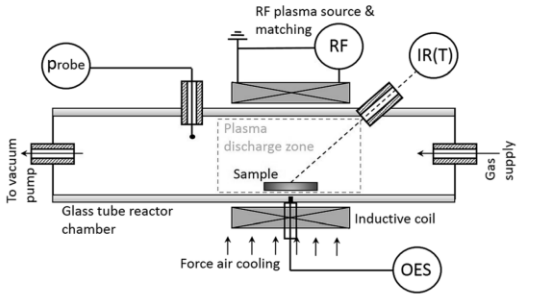


Fig. 1 Experimental setup of plasma rector and measurement systems.

This journal is © The Royal Society of Chemistry 2015

various oxygen species started with polymer surface. Predominant interacting species were neutral O atoms and positive O ions, which caused surface etching.[23] As a result of these interactions different products were released into plasma and many times disintegrated into smaller products. This etching process was seen from optical emission spectra and intensity of spectral emission lines. The intensity of various species as measured by OES at the end of 2nd and 18th pulses is shown in Fig. 2. Observed spectral features such as O atom emission lines, hydrogen Balmer series and molecular OH band are typical for plasmas containing water vapor and also as a byproduct of reactions of oxygen species with the hydrogen from the polymer. In the beginning of the single-first pulse we have typically pure oxygen plasma with only oxygen species or sometimes evaporating water from reactor walls or sample surface as well as from polyphenol which results in molecular OH peak and H lines. Other spectral features like molecular CN, NH and CO or even Na are the result of sample etching, when reaction products are desorbed from surfaces into plasma. The species CN and NH are seen in the beginning of the treatment as an etching byproduct of the reaction between the polymers and nitrogen (air) desorbed from the surface of composite samples during degassing. When the etching is slowed down or almost over (seen from Fig. 2, 18th pulse), the spectra becomes similar to the initial – empty plasma conditions with only oxygen species and lower contents of OH coming from underlayers of polyphenol or water vapor. By these means OES offers unique opportunity to efficiently monitor plasma etching process and reactions occurring on surface in real-time. This was clearly perceived from Fig. 3, where the time evolution of selected emission peaks are drawn.

Later, there is significant decrease in CO peak intensity until it is almost vanished after prolonged treatment. On the other hand, the pretty rich OH emission at 309 nm ($A^2\Sigma^+ - X^2\Pi$) still persists for the maximum treatment time of 60 s, and it is originated by the reaction between the polymer and the oxygen neutrals as well as the dissociation of water vapor inside the plasma chamber.[24,25] One of more important oxygen species recorded during our experiments was triplet atomic oxygen, at wavelength of 615 nm. The intensity of O is lower for the first

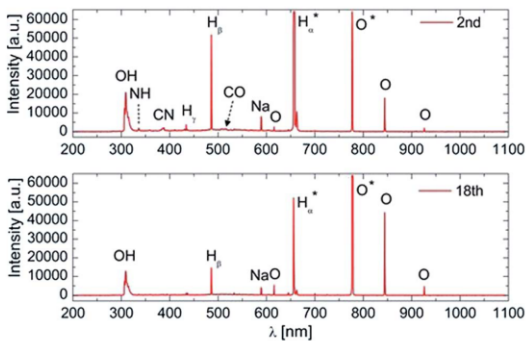


Fig. 2 OES spectra of plasma taken during the processing at the end of 2nd and 18th pulse.

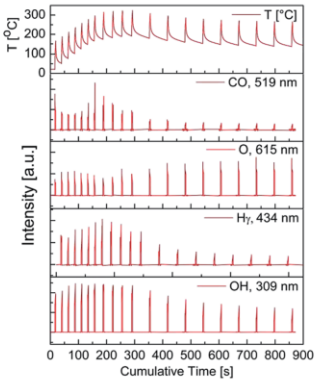


Fig. 3 Surface temperature measurements and corresponding OES spectra for selected emission lines presenting typical species during the treatment process.

few pulses and thereafter increases.[26] This is attributed to the higher consumption of oxygen species for interactions with surface and consequent etching. Secondly, the Hα line at 434 nm and molecular OH band at 309 nm show same trends, increasing with surface temperatures and slowly decreasing with treatment times. During the treatment, the surface temperature increases also to up to around 300 °C, with steady increase for first 8 pulses, reaches saturation for next 4 pulses and then slowly decreases due to increased cooling time (Fig. 3). The surface temperature results from the exothermic carbon oxidation as well as the ion bombardment and neutral atom recombination on the composite surface. Such increase in the surface temperature can affect the overall bulk properties of the material. To prevent such adverse effects, the sample surface was allowed to cool down by keeping sufficient time intervals

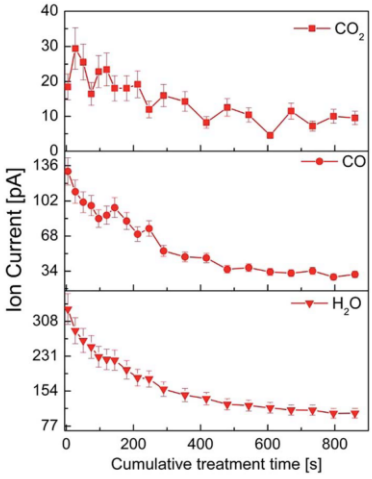


Fig. 4 Intensities of CO, CO_2 and H_2O species as observed by mass spectroscopic measurement during the treatment.

between successive pulses. Despite this, there was still accumulation of heat in the bulk which is seen as a background temperature and would require longer cooling times between sequential pulses. Additionally, mass spectroscopy analysis of the residual gas was performed in a remote chamber at the end of plasma reactor on the way to vacuum pump, which allowed monitoring of the etching products, namely CO, CO_2 and H_2O molecules, which reform into stable molecules upon exiting plasma discharge. From all mass spectra, the gradual drop in the densities of oxidized carbon species CO and CO_2 as well as H_2O is observed (Fig. 4).

This is indication of the reduced carbon mass on the material surface due to etching of material from the surface, especially polymers. Similar holds for detected H_2O species from the residual gas mixture, whose peak in mass spectra showed similar trend with the OH band intensity in observed OES spectra. However, it is important to mention that optical emission spectra doesn't overlap with mass spectroscopy measurements, since in OES we count only for excited plasma species which emit photons during deexcitations. This is seen in the first stages of etching, where not all species leaving the surface are excited with electron collisions.

After the surface treatment with plasma and consequent etching, the samples were subjected to CTI index testing. The average results of ten samples tested are presented in Fig. 5a and display significant increase in the CTI index values of the material with increasing plasma running time. The CTI performances were increased from 225 V to 350 V after an accumulative treatment of 60 s of 3 s pulses. The most significant increase happened between 5 and 10 pulses in accumulative time of 15 s to 30 s.

After this the trend slowly starts to reach saturation profile. Surprisingly the short treatment times lead to 56% improvement of CTI index, and better tracking performance. As seen from OES and mass spectra in combination with SEM images the etching occurs on the surface and leads to reduced carbon content. As a result the reduced amount of carbon on the surface lowers potential carbonization by electrical current and thereby increases the tracking voltage. To confirm the effect of glass fillers on the surface, the samples with different filler content were treated with plasma for 60 s and tested for CTI performances. The sample containing ~20% of fillers showed only 13% of increase in CTI index. But, as we increased the filler content to ~70%, the tracking performance reached a value 56% higher than that of the non-treated composite (Fig. 5b).

The reason behind the significant increase of CTI was due to selective removal of the polymer, which was confirmed by SEM of sample surfaces after different treatment times in Fig. 6, where exposure of composite fillers is observed. These glass fillers act as an additional insulating layer towards surface tracking measured by CTI index. Higher content of fillers therefore simply leads to more significant improvements of CTI. As seen from SEM images (Fig. 6), the surface of the untreated sample composite is almost completely covered with polymer. By increasing the treatment time, the polymer covered on the surface is gradually removed and the fillers (glass fibers and

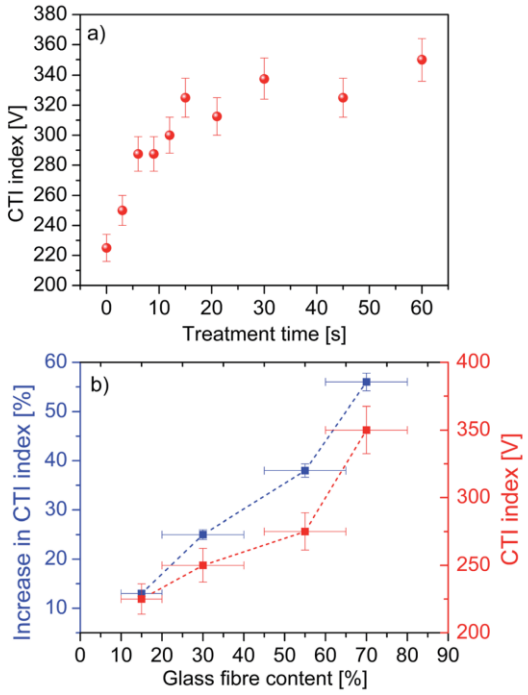


Fig. 5 (a) Composite tracking properties (CTI) with respect to accumulated pulse treatment time; (b) the CTI index of the composites with different glass filler content, when treated for 60 s.

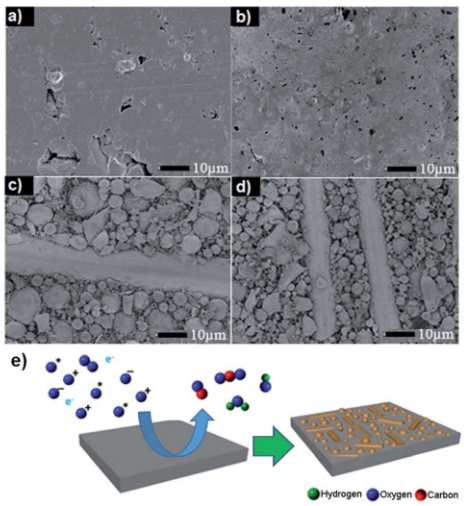


Fig. 6 SEM images of (a) non-treated sample, plasma treated for (b) 6 s (2 pulses), (c) 15 s (5 pulses) and (d) 60 s (20 pulses) as well as (e) schematic representation of plasma etching with corresponding plasma species and resulted products.

This journal is © The Royal Society of Chemistry 2015

spheres) become clearly visible. This process is schematically shown in Fig. 6e. Increasing the treatment times up to 20 pulses yields also etching of composite under surface layers where polymer is removed from the inner parts of composite and the fillers are further revealed. This results in gradual increase in the CTI performances and eventual decrease in the potential surface carbonization level enabling electrical current.

To confirm visual observations of selective etching, the XPS and EDXS analyses of composite surfaces (Fig. 7) were performed to monitor the surface chemistry changes and surface etching with respect to treatment time. Both methods gave almost identical results in the frame of measurement errors and restrictions of used analyses. On the surface, the gradual and selective removal of the surface polymer was observed from the carbon content, whereas the exposed composition of elements such as Si, O, Mg, Na, Mg, *etc.* originated mostly from the fillers inside. The first selective removal occurred in 6 to 30 s of accumulative plasma treatment time. The oxygen content increases slightly more than silicon, due to combined effect of the functionalization of the surface carbon and exposition of the glass fillers from SiO_2. This is observed also from XPS high resolution peaks C1s and O1s, where primary rise of peaks is due to C–O, C=O and COO functional groups. However this functionalization starts to reduce due to heating effects and etching of polymer and after 15 s C/O ratio tend to increase slowly.[27] Result of sample heating and increased surface tension is also the creeping of polymer to the surface, which comes from slight increase in carbon content at prolonged treatment times. The amount of surface functionalization with oxygen polar groups in dependence of progressing etching of the polymer is indirectly estimated from surface wettability measurements. Plasma treatment itself enhances the surface energy of the composite, which results in decreased water contact angle. This is a simultaneous effect of polar group incorporation and roughening of the surface.[28,29] Surface roughening is a permanent change on the surface, while the functional groups will be moved into the bulk of the material, be degraded or/and removed by recombination with impinging air gas molecules with time. The surface functionalization and sequenced surface ageing are perceived from the water contact angle (WCA) for various time intervals of treatment (Fig. 8). The surface becomes superhydrophilic only after treating the surface for 9 s (3 pulses), which means that this is the optimal ratio between incorporation of polar O groups and surface etching. However, due to persisting polymer this is not a very lasting effect, since surface is pretty quickly influenced by polymer ageing. Longer lasting effects of this phenomena are achieved after 30 s or even 45 s treatments, when polymer is almost completely removed. In these cases, the surface is

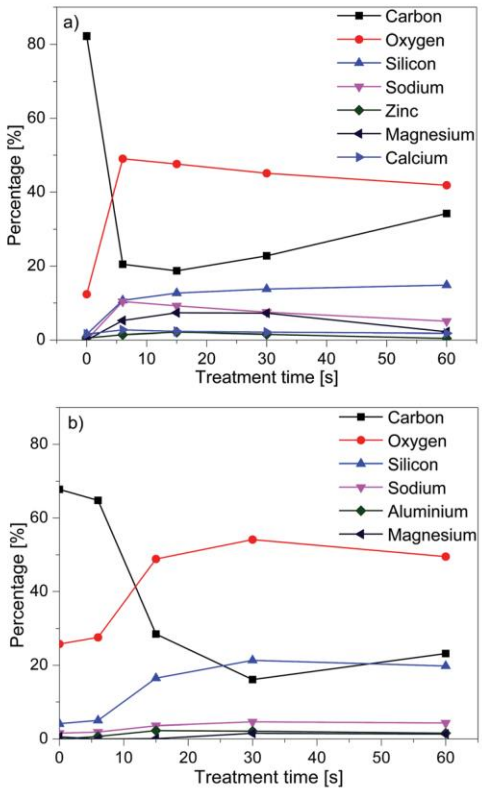


Fig. 7 Surface elemental composition analyzed with (a) XPS measurements from survey spectra and (b) from EDXS measurements.

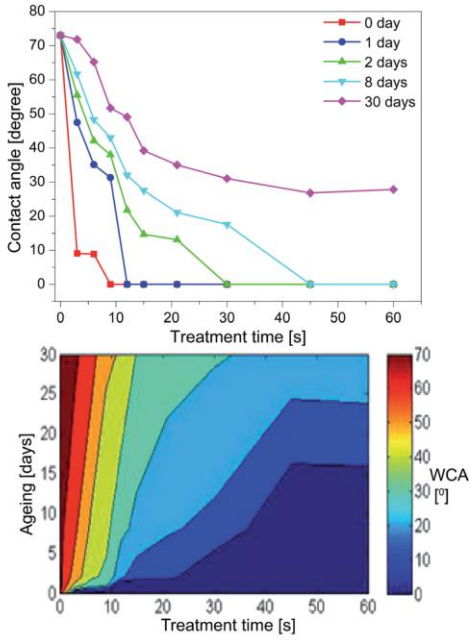


Fig. 8 Wettability of composites surfaces for different accumulative time treatments and time aging of those surfaces presented in *x*–*y* graph (top) and 2D contour plot (bottom).

superhydrophilic even after a period of 8 day ageing, whereas for the 60 s treatment surface turned from superhydrophilic to merely hydrophilic only after 30 days of ageing.

The results from the SEM, XPS, OES, TGA (see ESI†) and WCA confirmed that plasma is selectively removing carbon (polymers) from the surface and exposing the glass fillers. With less and less of carbon on the surface, insulating properties of the composite, depending on glass filler content, increased for up to 56%. Prolonged plasma treatment of the composite led to stabilization of insulating properties of material. This is due to removal of the polymer from the surface and exposure of homogeneously dispersed fillers. These glass fillers are resistant to oxygen plasma.

Conclusions

In this paper, a new method for improving the tracking performances of insulating composite materials was presented. This was achieved by the selective removal of the polymer layer from the surface by means of oxygen plasma treatment. During the plasma treatment, the carbon content on the polyphenolic composite surface is drastically decreased because of the etching by oxygen neutral atoms and ions. This decrease reduces the possibility of carbon layer oxidation and thereby tracking in the presence of high voltage arcing on the material surface. Furthermore, the exposed glass fibers on the surface, as observed by SEM after the oxygen plasma treatments, act as a protective surface layer against high voltage arcing. The repetition of the experiment with lower filler content further confirmed this argument. Thus, it was demonstrated that the tracking properties of composite materials could be improved simply by surface modifications. This proved that selective oxygen plasma etching is an effective and very fast surface processing method for achieving this goal, and that is a very valuable tool in designing novel cost-effective high-voltage electrical insulators.

Acknowledgements

Authors gratefully acknowledge Slovenian Research Agency (ARRS) for financial assistance and Nejc Rozman (ZAG) for technical support. H. P. thanks Jozef Stefan International Postgraduate School for the PhD grant from Innovative Scheme.

Notes and references

1 C. L. Beyler and M. M. Hirschler, Thermal Decomposition of Polymers, *SFPE Handbook of Fire Protection Engineering*, 3rd edn., 2001, sect. 1, ch. 7, pp. 1–110.
2 M. Ugur, O. N. Ucan, A. Kuntman, N. Ozmen and A. Merev, *Annual Report Conference on Electrical Insulation and Dielectric Phenomena*, 1999, Vol. 1, pp. 154–157.
3 IEC 112. Recommended method for determining the comparative tracking index in solid insulating materials under moist conditions.
4 S. Sullalti, M. Colonna, C. Berti, M. Fiorini and S. Karanam, *Polym. Degrad. Stab.*, 2012, **97**, 566–572.
5 D. J. Parr and R. M. Scarisbrick, *Proc. Inst. Electr. Eng.*, 1965, **112**, 1625–1632.
6 E. Schmitt, *Plast. Addit. Compd.*, 2007, **9**, 26–30.
7 F. Guastavino, A. S. Thelakkadan, G. Coletti and A. Ratto, *IEEE Conference on Electrical Insulation and Dielectric Phenomena*, 2009, pp. 701–704.
8 A. Turner, *Wiring Installations and Supplies*, 1985, **1985**, pp. 17–19.
9 P. Slobodian, P. Riha, P. Cavallo, C. A. Barbero, R. Benlikaya, U. Cvelbar, D. Petras and P. Saha, *J. Nanomater.*, 2014, **2014**, 1–8.
10 A. A. Kafi, K. Magniez and B. L. Fox, *Compos. Sci. Technol.*, 2011, **71**, 1692–1698.
11 K. Tamargo-Martínez, A. Martínez-Alonso, M. A. Montes-Morán and J. M. D. Tascón, *Compos. Sci. Technol.*, 2011, **71**, 784–790.
12 A. R. Horrocks, S. Nazaré, R. Masood, B. Kandola and D. Price, *Polym. Adv. Technol.*, 2011, **22**, 22–29.
13 J. Alongi, J. Tata and A. Frache, *Cellulose*, 2011, **18**, 179–190.
14 F. Carosio, J. Alongi and A. Frache, *Eur. Polym. J.*, 2011, **47**, 893–902.
15 J. Alongi, F. Carosio and G. Malucelli, *Polym. Degrad. Stab.*, 2014, **106**, 138–149.
16 E. Gogolides, V. Constantoudis, G. Kokkoris, D. Kontziampasis, K. Tsougeni, G. Boulousis, M. Vlachopoulou and A. Tserepi, *J. Phys. D: Appl. Phys.*, 2011, **44**, 174021.
17 N. De Geyter, A. Sarani, T. Jacobs, A. Nikiforov, T. Sesmet and P. Dubruel, *Plasma Chem. Plasma Process.*, 2013, **33**, 165–175.
18 K. Tsougeni, N. Vourdas, A. Tserepi and E. Gogolides, *Langmuir*, 2009, **25**, 11748–11759.
19 M. Mozetič, A. Zalar, P. Panjan, M. Bele, S. Pejovnik and R. Grmek, *Thin Solid Films*, 2000, **376**, 5–8.
20 M. Kunaver, M. Klanjsek-Gunde, M. Mozetic, M. Kunaver and A. Hrovat, *Surf. Coat. Int., Part B*, 2003, **86**, 175–179.
21 U. Cvelbar, S. Pejovnik, M. Mozetiè and A. Zalar, *Appl. Surf. Sci.*, 2003, **210**, 255–261.
22 U. Cvelbar, M. Mozetic and M. Klanjsek-Gunde, *IEEE Trans. Plasma Sci.*, 2005, **33**, 236–237.
23 C. Fernández-Sánchez, E. Pellicer, J. Orozco, C. Jiménez-Jorquera, L. M. Lechuga and E. Mendoza, *Nanotechnology*, 2009, **20**, 335501.
24 D. Vujosevic, M. Mozetic, U. Cvelbar, N. Krstulovic and S. Milosevic, *J. Appl. Phys.*, 2007, **101**, 103305–103307.
25 E. Vassallo, A. Cremona, F. Ghezzi and D. Ricci, *Vacuum*, 2010, **84**, 902–906.
26 V. Milosavljević, M. Donegan, P. J. Cullen and D. P. Dowling, *J. Phys. Soc. Jpn.*, 2013, **83**, 014501.
27 A. Vesel and M. Mozetic, *Vacuum*, 2012, **86**, 634–637.
28 M. J. Perez-Roldan, D. Debarnot and F. Poncin-Epaillard, *Rsc Adv.*, 2014, **4**, 31409–31415.
29 M. J. Perez-Roldan, D. Debarnot and F. Poncin-Epaillard, *Rsc Adv.*, 2014, **4**, 64006–64013.

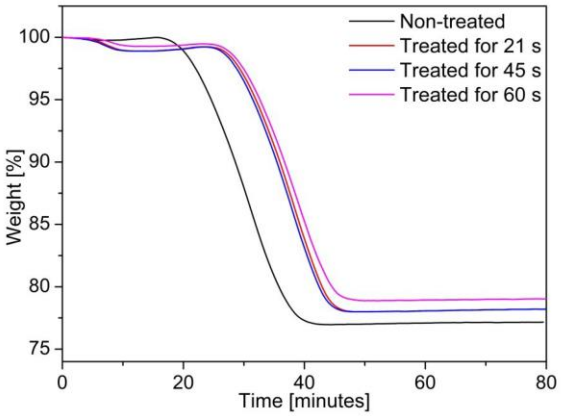
 This journal is © The Royal Society of Chemistry 2015

Electronic Supplementary Material (ESI) for RSC Advances.
This journal is © The Royal Society of Chemistry 2015

Supporting information:

Thermogravimetric analysis (TGA)

NETZSCH STA 409 PC/PG was employed to study the pyrolytic degradation of the composite material. A thin layer from the plasma modified surface (41mg) was cut using a diamond saw for the analysis. The samples were heated in an alumina crucible at a heating rate of 10°C/min. In the TGA spectrum, for the non-treated sample, the degradation was observed only in one stage whereas the plasma modified samples showed degradation in 2 stages. The first stage of degradation during pyrolysis, which is only observed for the plasma treated samples shows the existence of smaller polymer or volatile fragments created by plasma degradation and etching. The increased mass loss due to the pyrolysis was much higher for the non-treated sample, which seen from decreased loss within prolonged treatment times, indicating larger quantities of polymer on the sample surface. Beside this results also demonstrate that the char formation possibility decreases with selective etching of polymer.



Chapter 5

Optimization of Plasma Etching Process in Ar/O_2 Plasma for Improved Surface Tracking Properties

In the previous chapter, we demonstrated that the surface tracking properties of polymer composites, measured in terms of CTI are improved by the selective removal of the superficial polymer layer. This was achieved with the plasma process in pure O_2 plasma, where the process was not optimized. In this chapter, the selective polymer removal is carried out by treating the composite material with low pressure Ar/O_2 gas discharge. The plasma is quantitatively analyzed by combining various probe measurement techniques. The increase in the number of electrons with Ar addition increased the efficiency of plasma etching due to increased density of dissociated atomic O, which was the major etchant presented in the system. The result density of atomic O is also related to the partial pressure of the feeding O_2. This study further reveals that the ionic species predominantly contribute to surface heating during processing. Furthermore, this study prove that the molecular O_2 itself is not able to chemically react with the carbon layer, whereas it points towards the possibility of the reaction between the surface polymer and the metastable oxygen species.

This chapter addresses thesis Objectives 2 and 3.

Regarding my contribution: I performed the plasma treatments, CTI measurements and jointly wrote the manuscript with co-authors.

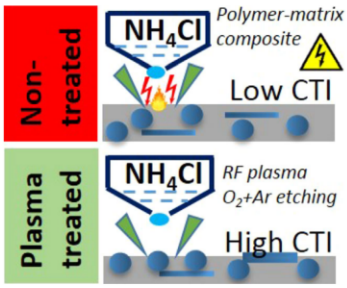
Full Paper

Plasma Processes and Polymers

Selective Plasma Etching of Polyphenolic Composite in O_2/Ar Plasma for Improvement of Material Tracking Properties

Harinarayanan Puliyalil, Gregor Filipič, Uroš Cvelbar*

Compositing with suitable fillers is a common strategy to improve the electrical insulation properties of polymer materials, which is limited by the carbonization of protruding surface polymer. To resolve this, we performed an Ar/O_2 plasma etching on glass-filled polyphenolic composite to uncover the fillers by selective removal of the surface polymer. Exposure of the glass fillers increased the performance level up to 65%, which enabled the material to be used as insulator for commercial applications. Plasma diagnostics with probe measurements and emission spectroscopy revealed that the etching rate was mostly influenced by the neutral oxygen atom density rather than O_2 or Ar ions. Additionally, Ar content in the reactor chamber could control the densities of species, i.e., neutral oxygen density, and thereby polymer etching rate.



1. Introduction

For past few decades, plasma functionalization and etching were recognized as efficient tools for the processing of polymer or polymer-based materials for energy storage, biomedical applications, automotive industry, and sensing devices.[1–5] Surface modification of polymer materials by functionalization or etching was used for the surface nanostructuring, improved adhesion, water repellence, or grafting of suitable surface coatings.[6,7] Among various surface properties, the degradation of polymer materials was studied extensively under various chemical and physical environments due to interest for technology transfer into the industrial scale processing. To monitor the surface processing and kinetics, infrared microscopy was found to be one of the efficient tools for monitoring the polymer degradation mechanisms in various physical and chemical environments.[8] Among different plastic materials, the thermal and chemical degradation rates were highly influenced by the extent of antioxidants lost during the material processing or with aging.[9,10] When dealing with the stability of polymers under high voltage electric arcing, the comparative tracking index (CTI) is the standardized measurement (by International Electrotechnical Commission IEC 60112 standards), which represents the basic safety test for any material used as an electrical insulator.[11] The test apparatus includes two metallic electrodes (usually made of Pt) which induce electric stress on the horizontal plane of the material to be tested. During the experiment, the surface is moistened with 0.1% NH_4Cl solution having a conductivity less than 1 mS m^{-1}. Tracking voltage of a particular material is the maximum voltage at which there is no tracking (surface sparking, burning) after wetting the surface with 50 drops of NH_4Cl. According to the IEC standards, materials are placed in performance levels,

H. Puliyalil
Jozef Stefan International Postgraduate School, Jamova cesta 39, 1000 Ljubljana, Slovenia
Prof. U. Cvelbar, H. Puliyalil, Dr. G. Filipič
Jozef Stefan Institute, Jamova cesta 39, 1000 Ljubljana, Slovenia
E-mail: uros.cvelbar@ijs.si

© 2016 WILEY-VCH Verlag GmbH & Co. KGaA, Weinheim

where the level 0 is of the highest quality with CTI over 600 V. For polymeric materials used in commercial devices, the materials should be at least in performance level 2 (250–399 V). Typically, the improvement in CTI performances of polymer materials is done by the addition of suitable fillers, which do not form condensed char and act as a barrier against tracking.[12]

The major disadvantage of polymer composites as insulating materials is the superficial polymer layer, which covers the fillers and is prone to the CTI test failure. The efficient removal of the thin surface layer is of at most importance for improving the CTI properties of the polymer composite. This is easily achieved by the plasma selective etching, and thus utilizing the distinct chemical stability of various fillers inside.[13] Recently, the selective oxygen plasma etching of glass filled polyphenolics was reported for the improved tracking resistance.[14] However, more studies are needed for understanding the process mechanisms, the optimization of plasma parameters, and to increase the etching efficiency with controlled surface temperature during the process. Herein, we address these issues and use O_2 plasma with Ar addition for improvement of etching efficiency and discuss the role of different plasma species in the process. The introduced processing method improves the tracking resistance properties of glass filled polyphenolic composites even better than just reported O_2 plasma, and opens an inexpensive route for reducing the amount of expensive fillers needed in composites for the electric insulation. A polyphenolic matrix is specifically chosen as a test subject because it is extensively used in insulating and engineering devices. The additives are from glass despite its poor tracking properties, since they are inexpensive compared to the melamine filled polyesters or polyamides, which are typically used in insulating devices.

2. Experimental Section

The chemical structure of the used polymer resin is presented in Figure 1. The polyphenol (phenol-formaldehyde Novolac resin) matrix composite material that contained 60–80% glass fibers (dimeter $< 8\,\mu m$ and length $> 10\,\mu m$) and micro glass spheres (dimeter 3–8 μm) was used for our experiments. The composites were commercially bought and prepared by injection molding process. The molded composites were cured in three stages: in the initial stage for 2 h at 160 °C, which was followed by 4 h at 180 °C, and the last for 4 h at 210 °C (information provided by the manufacturer: Vyncolit Sumitomo Bakelite Co. Ltd.).[14] The inductively coupled plasma was generated by AE Cesar RF 13.56 MHz generator at a total pressure of 80 Pa and a discharge power of

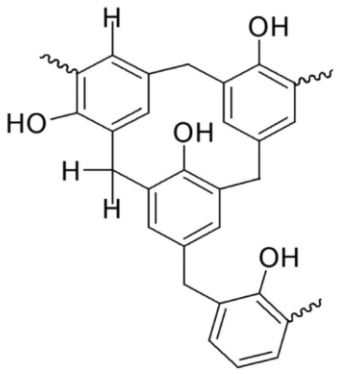


Figure 1. Chemical structure of the polymer matrix.

100 W. The pressure inside the chamber was maintained at 80 Pa for all Ar/O_2 gas mixtures by adjusting the gas flow rates. During the process, the induction coil and plasma chamber were cooled with water flow and forced air, respectively. The samples were treated inside the glass chamber, 3 cm away from the coil to control the sample overheating due to the intense exposure of reactive plasma species. A schematic of the plasma reactor used for experiments is presented in Figure 2. The excited plasma species inside the chamber were monitored from a side by optical emission spectroscopy (OES) with Avantes AvaSpec-3648 spectrometer. During plasma treatment, the temperature on the sample surface was monitored by thermal imaging using IR camera FLIR SC5600. The density of neutral oxygen atoms and ions generated inside the empty plasma reactor were determined by nickel catalytic probe and symmetric Pt double Langmuir probe, respectively. The samples were weighed before and after the plasma treatment to compare the etching rates in terms of mass lost per cm^2 on the exposed surface, where the possible mass loss due to filler detachment was disregarded. CTI performance levels of composite samples were analyzed with PTL Tracking Test Apparatus M31.10 according to IEC 60112:2003 standard. The apparatus consisted of two Pt electrodes having a rectangular cross section of 5 mm × 2 mm, which had a cutting edge. The cutting edges that had

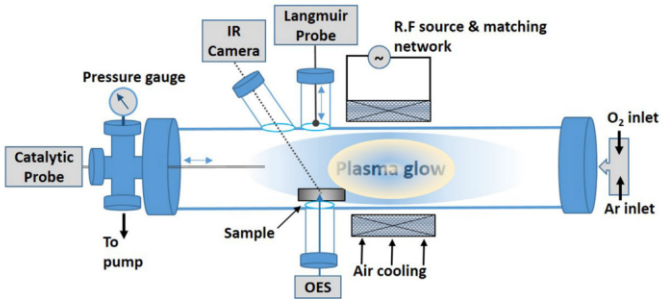


Figure 2. Schematic of plasma etching system equipped with the inductively coupled RF generator.

© 2016 WILEY-VCH Verlag GmbH & Co. KGaA, Weinheim
DOI: 10.1002/ppap.201600005

width > 0.1 mm were touching the sample specimen, separated by a distance of 4 mm. A power supply was connected to the electrodes which provided a variable voltage in the range of 100–600 V. Analytical reagent grade 0.1% NH_4Cl solution was allowed to drop centrally between the electrodes from a height of 35 mm. The time required for dropping 50 drops was 25 ± 2 min. The tracking voltage was estimated as the highest voltage at which there was no surface tracking after moistening the surface with 50 drops of 0.1% NH_4Cl solution. The surface morphology was imaged with FE-SEM Jeol JSM-7600F with electron beam energy of 2 kV. For the additional testing to study temperature effects, the samples were heated inside OTF-1200X Dual Zone Split Tube Furnace, which was connected to mass flow controllers and rotary pump to achieve desired gas compositions and pressures comparable to the plasma chamber.

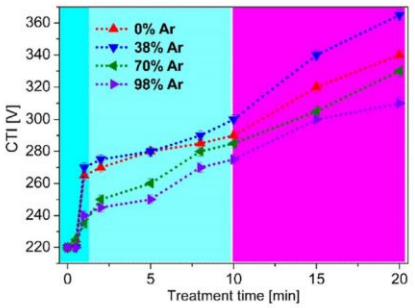


Figure 4. Comparative tracking index (CTI) values in respect to plasma treatment time within different Ar/O_2 gas compositions.

3. Results and Discussion

After the selective plasma removal of the polymer, the surface was left with exposed glass fibers and glass balls embedded in the polyphenol-matrix. As seen from the SEM images (Figure 3), the polymer removal from the surface was complete after exposing to 38% Ar in O_2 plasma (Figure 3B), whereas in the case of 98% Ar in O_2 plasma (Figure 3C), the polymer removal was not so efficient. The non-efficient removal is seen from a large amount of polymer residue on top of the glass fillers. During plasma etching, the polymer is removed to a depth around a few micro meters as the micro sized fillers became well exposed and visible on the surface. On the other hand, the glass fibers are unaffected by the plasma reactive species due to the resistance of the glass substrate toward oxygen radicals and ions. As a result of polymer removal, the CTI index of surface increases from initial 220 up to 365 V, which is a great improvement.

The variation of CTI values for samples etched in various Ar/O_2 gas compositions is presented in Figure 4. For the non-treated samples, the tracking index value was 220 V. When the non-treated sample was subjected to the test, it failed with an immediate appearance of a flame that resulted from the charred polymer surface layer (as schematically presented in Figure 5). However, after treating the samples with a gas mixture of 38% Ar in O_2, the tracking performances increased to a value of 365 V after 20 min. In all the gas compositions, the samples reached performance level 2 and are thus allowed to be used for commercial purposes. Further increase in CTI values is restricted in our case by the presence of small polymer residues left on the surface. Prolonged treatments just lead to detachment of the fillers from the matrix causing high extent of damages and defects on the surface.

To reveal how the etching process actually occurs, the plasma species involved in the etching process and etch products need to be determined and monitored. For this reason, the OES measurements are utilized, which provided the information on the excited plasma species inside the chamber during the processing (Figure 6). Emission spectra were dominated by two characteristic lines from excited oxygen atom at 777 nm $[O(3p^5P \rightarrow 3s^5S)]$ and 844 nm $[O(3p^3P \rightarrow 3s^3S)]$.[15] These observed species are generated inside the plasma either by the dissociative excitation or direct electron impact excitation of the molecular oxygen. After Ar gas is added, the spectra are populated by excited Ar species as presented in Figure 6. The most prominent Ar

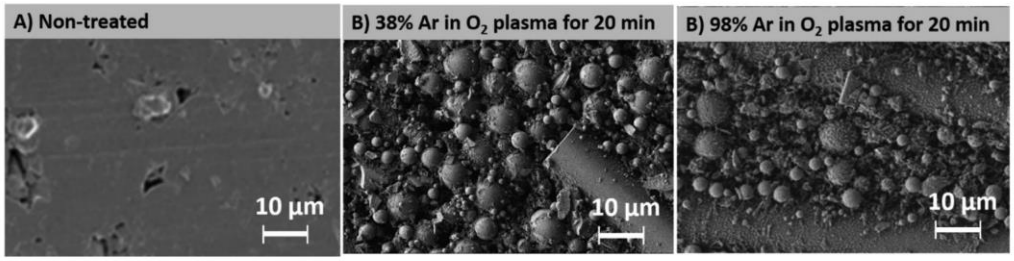


Figure 3. SEM images of (A) non-treated sample; (B) plasma treated sample in gas mixture 38% Ar in O_2 for 20 min or (C) 98% Ar in O_2 for 20 min.

© 2016 WILEY-VCH Verlag GmbH & Co. KGaA, Weinheim

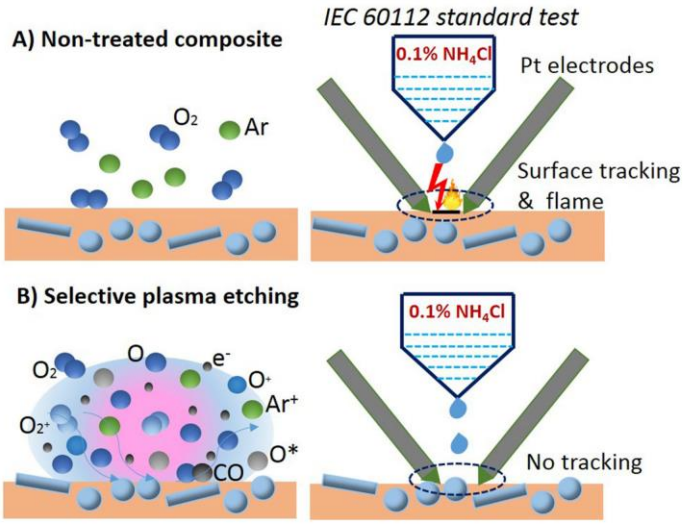


Figure 5. Schematic of CTI performances on surfaces of non-treated and plasma exposed samples.

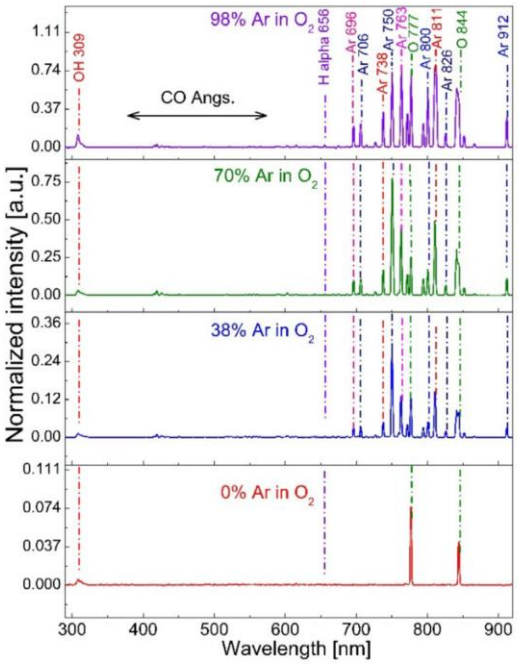


Figure 6. Representative optical emission spectra at 10th minute during the treatment for various gas mixtures of Ar–O_2.

lines are observed at wavelengths 750.4 nm ($2p_1$–$1s_2$), 763.5 nm ($2p_6 \rightarrow 1s_5$), 794 nm ($2p_4 \rightarrow 1s_3$), and 811 nm ($2p_9 \rightarrow 1s_5$).[16] The lines become more intensive with the higher Ar gas ratio. Due to the limitation in spectral resolution some lines are overlapped, e.g., the oxygen peak at 844 nm is merged with Ar peak emitted at 840 nm and appears now as a multiplet. However, the spectra indicate also the presence of hydrogen in the plasma with H_α transition at 656 nm as well as the molecular OH ($A^2\,\Sigma^+ - X^2\,\Pi$ (0,0)) band at 309 nm. Hydrogen is produced by the dissociation of the desorbed water vapor from the plasma chamber walls and the sample surface. In addition, it can be a by-product of polymer etching. In our case, the intensity of H_α band is very weak as seen from Figure 6. Polymer etching is suggested also by the presence of spectral lines from CO molecular bands, which were observed in the CO Angstrom region and are accompanying polymer etching process inside O_2 containing plasmas.[16,17] Intensities of all the emission peaks are increased with Ar content, which is ascribed to higher electron density and consequently higher excitation efficiency of plasma.

Despite indication of which species are created inside plasma during processing, there is a lack of quantified measurements. For this reason, the densities of neutral oxygen atoms were determined by standard thermocouple Ni catalytic probe, the operation of which is based on the heterogeneous recombination of O atoms on the metallic surface, where the probe surface temperature is correlated to O atom flux onto the probe tip (Figure 7A).[18] Moreover the quantitative analysis of major oxygen and argon ionic species (O_2^+ and Ar^+) were performed with a symmetric double Langmuir probe. In this analysis, we have neglected all other ion possibilities (O^+, O_2^-, O^-) on assumptions that: (i) the negative ions do not influence the Langmuir characteristics drastically because they are thermalized just slightly above the room temperature, and thus do not have sufficient energy to influence the Langmuir characteristics at the negative potential. In addition, the density and energy of electrons is much higher and they dump the negative ion influence in floating and positive probe regime; (ii) the positive oxygen ion O^+ density is negligible, because the reaction rate for electron impact ionization of O_2 directly to O^+ is small, and the electron ionization of O atom is a two-step process that also involves the splitting of oxygen molecule in the first place, and thus the overall reaction rate is much smaller to reaction rate for O_2^+

© 2016 WILEY-VCH Verlag GmbH & Co. KGaA, Weinheim

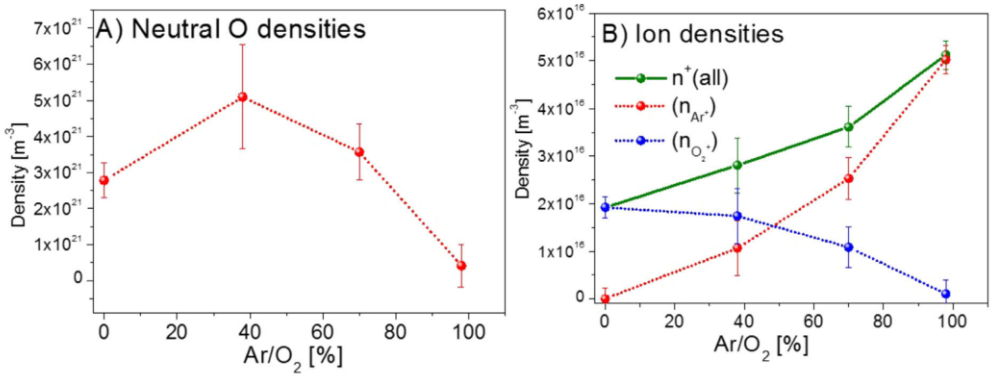


Figure 7. Measured densities of oxygen atoms and plasma ions at various gas mixture compositions of Ar–O_2: (A) neutral oxygen atom densities and (B) densities of ions for Ar^+ and O_2^+.

ionization by electron impact.[19] The distinction between O_2^+ and Ar^+ species was roughly estimated by assuming that Ar ionization inside the system is twice more efficient than the oxygen based on the rate coefficients for the electron impact ionization at presented pressure and electron temperature (approximately 4.8×10^{-15} and $2.2 \times 10^{-15}\,m^3\,s^{-1}$, respectively).[19] The ratio of number densities was correlated with the partial pressure of the gases and then applied to Langmuir probe analysis to estimate the absolute densities of each ions (Figure 7B).

The surface temperature variation during the treatment, which significantly influences etching dynamics, is another important factor (Figure 8A). Moreover, the temperature also reveals information about reactions on the surface, since it is the result of interacting species and exothermic reactions. Since plasma is applied to a composite surface, the thickness measurement is not suitable to assess the etching rate. However, we are able to estimate the etching rates from the total mass loss after exposing the samples to plasma (Figure 8B). The highest surface temperatures (~225 °C) and etching rate are found when the samples are treated with gas mixture 38% Ar in O_2.

One assumes that the ion and radical flux onto the surface are the key parameters which decide the etching rate of polymer inside the plasma and also attribute to surface heating. The kinetic energies of the ions bombarding the surface are estimated between 34 and 40 eV. For simplicity, equations for collisionless sheath were used.[19] On the surface, ions recombine to form neutral atoms with probability ~1, which adds this ionization energy to the

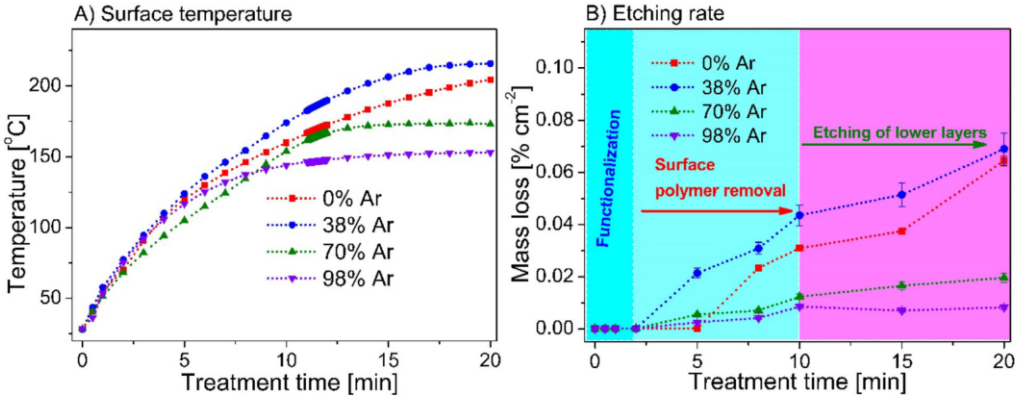


Figure 8. (A) Surface temperature during the plasma treatment of polymer composites with corresponding (B) etching rates in various gas compositions.

© 2016 WILEY-VCH Verlag GmbH & Co. KGaA, Weinheim

surface heating. However, despite extensive ion energy, the density of ions is relatively low and the resulting energy flux to the surface is low – approximately in the range 40–90 mW cm^{-2}. On the other hand, O atoms bring about 2.5 eV per atom to the surface when they recombine to form oxygen molecule. The probability for oxygen atom recombination is ~0.30 for the polypropylene material at the surface temperature of around 100 °C.[20] Due to much larger oxygen atom density (presented in Figure 7A), the energy flux from the atomic species to the sample surface is much higher than ion's (in the range 4000–12 000 mW cm^{-2}).Our hypothesis is that the ions contribute a minor part to the localized surface heating whereas O atoms react with the exposed surface to form oxidized products.[21] Here it is worth noticing that the thermal energy contribution from the polymer-plasma radical reaction to the surface heating is difficult to evaluate.

As we compare the etching rate, we find that small addition of Ar to oxygen increases the etching rate. However, larger amount of Ar in the system decreases the etching rate. When the gas composition was 98% Ar in O_2, the total ion density (Ar^+ and O_2^+) was found to be 5×10^{16} m^{-3}. On the other hand, when the plasma was generated without Ar, the ion density was about 2.5-times lower, although the etching rate was higher. Moreover, the oxygen atom density is approximately 3×10^{21} m^{-3} with no argon, and only 4×10^{20} m^{-3} at 98% Ar. Thus, it becomes more evident that the predominant species which induced the etching are the dissociated atoms and not ions. The addition of Ar increases plasma density and consequently the dissociation of oxygen molecules, since it has higher electron impact dissociation cross-section.[22] Based on results as from Figure 8B, one presumes that the etching process efficiently starts only after 2 min of exposure. Until then the functionalization with polymer bond breaking is the leading process. Along with increased exposure time, the surface temperature started to increase and the etching rate is enhanced, leading away from mere functionalization to polymer bond breaking. On the other hand, an increase in the surface temperature increases the softness of the polymeric substrate and provides an additional kinetics to the etching mechanism. One possible etching route is also the direct reaction between the molecular oxygen with the polymer. This was rechecked with experiments in the hot furnace at the same pressure, gas composition, and at the temperature of 200 °C. Results confirmed that the molecular oxygen is incapable to induce etching at the tested conditions.

As revealed by the probe measurements, the neutral O atom density was slightly higher when the feeding gas contained 70% Ar in O_2 compared to that of pure O_2 plasma. However, the etching rate was higher in the latter case. The reason of reduced etching with higher Ar content might be due to the lower concentrations of oxygen metastable and excited species, which we were not able to measure in our system. In general, the influence of metastable atoms on the etching is discarded in many reports due to their low potential energy and density compared to the neutral oxygen atoms.[23] However, some recent reports disclose that metastables are efficient enough to etch away relatively unstable residues from the surface of carbonaceous materials.[24,25] The effect of such metastable atoms is potentially pronounced especially at elevated surface temperature due to the lower chemical activation energy barrier of the polymer molecules toward oxygen. Further, as reviewed by Schweitzer and Schmidt, one of the major quenching mechanism of the excited singlet metastable oxygen species include chemical bonding with the molecules in the medium.[26] The report by Gudmundsson and Thorsteinsson, revealed that the metastable oxygen atom densities at lower pressures (below 15 Pa) increased for 15% with Ar addition (up to ~43%).[27] Oxygen metastables at higher pressures (above 100 Pa) were measured by Rakhimova et al. and showed that the number density of metastable oxygen molecules and atoms decreased with the increase in the concentration of argon.[28] In the case of 98% Ar gas mixture, the poor etching rate seems obvious, due to the lack of chemical assistance in the absence of dissociated O atoms.[29,30] The preferential removal of the polyphenolic component from the composite surface enabled the composite to be used in insulating devices as per the norms of IEC safety standards. The removal of the polymer was mostly done by the radical atoms, whereas the incoming ions contributed to surface heating. One possible technique to increase the etching rate is sample biasing, which will result in higher surface temperature and even sputtering due to increased ion collisions.[21,31] This is not advisable since elevated temperature can adversely affect the properties of the matrix underneath. Comparison of the plasma characteristics with the etching rate pointed toward the possible involvement of metastable species in the chemical reactions of etching. However, to get more evidence to this speculation both qualitative and quantitative analytical techniques (e.g., absorption spectroscopy) should be combined with the probe measurements and the optical emission spectroscopy.

4. Conclusion

The effect of Ar addition in to O_2 plasma on the etching rate of polymeric composite is presented for optimization of a new innovative technology for improvement in the CTI performances. The selective removal of the polymer is achieved by utilizing the difference in the chemical bond stability and probability for reaction with reactive plasma species of glass fillers and the polyphenolic matrix. The dissociation of oxygen molecules into reactive atoms is

© 2016 WILEY-VCH Verlag GmbH & Co. KGaA, Weinheim

enhanced due to the increased number of available electrons with the addition of Ar. The contribution of oxygen neutrals is directly linked to the chemical reaction with the carbon layer, whereas the ionic species contributed mostly to the surface heating. On the basis of comparison of radical densities and etching, we presumed the importance of the chemical assistance of reactive metastable oxygen species for etching at lower oxygen concentrations.

The etching rate was measured by the mass loss after plasma exposure and was in good agreement with the CTI performances, which revealed that the surface tracking is directly associated with the surface polymer removal. The best tracking performance was obtained after exposing the samples with 38% Ar in O_2, which had the highest density of dissociated oxygen atoms of the order of $5 \times 10^{21}\,m^{-3}$. With higher concentrations of argon (98%), the background density of neutral oxygen molecules decreased, and thus also the oxygen atom density decreased. The etching rate was the lowest at 2% O_2 in the gas mixture due to very small oxygen reactive species density in the system. Although the embedded glass fibers were moderately exposed after etching in 98% Ar in O_2 plasma, the observed polymer residues resulted in a failure at lower voltage during CTI tests.

Acknowledgements: Authors gratefully acknowledge Slovenian Research Agency (ARRS) program P2-0082 and grant L2-6769 for the financial support, and Faculty of Electrical Engineering, University of Ljubljana for lending the IR camera and Matic Hajdič for his assistance with thermal imaging. H. P. thanks Jozef Stefan International Postgraduate School for the grant from Innovative Scheme for Research

Supporting Information is available from the Wiley Online Library or from the author.

Received: January 14, 2016; Revised: April 8, 2016; Accepted: April 29, 2016; DOI: 10.1002/ppap.201600005

Keywords: composites; etching selectivity; plasma etching; surface tracking

[1] M. R. Sanchis, O. Calvo, O. Fenollar, D. Garcia, R. Balart, *Plasma Process. Polym.* **2007**, *4*, S1091.
[2] G. Filipič, O. Baranov, M. Mozetič, K. Ostrikov, U. Cvelbar, *Phys. Plasmas (1994-present)* **2014**, *21*, 113506.
[3] J. Shen, Q. Sun, Z. Zhang, C. Cheng, Y. Lan, H. Zhang, Z. Xu, Y. Zhao, W. Xia, P. K. Chu, *Plasma. Process. Polym.* **2015**, *12*, 252.
[4] U. P. M. Ashik, W. M. A. Wan Daud, H. F. Abbas, *Renew. Sustain. Energy Rev.* **2015**, *44*, 221.
[5] L. Saša, P. Nevena, M. Maja, P. Dušan, J. Milena, B. Diana, M. Slavko, M. Dejan, M. Gordana, M. Pavle, P. Zoran, *New J. Phys.* **2010**, *12*, 083037.
[6] H. Yu, Z. Z. Chong, S. B. Tor, E. Liu, N. H. Loh, *RSC Adv.* **2015**, *5*, 8377.
[7] P. Slobodian, P. Riha, R. Olejnik, U. Cvelbar, P. Saha, *Compos. Sci. Technol.* **2013**, *81*, 54.
[8] S. Damodaran, T. Schuster, K. Rode, A. Sanoria, R. Brüll, M. Wenzel, M. Bastian, *Polym. Degrad. Stab.* **2015**, *111*, 7.
[9] N. Chandran, S. Chandran, H. J. Maria, S. Thomas, *RSC Adv.* **2015**, *5*, 86265.
[10] S. Damodaran, T. Schuster, K. Rode, A. Sanoria, R. Brüll, N. Stöhr, *Polymer* **2015**, *60*, 125.
[11] M. Ugur, O. N. Ucan, A. Kuntman, N. Ozmen, A. Merev, Electrical Insulation and Dielectric Phenomena, 1999 Annual Report Conference, **1999**, *151*, 154–157.
[12] S. Sullalti, M. Colonna, C. Berti, M. Fiorini, S. Karanam, *Polym. Degrad. Stab.* **2012**, *97*, 566.
[13] U. Cvelbar, S. Pejovnik, M. Mozetič, A. Zalar, *Appl. Surf. Sci.* **2003**, *210*, 255.
[14] H. Puliyalil, U. Cvelbar, G. Filipič, A. D. Petric, R. Zaplotnik, N. Recek, M. Mozetič, S. Thomas, *RSC Adv.* **2015**, *5*, 37853.
[15] N. Krstulović, I. Labazan, S. Milošević, U. Cvelbar, A. Vesel, M. Mozetič, *J. Phys. D: Appl. Phys.* **2006**, *39*, 3799.
[16] M. Schulze, A. Yanguas-Gil, A. v. Keudell, P. Awakowicz, *J. Phys. D: Appl. Phys.* **2008**, *41*, 065206.
[17] Z. Kregar, M. Bišćan, S. Milošević, M. Mozetič, A. Vesel, *Plasma Process. Polym.* **2012**, *9*, 1020.
[18] D. Babič, I. Poberaj, M. Mozetič, *Rev. Sci. Instrum.* **2001**, *72*, 4110.
[19] M. A. Liberman, A. J. Lichtenberg, *"Principles of Plasma Discharges and Materials Processing"*, 2nd Edition, John Wiley & Sons, Hoboken, New Jersey, USA **2005**.
[20] S. Gomez, P. G. Steen, W. G. Graham, *Appl. Phys. Lett.* **2002**, *81*, 19.
[21] G. Filipič, O. Baranov, M. Mozetič, U. Cvelbar, *J. Appl. Phys.* **2015**, *117*, 043304.
[22] J. T. Gudmundsson, E. G. Thorsteinsson, *Plasma Sources Sci. Technol.* **2007**, *16*, 399.
[23] T. Vrlinič, A. Vesel, U. Cvelbar, M. Krajnc, M. Mozetič, *Surf. Interf. Anal.* **2007**, *39*, 476.
[24] L. G. Nair, A. S. Mahapatra, N. Gomathi, K. Joseph, S. Neogi, C. P. R. Nair, *Appl. Surf. Sci.* **2015**, *340*, 64.
[25] J. Y. Jeong, S. E. Babayan, V. J. Tu, J. Park, I. Henins, R. F. Hicks, G. S. Selwyn, *Plasma Sources Sci. Technol.* **1998**, *7*, 282.
[26] C. Schweitzer, R. Schmidt, *Chem. Rev.* **2003**, *103*, 1685–1758.
[27] J. T. Gudmundsson, E. G. Thorsteinsson, *Plasma Sources Sci. Technol.* **2007**, *16*, 399.
[28] T. V. Rakhimova, A. S. Kovalev, A. T. Rakhimov, K. S. Klopovsky, D. V. Lopaev, Yu. A. Mankelevich, O. V. Proshina, O. V. Braginsky, A. N. Vasilieva, *34th AIAA Plasmadynamics and Lasers Conference, American Institute of Aeronautics and Astronautics* **2003**, 4306.
[29] K. S. Siow, S. Kumar, H. J. Griesser, *Plasma Process. Polym.* **2015**, *12*, 8.
[30] D. Kontziampasis, T. Trantidou, A. Regoutz, E. J. Humphrey, D. Carta, C. M. Terracciano, T. Prodromakis, *Plasma Process. Polym.* **2016**, *13*, 324.
[31] P. Knoll, J. Reynvaan, M. Mayer, S. Surnev, P. Geistlinger, K. Krenn, K. Ettinger, C. Prietl, A. Hohenau, J. Gruenwald, B. Kunert, R. Resel, *Diam. Relat. Mater.* **2016**, *65*, 96–104.

© 2016 WILEY-VCH Verlag GmbH & Co. KGaA, Weinheim

Chapter 6

Comparison of Selective Plasma Etching in Various RF Gas Discharges

The importance of selective removal of the surface polymer from glass-filled polyphenolic composites is presented in the previous chapters. The efficiency of O_2 or Ar/O_2 plasma was presented and the process was optimized. However, for the commercial applications, the other feeding gases including H_2, N_2, and NH_3 are also widely used.
This chapter focuses on the systematic comparison of the etching efficiency of H_2, N_2, and NH_3 with the most frequently used O_2 plasma. The etching rates were measured in terms of the mass removed from the surface after the plasma treatment. The study reveals that the etching rates inside various RF gas plasmas increase as a function of applied power. However, the etching efficiency in H_2 and N_2 plasma is much lower than that of O_2 plasma, whereas NH_3 plasma shows a moderate etching efficiency. The etching process usually propagates through functionalization, where the primary bond breaking occurs at the bond with the lowest bond energy. To confirm this speculation, we tried to unravel this with the support of optical emission spectroscopy and XPS analysis during and after plasma interaction with polyphenolic resin.

This chapter addresses thesis Objective 4.

Regarding my contribution: I contributed to the plasma treatments, emission spectroscopy, XPS analysis and prepared the manuscript.

RSC Advances

ARTICLE

Tackling chemical etching and its mechanisms of polyphenolic composites in various reactive low temperature plasmas

Received 00th January 20xx,
Accepted 00th January 20xx

DOI: 10.1039/x0xx00000x

www.rsc.org/

H. Puliyalil[ab], G. Filipič[a], J. Kovač[ab], M. Mozetič[ab], S. Thomas[c], U. Cvelbar[ab]*

Selective removal of the surface polymer layer from the glass filled polyphenolic composite is important while using them for applications in extreme environments. Inductively coupled low temperature plasma discharge was verified to facilitate chemical etching to selectively remove the surface polymer from the glass filled polyphenolic composite. The etching rate inside the plasma was compared with commercially important feeding gases including H_2, N_2, O_2 and NH_3 as a function of discharge power. The protruding surface polymer was removed in volatile molecular fragments, whereas the glass additives stayed unaffected. The etching rate is shown to increase as a function of applied power inside all used gas discharges. Irrespective of the applied power, O_2 plasma displayed the highest etching rate. Furthermore, by combining optical emission spectroscopy (OES) and X-ray photoelectron spectroscopy (XPS) analyses, the work is extended to mechanistically present the possible chemical pathways which lead to creation of various functional groups on the surface during the plasma-surface interactions. This gives a new outlook towards the future applications of low temperature plasma processing in composite industry for surface modification and selective etching.

Introduction

Plasma is denoted as the complex mixture of high energy ions, radicals, excited atoms and electrons which was successfully implemented for fabrication of high performing micro/nanodevices including nanofibres, graphene sheets, thin coatings, quantum dots, etc.[1-5] Plasma processing is always associated with complex physical and chemical interactions in gaseous phase as well as at the plasma-surface interface. However, one of the major challenges is the precise understanding of chemical interactions and reaction pathways of different energetic plasma particles on the designated surfaces. This is extremely important when plasma is used for surface modification of delicate materials including polymeric substrates which are important in countless applications in chemistry, chemical engineering, physics, biology and even medicine.[6-8] Surface modifications including functionalization and etching are preferred with low energy particles due to the high heat sensitivity of polymeric substrates. For treating such heat sensitive materials, weakly-ionized highly-dissociated plasmas in thermal non-equilibrium are more suitable, since they are able to restrict the thermal damages caused by extensive ion bombardment on the surface.[9]

The solidity of various materials towards the plasma interacting particles has strong correlation with the type and energy of the bonds in the molecular or solid material formation. The typical example for this is the etching of graphene sheets with H_2 plasma. Due to the higher reactivity of the C-C bonds at the edge, functionalization and followed carbon removal is faster from the edge of the graphene sheet compared to the basal planes.[10,11] These differences observed in the materials etching rates with respect to their chemical stability or structures are relevant for the polymeric substrates as well. Various polymers are etched at different rates depending upon their physical and chemical properties including the bond strength, crystallinity and the ability to cross link on the surface upon irradiation, etc.[12,13] This is the general outset for preferential plasma removal of one material over another.

The etching rates inside the plasma are typically higher for macromolecular carbon chains comparing to the inorganic materials (minerals, glass, etc.) or the elemental forms of carbon (graphite, carbon nanotubes, etc.). Various polymer materials are usually composited with these organic or inorganic materials in order to improve their material performance in numerous applications.[14-16] In many cases, preferential removal of the polymer matrix or the embedded fillers is utilized for upgrading the properties of such fabricated composites. For better accuracy and precision during such preferential plasma etching, clear understanding of the fundamental chemistry involved is essential. However, the field of plasma science is notably application driven which leads to lack of

[a] Jozef Stefan Institute, Jamova cesta 39, 1000 Ljubljana, Slovenia.
[b] Jozef Stefan International Postgraduate School, Jamova cesta 39, 1000 Ljubljana, Slovenia.
[c] School of Chemical Sciences, Mahatma Gandhi University, PD Hills, Kottayam, Kerala, India
* email: uros.cvelbar@ijs.si

This journal is © The Royal Society of Chemistry 20xx

fundamental understanding of the elemental mechanisms involved in the process. More particularly, when it comes to plasma surface interactions, the basic chemical reactions involved are often on the side track of investigations. One of the main challenges for the plasma community is to control the efficiency of the etching process at atomic or molecular level, which requires a detailed understanding of the processes. Some of the recent articles tried to explore the precise chemical interactions between the plasma particles and polymeric substrates, however the research was limited to atmospheric pressure plasma treatments or limited number of feeding gases.[17]

The fabrication of various composite materials and their suitable surface modifications are essential to devise suitable materials for delicate applications.[1, 18-21] Glass filled polyphenolic composites which are important for engineering applications in aerospace and insulating devices.[22] However, the very thin surface polymer layer found to restrict their performance level in electrical insulation devices, which was found to be improved by the selective plasma etching of the superficial polymer layer.[20] Herein we present a systematic study of plasma chemistry which influences the etching rate and its selectivity for the example case of glass filled polyphenolic resin. Moreover we compare the etching rates of the composite resin for different plasma feeding gases including H_2, N_2, O_2 and NH_3. The fundamental chemical interactions and mechanisms during the treatment process are unravelled by combining various plasma diagnostics and surface analytical techniques.

Materials and methods

Plasma was generated with an inductively coupled RF discharge using AE Cesar plasma generator at a frequency of 13.56 MHz inside a borosilicate glass tube of 80 cm length (Figure 1).[20] Before that the chamber was evacuated to a base pressure (< 1 Pa) using a two-stage rotary pump, and then commercially available gases H_2, N_2, O_2 and NH_3 (Messer) were leaked individually into the system through mass-flow controller (Aera Transformer 785X by Hitachi Metals). The gas flows were controlled to keep the pressure inside the chamber at a constant value of 40 Pa. The plasma was generated at 3 different discharge input powers 100 W, 150 W and 250 W. The inductive coil and the reactor chamber were cooled with chilled water and forced air flow, respectively. The testing samples – commercially bought polyphenolic resins (phenol-formaldehyde Novolac resin) filled with 60-80% of glass fibres and glass spheres were prepared, according to the manufacturer: Vyncolit Sumitomo Bakelite Co. Ltd., by injection moulding process. During the moulding process, the temperature inside the tool cavity was kept at 160 - 170 °C. The samples thus obtained were cured in three stages: i) 2 h at 160 °C, ii) 4 h at 180 °C and iii) 4 h at 210 °C. For the treatments, the samples were cut to dimensions 1cm × 1cm × 5mm (lbh) and placed on a glass substrate inside the plasma chamber. The etch rates were calculated from the mass lost after the plasma exposure, where the possible mass loss from the filler detachment was neglected. During the processing, the qualitative analysis of the plasma was carried out by Avantes AvaSpec-3648 optical emission spectrometer. The sample surface temperature was measured with an infrared pyrometer (Raytek Raynger MX4+) through the CaF_2 window with linear transmissivity in the IR region of interest. The surface characterization was done after treatments with X-ray photoelectron spectroscopy (XPS) using the PHI-TFA XPS instrument (Physical Electronics Inc). The sample morphology was imaged with a scanning electron microscope (SEM) FE-SEM Jeol JSM-7600F at electron beam energy of 15 kV.

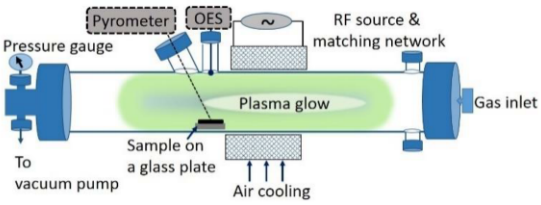


Figure 1. Schematic of the inductively coupled low pressure RF plasma reactor chamber used for the treatment process.

Results and discussion

The etching rates of the polymer-matrix composite were measured in terms of the mass lost after exposing it to various gas plasmas and is presented in figure 2. The etching was done selectively for polymer over inert glass fillers. The comparison of the etching rates revealed that the etching rates were maximal for O_2 plasma at all the 3 discharge powers used for the treatment process. Additionally, the etching rates showed an increasing trend with the increase in the discharge power. This was evidently due to the higher degree of dissociation of the feeding gas with the increase in applied discharge power.[23,24] While comparing the etching rates at lower discharge power (100 W), the etching rates inside H_2, N_2 and NH_3 were very close to each other, whereas the etching rate inside the O_2 plasma was comparatively higher. At 100 W discharge power, the observed etching inside the O_2 plasma was around 90%

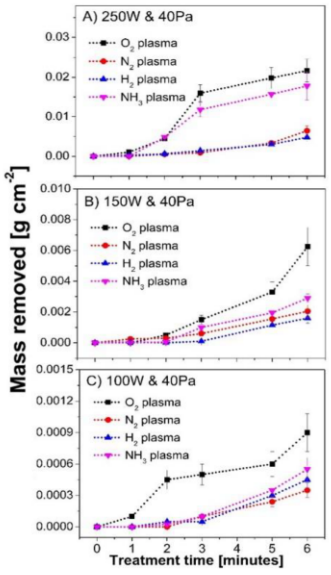


Figure 2. Etching rates in various gas plasmas generated at pressure 40 Pa and different discharge powers A) at 250 W B) at 150 W and C) at 100 W.

This journal is © The Royal Society of Chemistry 20xx

higher than that of H_2 plasma after 6 minutes of exposure. When the discharge power was increased to 250 W, this difference increased up to 3.5 times. This clearly indicated that the etching efficiency as a function of discharge power was more pronounced in the case of O_2 plasma. The plausible explannation for the lower etching rate inside other gas plasmas could be explained in terms of difference in the reactivity of various atomic and molecular species produced during discharge, which is described in the latter section of this article.[25,26]

As seen from the SEM images, the surface of the non-treated composite was completely covered with the polymer and the fillers were well embedded into the matrix (Figure 3A). However, after exposing it to various gas plasmas, the polymer was selectively removed from the surface and the fillers got exposed. The SEM images of the samples treated with these plasmas at 250 W for 3 minutes were compared in figures 3B-3E. This revealed that the surface of the samples treated in O_2 and NH_3 plasma (Figures 3D and 3E) was predominantly polymer residue free. On the other hand, the polymer residue partially covered the embedded fillers on the surface of the samples treated with N_2 and H_2 plasma (Figures 3B and 3C), respectively.

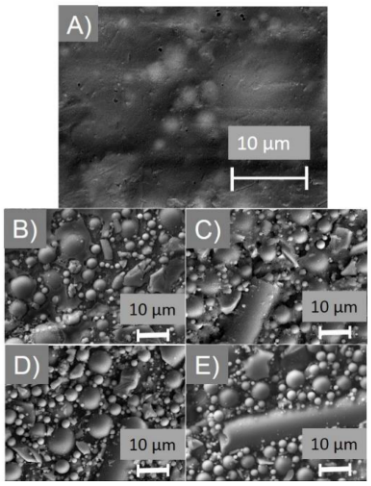
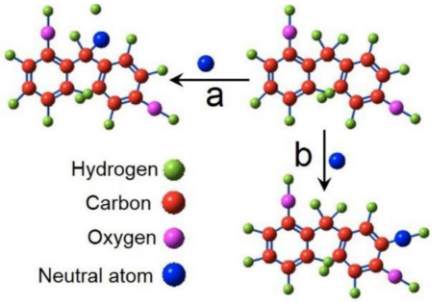


Figure 3. SEM images of non-treated and various plasma treated samples at 250 W for 3 minutes A) non-treated sample B) treated in N_2 plasma C) treated in H_2 plasma D) treated in O_2 plasma and E) treated in NH_3 plasma

Unravelling the origin of etching, the energies of various bond types in the polymer chain play one of the most important roles which determinate the bond breaking mechanism and consequent removal. The bond energy of the aromatic C-C bond is roughly estimated to a value of 4.8 eV. The other possible bond breakings are at the benzylic C-C (3.9 eV) or benzylic C-H (3.8 eV) positions. Compared to the benzylic C-H, the aromatic C-H bond has much higher bond dissociation energy of ~4.2 eV.[27] The primary bond cleavage is always expected at the position with the lowest bond energy. The extra stability is provided by the energy of aromatization, which retards the possibility of ring rupture compared to the stated competing reactions. Thus, one should expect the functionalization to be initiated at the benzylic position. Another major reaction that could be possible is also the quenching of the neutral atomic species by the functionalization of aromatic rings.[28] Namely, the incoming atomic species, generated by the dissociation of the feeding gas in the plasma, react with the aromatic ring in such a way that the proton from the aromatic ring is transferred to the incoming heteroatom causing a functionalization of aromatic ring. During such neutral atom quenching, the incoming plasma species preferably attack the ortho position due to their high electrophilic nature.[29] These two major initiation reactions between the incoming atom and the polymer substrate are represented in Scheme 1. However, further proceedings of the etching process is hard to explain due to the complexity of the competing reactions.



Scheme 1. A) Plasma neutral atom substitutes the hydrogen at the benzylic position B) Neutral atom quenching by proton abstraction from the aromatic ring.

To gain more understanding on the chemical composition and the modifications of surface chemistry during plasma treatments, the XPS analyses were carried out. XPS survey spectrum (0-800 eV) revealed the elemental composition on the surface before and after exposure to different gas plasmas generated at various discharge powers. The case of 250 W treatment for 6 minutes is presented in figure 4. The non-treated sample surface contained mostly carbon (89.4%) and very little of oxygen (9.1%). After the exposure of polymer-matrix composites, the surface carbon content drastically decreased for all tested gas plasmas, whereas the concentration of the oxygen significantly increased. Additionally, the Si content was also increased after the plasma treatment. The Si signal originated from the exposed glass fillers, leading us to the confirmation that fillers are exposed and polymer is removed. After the polymer removal, notable amount of Na and traces of other minerals including Zn and Mg are also observed on the surface as additives to fillers. All these observations pointed out that the plasma treatment reduced the carbon content on the surface by the selective removal of the surface polymer. Another interesting observation is that the nitrogen content was slightly higher for the samples exposed to N_2 plasma rather than the one for NH_3 plasma.

This journal is © The Royal Society of Chemistry 20xx

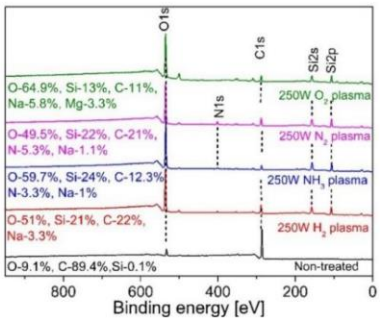


Figure 4. XPS survey spectrum with major elemental compositions for the non-treated sample and the ones treated in various gas plasmas for 6 minutes at an applied power of 250 W.

To compare the surface chemistry before and after the treatments, the deconvolution of C 1s peak was essential. The high resolution (HR) C 1s spectrum of the non-treated sample was fitted with 3 peaks at 284.8 (C1), 285.9 (C2) and 288.6 eV (C3) respectively (Figure 5). The peak at lower binding energy was assigned to C-C/C-H bond types. Thus, the intensity of this peak is connected to the surface polymer content. The peak C2 could be assigned to the C-OH bond originated from the phenolic functionality on the resin matrix, whereas the peak C3 at binding energy around 288.6 eV was assigned to the O-C=O functional groups. However the concentration of O-C=O bonds is very low (~2%), and probably originate from the degraded polymer during the high temperature curing process. Namely, the reports of such effects of curing temperature on the pyrolytic degradation of phenolic resins are found in literature and support this argument.[30]

When the samples are treated with different gas plasmas (like presented case for 250 W and 6 minutes) and compared, the changes in the surface chemistry arise after plasma treatments. The comparison of various plasma treatments revealed that the notable change was in the intensity of the C-C/C-H bond types (Figure 6).

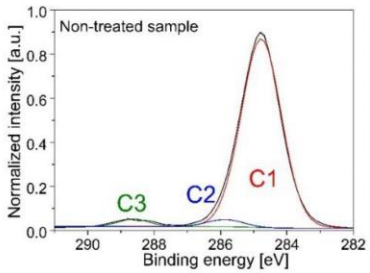


Figure 5. Deconvolution of XPS HR C 1s spectrum of the non-treated polyphenolic sample.

This was evident from the decrease in the intensity of the peak C1 at 284.7 eV. The decrease was more pronounced in the case of NH_3 and O_2 rather than of N_2 or H_2. The peak C3 in the case of O_2 plasma was assigned to the carboxylic functionalities. In the case of NH_3 or N_2 plasma, C2 can be a grouping of C-N and C-O functional groups due to their comparable binding energy. Moreover the peak C3 (below 289 eV) was assigned as the amide linkage formed as a result of post oxidation after exposing to the external atmosphere.[17] When the sample was exposed to H_2 plasma, such post oxidation gave rise to lower concentrations of carbon-oxygen bonds on the surface.[31,32]

Other origins of oxygen functionalities could be from the reaction between the polymer and the oxygen from the desorbed water molecules or water formed as a by-product of polymer etching.

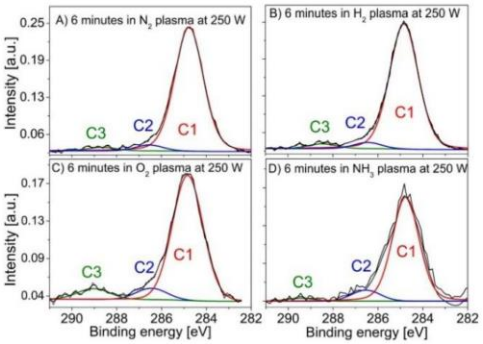


Figure 6. XPS HR C 1s spectrum deconvolution of the samples treated at 250 W for 6 minutes A) in N_2 plasma B) in H_2 plasma C) in O_2 plasma D) in NH_3 plasma.

To explore more information about the plasma surface interactions, plasma characterization is needed. Optical emission spectroscopy (OES) analysis is a useful characterization technique which enables the detection of various excited species in plasma. Monitoring of the OES spectra of N_2 plasma in the beginning of the 6th minute for various discharge powers revealed that the intensity of the bands increase consecutively with the increase in the discharge power. N_2 plasma emission bands mainly composed of N_2 first and second positive spectrum (N_2-FPS and N_2-SPS) (Figure 7).

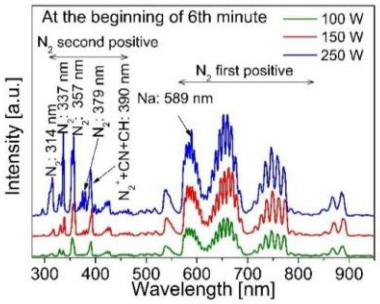


Figure 7. OES measurements during the N_2 plasma treatment of the composite at the 6th minute for various discharge powers.

The major lines gathered in the range 300 to 400 nm constitutes of N_2-SPS ($C^3\Pi_u \rightarrow B^3\Pi_g$).[33] The N_2-SPS band at 337 nm: N_2 ($C_3\Pi_u$) is principally responsible for N_2-SPS, which is produced as a binary collision product of $N_2(A_3\Sigma^+_u)$.[34] The existence of N_2-SPS can thus serve as the indication for $N_2(A_3\Sigma^+_u)$, which has an energy state of 6.2 eV.[35] These species can very easily break various bonds present in the polymer chain. However, due to the ease of reactivity,

This journal is © The Royal Society of Chemistry 20xx

primarily the bond breaking is expected at the benzylic position. Furthermore, the peak at 390 nm is assigned as a combination of N_2^+, CN and CH fragments, where CN and CH species originate after the plasma-polymer interactions.[36] Other possible etch product is NH species which are typically observed at around 336 nm in their excited state. However, this peak is not clearly visible as it can be merged with broad N_2-SPS band at 337 nm. Another possible species inside the reactor chamber is atomic N species, which can separately appear as peaks at 745 nm and 869 nm. However in our case these emission lines are probably embedded inside the molecular emission bands of N_2-FPS and not seen separately due to lower resolution of recorded spectrum.[37,38] Moreover, the intensity of emission line from excited Na species (589 nm) is predominantly seen only when the discharge power is 250 W. Such species usually originate from the organic salts added to improve the processability of the polymer material.[39] Interestingly, this can serve as another indication of enhanced etching rate at higher discharge powers.

The represented OES spectra during the NH_3 plasma treatment revealed that the major peaks are the atomic lines corresponding to hydrogen species includes Hα, Hβ and Hγ at respective wavelengths 686, 486 and 434 nm (Figure 8). The peaks corresponding to NH band at 336 nm ($A^3\Pi \rightarrow X^3\Sigma^-$) were also present at relatively high intensity. Additionally, the peaks corresponding to nitrogen molecular species in the N_2-SPS are present, whereas NH_2 species were hard to detect due to their faster quenching and lowered detection sensitivity, which is 200 times lower than that of the NH species.[17]

The major interacting species inside NH_3 plasma are NH_x and H atoms, whereas in the case of N_2 plasma the excited N_2 and N_2^+.[40,41] If NH_3 plasma is used, then there is a presence of H atoms. Moreover it is well known that NH_3 plasma can induce simultaneous nitrogen incorporation and reduction. On the other hand, the major interacting species in N_2 plasma are supposed to be $N_2(A_3\Sigma^+_u)$ and potentially dissociated N atoms, which induce polymer oxidation. Due to the lower stability of the C-H bond at the benzylic position, primary attack of the plasma particles will probably occur at this position. The possible amination mechanism inside NH_3 plasma is represented in Scheme 2A. Either by the direct reaction of NH_2 radical at the benzylic position to form C-NH_2 bonds, releasing atomic H or by the reaction of NH_2 species with the dangling bonds generated by the influence of H atoms. Additionally, amination at the aromatic ring is also possible by means of NH_2 quenching as explained previously in Scheme 1. Another one of the possible mechanistic routes for amination and nitrile bond formation in N_2 plasma is speculated in Scheme 2B, where diatomic or atomic nitrogen species are involved. However, the exact possible mechanism is hard to predict since plasma is composed of many species which can directly or synergistically influence chemical pathways. After the primary functionalization step, the process can go on through many complicated and competitive reactions. Here it is impossible also to neglect the possibility of interactions from complex radicals arisen from chain fragmentation. Additionally, the UV emission from the excited plasma species are capable of inducing homolytic bond fissions on the polymer surface.

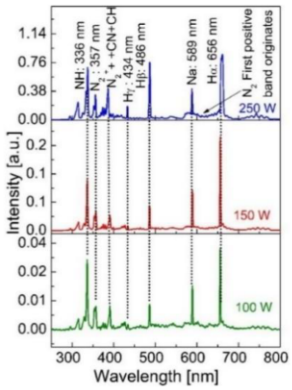
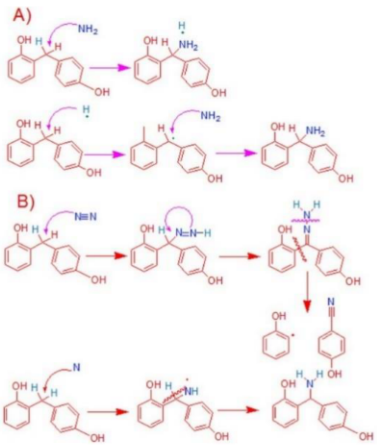


Figure 8. OES measurements recorded during the NH_3 plasma treatment of the composite material at the beginning of the 6th minute for various discharge powers.



Scheme 2 A) Amination mechanism in NH_3 plasma and B) Formation of nitrile and amine functionalities by atomic and molecular nitrogen species.

Among various gas plasmas used, H_2 plasma had the lowest etching rate. The etching inside H_2 plasma is expected to proceed through C-C and C-H bond breakings though hydrogenation reaction. The OES spectrum presented in Figure 9 revealed that the plasma contained atomic hydrogen observed from the emission lines at 434 nm, 486 nm and 656 nm.[42,43] The molecular bands corresponding to H_2 Fulcher and CH were present in the range 590-640 nm and 387 nm, respectively. The intensity of emission from the atomic Na at 589 nm was pronounced only for 250 W. This peak was much weaker in the case of lower discharge powers. In addition to this, the intensities of the etch products originated from the fragmentation of the macromolecules (e.g. CH peak 387 nm, C2 Swan peak at 413 nm) which were the highest at 250 W.[44]

Going further, O_2 plasma was the most active etcher and displayed the highest etching rates. From the OES measurements it is observed that spectra are dominated with excited atomic oxygen as major etcher at 777 nm $O(3p^5P \rightarrow 3s^5S)$ and 844 nm $O(3p^3P \rightarrow 3s^3S)$

(Figure 10). Other atomic line O($3p^5P–4d^5D^0$) was observed at 615 nm.[45] The spectra are populated with the emission lines from atomic hydrogen and molecular OH species (309 nm), which originate from the excited species released in to the system after the polymer etching as well as the dissociation of the desorbed water molecules. The emission lines observed from the excited CO species in the CO Angstrom region clearly indicated the chemical oxidation of the polymer.[20,45] The chemical etching of polymer material with O_2 plasma is well discussed in many articles, where the primary step is the functionalization of the exposed surface. After the surface is saturated with functional groups, the polymer starts to be removed as volatile neutral molecules from the surface including CO, CO_2 or H_2O.

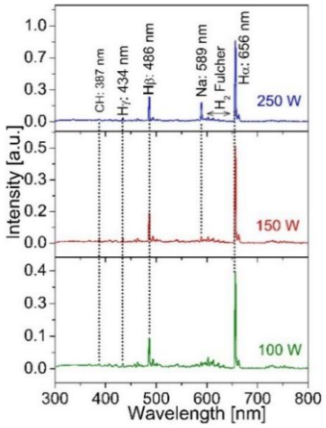


Figure 9. OES measurements recorded during the sample treatment inside H_2 plasma measured at the 6th minute.

In addition, the measured surface temperature is an important parameter among various factors which affects the etching rate of the polymer. The temperature was measured with the pyrometer and the time evolution for all types of plasma and all applied powers is presented in Figure 11.

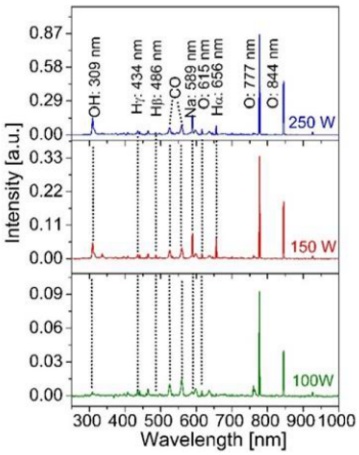


Figure 10. OES measurements recorded during the sample treatment inside O_2 plasma measured at the 6th minute.

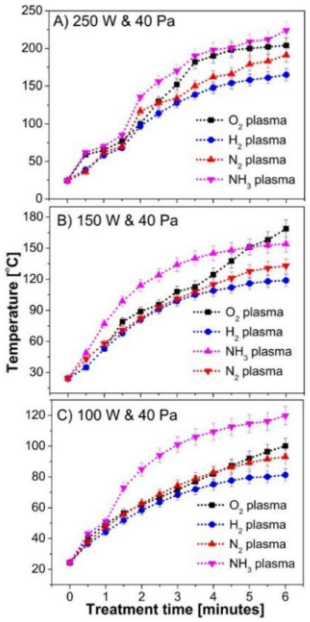


Figure 11. Measured temperature on the sample surface during the treatment in various gas plasmas A) at 250 W B) at 150 W and C) at 100 W.

The surface heating rate as a result of plasma-surface interactions were the lowest for 100 W and highest for 250 W. This power – temperature dependence is explained by increased density of reactive plasma particles which act as etchers with increasing power. As these particles react with surface, the heating of surface becomes more extensive. An interesting feature is the highest temperature achieved is for the case of NH_3 plasma. Since this doesn't correspond fully to previous statement, it suggests that other processes are occurring on the surface which lead to more extensive heating. In the case of NH_3, it seems that the heating of the sample surface is due to heterogeneous surface recombination of the NH_x species. These groups accommodate (adsorb) on the sample surface where they recombine back into ammonia. On other hand, small deviations in O_2 plasma can be explained with exothermic polymer oxidation prior polymer removal which can similarly contribute to the surface heating. However, after the polymer removal the major surface heating is due to radical and ion recombination. When the polymer component is removed due to chemical etching, the recombination occurs predominantly on glass fillers. The fact that the sample temperature is highest for the case of ammonia plasma indicates the recombination of NH_x occurs at somehow higher probability than recombination of N, O and H atoms to parent molecules. The effect is particularly pronounced at the lowest power of 100 W where heating by heterogeneous surface recombination usually prevails over other mechanisms such as accommodation of positively charged ions and neutralization of charged particles. For the future, we intend to investigate such

This journal is © The Royal Society of Chemistry 20xx

heating effects from the surface recombination by combining Langmuir and catalytic probe measurements.

Conclusions

The etching of polyphenolic-matrix composite in various gas plasmas at different discharge conditions is explored and differences are discussed. Among the various gases used, the etching rate was the highest with O_2 plasma. The increased etching rate at higher discharge powers was attributed to the increased density of excited and dissociated particles. The excited species inside various gas plasmas were monitored by OES analysis, which revealed the presence of dissociated atoms, other excited particles and molecules as well as ions. Various particles react with surfaces at different rates due to their potential energies. Impinging ionic species mostly recombine upon interaction with the surface and directly contribute to surface heating. On the other hand, metastables or neutral atoms can recombine on the surface with lower probabilities which are highly dependent on interacting material. The results of these interactions are then predominant formation of chemical bonds with the polymer.

During the treatment process, the polymer was selectively etched away while the glass fibres remained intact as observed by SEM images. Moreover by combining XPS analyses, OES measurements and information on strength of various bonds involved in the macromolecular chain, the surface reactions were mechanistically proposed and presented. The major etchers inside O_2 plasma are dissociated O atoms which give rise to oxidized carbon (CO or CO_2) and H_2O. The etching rate was the highest for O_2 plasma plausibly due to the higher reaction rates of the O reactive species with the polymer. In the case of H_2 plasma, the proposed etching is occurring through dissociated H atoms which reduce the C-C and C-H bonds to volatile hydrocarbons. When using N_2 plasma, the major etchers included excited ionic and molecular species. Whilst in the case of NH_3 plasma, dissociation of the feeding gas provided atomic H and NH species as observed by OES measurements. However, there are other possible species including NH_2. The existance of NH_2 is speculated due to the presence of NH and Hγ since the major formation of NH_2 species occurs through the reaction between NH_2 and H in NH_3 discharges (NH_2+H→ NH+H_2). Due to various excitation and quenching mechanisms, all the species involved cannot be detected with emission spectroscopy. For better validation of our proposed results, more detailed analysis of plasma with other sophisticated techniques including laser induced fluorescence and absorption spectroscopic studies and probe measurements (Langmuir and catalytic) should be combined with molecular modelling.

As a result of plasma-surface interactions, the surface temperature was increased during the treatment which represented an important parameter that influenced directly or synergistically the etching rate. The observed surface temperature was the highest for NH_3 plasmas, although the etching rate was lower compared to O_2 plasma. This discrepancies were explained in terms of higher probability of radical recombination which contributes to surface temperature in addition to polymer oxidation and ion collisions. Whilst it is really difficult to distinguish the individual effects of various heating mechanisms. Thus to conclude, this work will enlighten the applications of cold plasma processing in composite technology and provide more understandings on the plasma- surface interactions. To gain more understanding of these mechanisms, our future works will be more focused on plasma characterization which enables to estimate the concentration of various atomic and ionic species inside the plasma, electron temperature and ion energy flux onto the sample surface.

Acknowledgements

Authors gratefully acknowledge Slovenian Research Agency (ARRS) for financial support (Project grant L2-6767). H.P thanks Jozef Stefan International Postgraduate School for the PhD grant from innovative scheme.

References

1 H. Puliyalil and U. Cvelbar, Nanomaterials, 2016, **6**, 108, DOI:10.3390/nano6060108.
2 M. Alexander, V. Roumen, S. Koen, V. Alexander, Z. Liang, T. Gustaaf Van, V. Annick and H. Chris Van, *Nanotechnology*, 2008, **19**, 305604.
3 C. Yang, H. Bi, D. Wan, F. Huang, X. Xie and M. Jiang, *Journal of Materials Chemistry A*, 2013, **1**, 770-775.
4 A. Michelmore, D. A. Steele, J. D. Whittle, J. W. Bradley and R. D. Short, *RSC Advances*, 2013, **3**, 13540-13557.
5 Z. J. Han, I. Levchenko, S. Kumar, M. M. A. Yajadda, S. Yick, D. H. Seo, P. J. Martin, S. Peel, Z. Kuncic and K. Ostrikov, *Journal of Physics D: Applied Physics*, 2011, **44**, 174019.
6 S. Huet, T. Belmonte, J. M. Thiébaut, S. Bockel and H. Michel, *Thin Solid Films*, 2005, **475**, 63-67.
7 A. Sarani, A. Y. Nikiforov, N. De Geyter, R. Morent and C. Leys, *Applied Surface Science*, 2011, **257**, 8737-8741.
8 R. V. Goreham, A. Mierczynska, L. E. Smith, R. Sedev and K. Vasilev, *RSC Advances*, 2013, **3**, 10309-10317.
9 K. Bazaka, M. V. Jacob, W. Chrzanowski and K. Ostrikov, *RSC Advances*, 2015, **5**, 48739-48759.
10 L. Xie, L. Jiao and H. Dai, *Journal of the American Chemical Society*, 2010, **132**, 14751-14753.
11 A. Davydova, E. Despiau-Pujo, G. Cunge and D. B. Graves, *Journal of Physics D: Applied Physics*, 2015, **48**, 195202.
12 D. Hegemann, H. Brunner and C. Oehr, *Nuclear Instruments and Methods in Physics Research Section B: Beam Interactions with Materials and Atoms*, 2003, **208**, 281-286.
13 M. B. Olde Riekerink, J. G. A. Terlingen, G. H. M. Engbers and J. Feijen, *Langmuir*, 1999, **15**, 4847-4856.
14 S. Allauddin, M. K. Akhil Chandran, K. K. Jena, R. Narayan and K. V. S. N. Raju, *Progress in Organic Coatings*, 2013, **76**, 1402-1412.
15 A. Palanisamy, N. V. Salim, B. L. Fox, P. Jyotishkumar, T. Pradeep and N. Hameed, *RSC Advances*, 2016, **6**, 55792-55799.
16 F. Malara, M. Manca, L. De Marco, P. Pareo and G. Gigli, *ACS Applied Materials & Interfaces*, 2011, **3**, 3625-3632.

19 H. Puliyalil, P. Slobodian, M. Sedlacik, R. Benlikaya, P. Riha, K. Ostrikov and U. Cvelbar, *Frontiers of Chemical Science and Engineering*, 2016, **10**, 265-272.
20 H. Puliyalil, U. Cvelbar, G. Filipic, A. D. Petric, R. Zaplotnik, N. Recek, M. Mozetic and S. Thomas, *RSC Advances*, 2015, **5**, 37853-37858.
21 J. A. Kim, D. G. Seong, T. J. Kang and J. R. Youn, *Carbon*, 2006, **44**, 1898-1905.
22 A. Pizzi and C. C. Ibeh, in *Handbook of Thermoset Plastics (Third Edition)*, eds. H. Dodiuk and S. H. Goodman, William Andrew Publishing, Boston, 2014, DOI: http://dx.doi.org/10.1016/B978-1-4557-3107-7.00002-6, pp. 13-44.
23 N. Škoro, N. Puač, S. Lazović, U. Cvelbar, G. Kokkoris and E. Gogolides, *Journal of Physics D: Applied Physics*, 2013, **46**, 475206.
24 C. Canal, F. Gaboriau, A. Ricard, M. Mozetic, U. Cvelbar and A. Drenik, *Plasma Chem Plasma Process*, 2007, **27**, 404-413.
25 A. Vesel, I. Junkar, U. Cvelbar, J. Kovac and M. Mozetic, *Surface and Interface Analysis*, 2008, **40**, 1444-1453.
26 H. Nagai, S. Takashima, M. Hiramatsu, M. Hori and T. Goto, Journal of Applied Physics, 2002, **91**, 2615-2621.
27 D. F. McMillen and D. M. Golden, *Annual Review of Physical Chemistry*, 1982, **33**, 493-532.
28 G. N. Taylor and T. M. Wolf, *Polymer Engineering & Science*, 1980, **20**, 1087-1092.
29 E. Zadok, B. Sialom and Y. Mazur, *Angewandte Chemie International Edition in English*, 1980, **19**, 1004-1005.
30 W. M. Jackson and R. T. Conley, *Journal of Applied Polymer Science*, 1964, **8**, 2163-2193.
31 M. Pascu, D. Debarnot, S. Durand and F. Poncin-Epaillard, in *Plasma Processes and Polymers*, Wiley-VCH Verlag GmbH & Co. KGaA, 2005, DOI: 10.1002/3527605584.ch13, pp. 157-176.
32 Y. W. Park and N. Inagaki, *Polymer*, 2003, **44**, 1569-1575.
33 R. M. v. d. Horst, T. Verreycken, E. M. v. Veldhuizen and P. J. Bruggeman, *Journal of Physics D: Applied Physics*, 2012, **45**, 345201.
34 L. G. Piper, *The Journal of Chemical Physics*, 1988, **88**, 231-239.
35 T. H. Chung, Y. W. Lee, H. M. Joh and M. A. Song, *AIP Advances*, 2011, **1**, 032136.
36 M. Camero, F. J. Gordillo-Vázquez, J. Ortiz and C. Gómez-Aleixandre, *Plasma Sources Science and Technology*, 2004, **13**, 121.
37 K. J. Clay, S. P. Speakman, G. A. J. Amaratunga and S. R. P. Silva, Journal of Applied Physics, 1996, **79**, 7227-7233.
38 P. Anne-Marie, R. André, D. Bénédicte, O. Emmanuel, L. Juliette and G. Mihai, Journal of Physics D: Applied Physics, 2005, **38**, 1905.
39 M. A. Osman, A. Atallah and U. W. Suter, *Polymer*, 2004, **45**, 1177-1183.
40 C. López-Santos, F. Yubero, J. Cotrino and A. R. González-Elipe, *ACS Applied Materials & Interfaces*, 2010, **2**, 980-990.
41 J. E. Klemberg-Sapieha, O. M. Küttel, L. Martinu and M. R. Wertheimer, *Journal of Vacuum Science & Technology A*, 1991, **9**, 2975-2981.
42 A. Vesel, J. Kovac, R. Zaplotnik, M. Modic and M. Mozetic, *Applied Surface Science*, 2015, 357, Part B, 1325-1332.
43 M.-J. Wang, Y.-I. Chang and F. Poncin-Epaillard, *Langmuir*, 2003, **19**, 8325-8330.
44 A. Chingsungnoen, J. I. B. Wilson, V. Amornkitbamrung, C. Thomas and T. Burinprakhon, *Plasma Sources Science and Technology*, 2007, **16**, 434.
45 H. Puliyalil, G. Filipič and U. Cvelbar, *Plasma Processes and Polymers*, 2016, DOI: 10.1002/ppap.201600005.

This journal is © The Royal Society of Chemistry 20xx

Chapter 7

Conclusions and Future Outlook

This chapter summarizes all the experimental results and thesis objectives. Selective plasma etching of glass-filled polyphenolic composites was achieved in various gas plasmas, generated by RF frequency discharge. The effects of plasma surface modifications on surface wettability and comparative tracking index were studied. In addition to this, a systematic comparison of the etching process in various discharges was carried out.

Various results obtained are concluded under each stated objective.

Objective 1: Understand the effects of low-temperature plasma treatments on surface chemistry, topography and wettability of various industrially related composite surfaces.

The surface modification of industrially related polyphenolic matrix filled with glass fillers was achieved in various gas discharges. The combined effects of surface chemistry and topography were studied by various surface analyses of the composites treated inside CF_4 plasma generated at low pressure. It was demonstrated that the contribution from various chemical bonds towards the surface wettability is different. The $C-F_3$ bond types contributed more towards the hydrophobicity of the surface than $C-F_2$ or $C-F$ bond types. Along with this, the migration rates of $C-F_x$ bonds showed an increase with the increase in the number of F atoms attached to the carbon. The surface roughness after the plasma modification was relatively high due to the exposure of glass fillers. The water droplet was strongly pinned on the surface which led to the conclusion that the water droplet exhibited Wenzel state mechanism. On the other hand, fluorine-free plasma treatments tend to increase the surface energy by incorporating polar functional groups, providing superhydrophilicity to the treated surfaces.

The objective was achieved in Chapters 3 and 4.

Objective 2: To study the effects of selective plasma etching for improving the electrical insulation properties of glass-filled polyphenolic composites.

The surface polymer was selectively removed from the glass-filled polyphenolic composite so that the carbon content on the surface showed a substantial decrease. The reactive oxygen species inside the plasma removed the carbon layer in the form of volatile molecular fragments including OH, H_2O, CO and CO_2 which was confirmed by spectroscopic analysis. As observed from SEM images, after the selective polymer removal, the embedded fillers got exposed onto the surface. These fillers acted as a protective layer against surface tracking during CTI tests. The repetition of the experiment with lower filler content further confirmed this argument. The removal of surface polymer in both O_2 and O_2/Ar plasmas increased the CTI to above 250 V so that the material can be used for commercial applications according to IEC standards. Thus, it was demonstrated that the tracking properties of composite materials could be improved simply by plasma surface

modifications, which is an efficient and fast method, and is a valuable tool in designing novel cost effective high-voltage electrical insulators.

The objective was achieved in Chapters 4 and 5

Objective 3: To determine the influence of various plasma parameters on the etching efficiency and optimization of the process.

The surface polymer was selectively removed in Ar/O_2 discharge and various plasma reactive species were quantified. By changing the plasma feeding gas composition, atomic and ionic flux onto the surface were controlled, which enabled to control the polymer etching rate. The addition of Ar increased the electron density and consequently the dissociation of oxygen molecules. The contribution of oxygen reactive species was directly linked to the chemical reactions at the plasma-surface interface, whereas the ionic species contributed mostly to the surface heating. The etching rate was the lowest when the feeding gas contained 98% of Ar which was obvious due to the lack of chemical assistance from neutral O atoms.

The objective was achieved in Chapter 5

Objective 4: To systematically compare the etching process in various gas plasmas created within inductively coupled RF discharges.

The etching rate inside the plasma was compared with commercially important feeding gases including H_2, N_2, O_2 and NH_3 as a function of discharge power. The results demonstrated that the etching efficiency was the maximum for O_2 plasma due to the high affinity of neutral O atoms towards the carbonaceous layer. In addition to that, the etching rate was found to increase as a function of applied power. Sequential bond breaking was presented by considering the energy of various bond types presented on the polymer backbone. The observations revealed that the etching rate largely depends on the interacting plasma particle.

The objective was achieved in Chapter 6

Future work

Even though the selective removal of the polymer from the surface improved insulation properties sufficiently enough to be used in commercial applications, the polymer residue left underneath the glass fillers does not allow the material to reach the performance level 0. For this reason, we would need to improve the composition of the polymer-matrix composite.

Secondly, better plasma characterization would be needed in order to unravel more precisely the plasma-surface interactions. Due to various excitation and quenching mechanisms, all species involved cannot be detected with optical emission spectroscopy. For better validation of our proposed reaction mechanisms in Chapter 6, more detailed analysis of plasma with other sophisticated techniques including laser induced fluorescence and absorption spectroscopic studies as well as various probe measurements should be combined with molecular modelling. The analyses of plasma-surface interactions should be also done on more basic materials rather than on industrial samples like in our case.

Another part of future research should be also directed by selective plasma etching with atmospheric pressure plasmas, where selective removal of polymer could be done in open air in order to make production even more economical.

References

[1] M. Meyyappan, "Plasma nanotechnology: past, present and future," *Journal of Physics D: Applied Physics,* vol. 44, p. 174002, 2011.

[2] K. Ostrikov, U. Cvelbar, and A. B. Murphy, "Plasma nanoscience: setting directions, tackling grand challenges," *Journal of Physics D: Applied Physics,* vol. 44, p. 174001, 2011.

[3] L. Martinu and D. Poitras, "Plasma deposition of optical films and coatings: A review," *Journal of Vacuum Science & Technology A*, vol. 18, pp. 2619-2645, 2000.

[4] J. W. Coburn and H. F. Winters, "Ion- and electron-assisted gas-surface chemistry—An important effect in plasma etching," *Journal of Applied Physics,* vol. 50, pp. 3189-3196, 1979.

[5] P. Favia and R. d'Agostino, "Papers presented at the Fifth International Conference on Plasma Surface EngineeringPlasma treatments and plasma deposition of polymers for biomedical applications," *Surface and Coatings Technology,* vol. 98, pp. 1102-1106, 1998.

[6] F. Gou, A. W. Kleyn, and M. A. Gleeson, "The application of molecular dynamics to the study of plasma–surface interactions: CF x with silicon," *International Reviews in Physical Chemistry,* vol. 27, pp. 229-271, 2008.

[7] R. Hippler, S. Pfau, M. Schmidt, K. H. Schoenbach, "Low temperature plasma physics: Fundamental aspects and applications," Wiley VCH, Berlin, Germany, 2001.

[8] K. Pochner, S. Beil, H. Horn, and M. Blömer, "Treatment of polymers for subsequent metallization using intense UV radiation or plasma at atmospheric pressure," *Surface and Coatings Technology,* vol. 97, pp. 372-377, 1997.

[9] C. M. Chan, T. M. Ko, and H. Hiraoka, "Polymer surface modification by plasmas and photons," *Surface Science Reports,* vol. 24, pp. 1-54, 1996.

[10] M. Mikhaylova, D. K. Kim, C. C. Berry, A. Zagorodni, M. Toprak, A. S. G. Curtis*, et al.*, "BSA Immobilization on Amine-Functionalized Superparamagnetic Iron Oxide Nanoparticles," *Chemistry of Materials,* vol. 16, pp. 2344-2354, 2004.

[11] S. Lerouge, M. R. Wertheimer, and L. H. Yahia, "Plasma Sterilization: A Review of Parameters, Mechanisms, and Limitations," *Plasmas and Polymers,* vol. 6, pp. 175-188, 2001.

[12] M. B. Olde Riekerink, J. G. A. Terlingen, G. H. M. Engbers, and J. Feijen, "Selective Etching of Semicrystalline Polymers: CF4 Gas Plasma Treatment of Poly(ethylene)," *Langmuir,* vol. 15, pp. 4847-4856, 1999.

[13] I. Junkar, U. Cvelbar, A. Vesel, N. Hauptman, and M. Mozetič, "The Role of Crystallinity on Polymer Interaction with Oxygen Plasma," *Plasma Processes and Polymers,* vol. 6, pp. 667-675, 2009.

[14] S. J. Moss, A. M. Jolly, and B. J. Tighe, "Plasma oxidation of polymers," *Plasma Chemistry and Plasma Processing,* vol. 6, pp. 401-416, 1986.

[15] J. A. Kerr, *Handbook of Bimolecular and Termolecular Gas Reactions*: Taylor & Francis, Boca Raton, FL, USA, 1987.

[16] A. Ricard, C. Canal, S. Villeger, and J. Durand, "Transmission of Nitrogen Atoms through Porous Membranes for Nitrogen Flowing Post-Discharge Sterilization Processes," *Plasma Processes and Polymers,* vol. 5, pp. 867-873, 2008.
[17] G. N. Taylor and T. M. Wolf, "Oxygen plasma removal of thin polymer films," *Polymer Engineering & Science,* vol. 20, pp. 1087-1092, 1980.
[18] D. Hegemann, H. Brunner, and C. Oehr, "Plasma treatment of polymers for surface and adhesion improvement," *Nuclear Instruments and Methods in Physics Research Section B: Beam Interactions with Materials and Atoms,* vol. 208, pp. 281-286, 2003.
[19] L. Xie, L. Jiao, and H. Dai, "Selective Etching of Graphene Edges by Hydrogen Plasma," *Journal of the American Chemical Society,* vol. 132, pp. 14751-14753, 2010.
[20] U. Cvelbar, S. Pejovnik, M. Mozetiè, and A. Zalar, "Increased surface roughness by oxygen plasma treatment of graphite/polymer composite," *Applied Surface Science,* vol. 210, pp. 255-261, 2003.
[21] U. Cvelbar, M. Mozetic, and M. Klanjsek-Gunde, "Selective oxygen plasma etching of coatings," *IEEE Transactions on Plasma Science,* vol. 33, pp. 236-237, 2005.
[22] M. Kunaver, M. Mozetič, and M. Klanjšek-Gunde, "Selective plasma etching of powder coatings," *Thin Solid Films,* vol. 459, pp. 115-117, 2004.
[23] L. Jiao, L. Zhang, X. Wang, G. Diankov, and H. Dai, "Narrow graphene nanoribbons from carbon nanotubes," *Nature,* vol. 458, pp. 877-880, 2009.
[24] S. Joseph, M. S. Sreekala, Z. Oommen, P. Koshy, and S. Thomas, "A comparison of the mechanical properties of phenol formaldehyde composites reinforced with banana fibres and glass fibres," *Composites Science and Technology,* vol. 62, pp. 1857-1868, 2002.
[25] Z. Laušević and S. Marinković, "Proceedings of the Conference on Strength and Structural in Carbons and Graphites Mechanical properties and chemistry of carbonization of Phenol formaldehyde resin," *Carbon,* vol. 24, pp. 575-580, 1986.
[26] J. K. Park and T. J. Kang, "Thermal and ablative properties of low temperature carbon fiber–phenol formaldehyde resin composites," *Carbon,* vol. 40, pp. 2125-2134, 2002.
[27] Effect of phosphorus based flame retardants on UL94 and Comparative Tracking Index properties of poly(butylene terephthalate)," *Polymer Degradation and Stability,* vol. 97, pp. 566-572, 2012.
[28] B. X. Du, "Discharge energy and dc tracking resistance of organic insulating materials," *IEEE Transactions on Dielectrics and Electrical Insulation,* vol. 8, pp. 897-901, 2001.

Bibliography

Journal Articles

[1] H. Puliyalil and U. Cvelbar, "Selective Plasma Etching of Polymeric Substrates for Advanced Applications," *Nanomaterials*, vol. 6, pp. 108, 2016.

[2] H. Puliyalil, U. Cvelbar, G. Filipič, A. D. Petric, R. Zaplotnik, N. Recek, M. Mozetič, S. Thomas, "Plasma as a tool for enhancing insulation properties of polymer composites," *RSC Advances*, vol. 5, pp. 37853-37858, 2015.

[3] H. Puliyalil, G. Filipič, and U. Cvelbar, "Selective Plasma Etching of Polyphenolic Composite in O_2/Ar Plasma for Improvement of Material Tracking Properties," *Plasma Processes and Polymers*, 2016, DOI: 10.1002/ppap.201600005

[4] R. Thomas, C. Sinturel, J. Pionteck, H. Puliyalil, and S. Thomas, "In-situ Cure and Cure Kinetic Analysis of a Liquid Rubber Modified Epoxy Resin," Industrial & Engineering Chemistry Research, vol. 51, pp. 12178-12191, 2012/09/26 2012.

[5] H. Puliyalil, P. Slobodian, M. Sedlacik, R. Benlikaya, P. Riha, K. Ostrikov, U Cvelbar, "Plasma-enabled sensing of urea and related amides on polyaniline," Frontiers of Chemical Science and Engineering, vol. 10, pp. 1-8, 2016.

[6] H. Puliyalil, N. Recek, G. Filipič, M. Čekada, I. Jerman, M. Mozetič, S. Thomas, U. Cvelbar, "Mechanisms of hydrophobization of polymeric composites etched in CF_4 plasma," *Surface and Interface Analysis*, 2016, DOI: 10.1002/sia.6104.

[7] H. Puliyalil, G. Filipič, J. Kovač, M. Mozetič, S. Thomas, U. Cvelbar, " Tackling chemical etching and its mechanisms of polyphenolic composites in various reactive low temperature plasmas," Submitted to: *RSC Advances*, Manuscript number: RA-ART-06-2016-015923.

Patent Application

[1] H. Puliyalil, U. Cvelbar, M. Mozetič, S. Thomas, "Method for improving comparative tracking index (CTI) of polymer composites," Indian patent (Filed), Application number: 4239/CHE/2014.

Book Chapter

[1] H. Puliyalil, G. Filipič, U. Cvelbar, "Recent advances in the methods for designing superhydrophobic surfaces, " edited by M. Salih, *Surface energy*, InTech. Publishers, Rijeka, Croatia, 2015,

Published scientific conference contribution (Invited)

[1] H. Puliyalil, P. Slobodian, P. Riha, U. Cvelbar, "Atmospheric pressure plasma modified polyaniline crystals for detection of volatile organic compounds, " V: *2014 ECS and SMEQ Joint International Meeting*, *226th ECS Meeting of the Electrochemical Society*, Cancun, Mexico, 2014.

[2] H. Puliyalil, G. Filipič, U. Cvelbar, "Plasma selective etching: a green route for tackling electrical insulation properties, " V: *E-MRS 2015 Fall Meeting & Exhibit,* Warsaw, Poland, 2015.

[3] H. Puliyail, P. Slobodian, U. Cvelbar, "Improving the vapor detection properties of polyaniline composites by plasma surface modifications," *iPlasmanano V,* Malaga, Spain, 2014.

Published scientific conference contribution

[1] H. Puliyalil, M. Mozetič, U. Cvelbar, "Oxygen plasma selective etching for the enhanced electrical insulation properties of polyphenol composites," *9th EU-Japan Joint Symposium on Plasma Processing*, Bohinjska Bistrica, Slovenia, 2014.

[2] H. Puliyalil, G. Filipič, U. Cvelbar, "Plasma selective etching of composite surfaces for improved tracking resistance properties," *29th National Symposium on Plasma Science and Technology & International Conference on Plasma and Nanotechnology*, Kerala, India, 2014.

[3] H. Puliyalil, G. Filipič, U. Cvelbar, "Superhydrophilic surface of selectively plasma etched polyphenol composite," *6th Jožef Stefan International Postgraduate School Students' Conference*, Ljubljana, Slovenia, 2014.

[4] M. K. A. Chandran, V. Srdic, G. Stojanovi, H. Puliyalil, G. Filipič, and U. Cvelbar, "Investigation on band gap energy and effect of various surface plasma treatments on nano structured SnO_2 semiconductor," *IEEE 15th International Conference on Nanotechnology (IEEE-NANO)*, 2015.

[5] G. Filipič, M. Eleršič, H. Puliyalil, U. Cvelbar, "Microscopic study of metal-oxide nanowire growth mechanism," *1st Slovene Microscopy Symposium*, Piran, Slovenia, 2015.

[6] G. Filipič, O. Branov, H. Puliyalil, U. Cvelbar, "Ion influence on metal-oxide nanowire growth in low-pressure plasma oxidation," *E-MRS 2015 Spring Meeting*, Lille, France, 2015.

[7] M. Kulkarni, I. Junkar, H. Puliyalil, A. Iglič, "Wettability switch of anodic titanium dioxide nanotubes with various diameters," *Biophysical Journal*, vol. 100, p 339a, 2016.

[8] G. Filipič, J. Grunwald, H. Puliyalil, J. Zavašnik, J. Kovač, U. Cvelbar, "Gas sensing with CuO nanoflakes deposited at atmospheric conditions," *2nd International Conference Functional Integrated Systems, nanoFIS 2016,* Graz, Austria. 2016.

Biography

The author of this thesis received his Bachelor degree in Chemistry from University of Calicut, Kerala, India in 2008. In 2011, he received his Master of Science degree in Organic Chemistry from School of Chemical Sciences, Mahatma Gandhi University, Kottayam, India. He also holds a Master of Philosophy degree in Polymer Chemistry from School of Chemical Sciences, Mahatma Gandhi University, Kottayam, India. In 2012, he started his doctoral studies at Jožef Stefan International Postgraduate School, Slovenia. He has 5 years of research experience in different fields including carbohydrate chemistry, plasma etching, plasma nanostructuring, development of various polymer blends and composites.